Acta Pharmaceutica Sinica B 2021;11(8):2362–2395

Chinese Pharmaceutical Association
Institute of Materia Medica, Chinese Academy of Medical Sciences

Acta Pharmaceutica Sinica B

www.elsevier.com/locate/apsb
www.sciencedirect.com

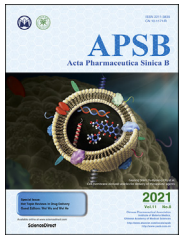

REVIEW

Metal-organic frameworks for advanced drug delivery

Siyu He[a,b], Li Wu[a], Xue Li[c], Hongyu Sun[a], Ting Xiong[a,d], Jie Liu[e], Chengxi Huang[a,b], Huipeng Xu[a], Huimin Sun[f], Weidong Chen[e,*], Ruxandra Gref[c,*], Jiwen Zhang[a,b,d,f,*]

[a]*Center for Drug Delivery Systems, Shanghai Institute of Materia Medica, Chinese Academy of Sciences, Shanghai 201203, China*
[b]*University of Chinese Academy of Sciences, Beijing 100049, China*
[c]*Institut de Sciences Moléculaires D'Orsay, Université Paris-Saclay, Orsay Cedex 91400, France*
[d]*Key Laboratory of Modern Chinese Medicine Preparations, Ministry of Education, Jiangxi University of Traditional Chinese Medicine, Nanchang 330004, China*
[e]*School of Pharmaceutical Sciences, Anhui University of Chinese Medicine, Hefei 230012, China*
[f]*NMPA Key Laboratory for Quality Research and Evaluation of Pharmaceutical Excipients, National Institutes for Food and Drug Control, Beijing 100050, China*

Received 3 November 2020; received in revised form 25 December 2020; accepted 15 January 2021

KEYWORDS

Metal-organic frameworks;
Drug loading;
Drug delivery systems;
Synthesis and characterization;
Diseases therapy;
Pharmaceutics;
Biopharmaceutics;
Biosafety

Abstract Metal-organic frameworks (MOFs), comprised of organic ligands and metal ions/metal clusters *via* coordinative bonds are highly porous, crystalline materials. Their tunable porosity, chemical composition, size and shape, and easy surface functionalization make this large family more and more popular for drug delivery. There is a growing interest over the last decades in the design of engineered MOFs with controlled sizes for a variety of biomedical applications. This article presents an overall review and perspectives of MOFs-based drug delivery systems (DDSs), starting with the MOFs classification adapted for DDSs based on the types of constituting metals and ligands. Then, the synthesis and characterization of MOFs for DDSs are developed, followed by the drug loading strategies, applications, biopharmaceutics and quality control. Importantly, a variety of representative applications of MOFs are detailed from a point of view of applications in pharmaceutics, diseases therapy and advanced DDSs. In particular, the biopharmaceutics and quality control of MOFs-based DDSs are summarized with critical issues to be addressed. Finally, challenges in MOFs development for DDSs are discussed, such as biostability, biosafety, biopharmaceutics and nomenclature.

*Corresponding authors.
E-mail addresses: anzhongdong@126.com (Weidong Chen), ruxandra.gref@u-psud.fr (Ruxandra Gref), jwzhang@simm.ac.cn (Jiwen Zhang).
Peer review under responsibility of Chinese Pharmaceutical Association and Institute of Materia Medica, Chinese Academy of Medical Sciences.

https://doi.org/10.1016/j.apsb.2021.03.019

1. Introduction

With the cracking growth of materials chemistry, a great deal of efforts have been dedicated to build original micro or nano-platforms for controlled and intelligent drug release systems in the interest of maximizing therapeutic efficacy and minimizing side effects. Metal-organic frameworks (MOFs), comprised of organic ligands and metal ions/metal clusters *via* coordinative bonds into two-dimensional or three-dimensional network are highly porous and crystalline materials, offering structural control at the molecular level, and have appealed to widespread attention since they were first reported in 1989 by Hoskins and Robson[1]. Nowadays, there are more than 20,000 diverse frameworks of MOFs reported in Cambridge database[2]. The publications tendency revealed an exponential increase relevant to MOFs in the period 2006−2020 (Fig. 1A). This trend highlights that MOFs are appealing new systems of great potential in drug delivery.

By choosing judicious linkers and metal clusters, a variety of MOFs with tuned physicochemical properties (*e.g.*, surface area, pore diameter, morphology, hydrophilicity or hydrophobicity) can be engineered for specific applications, such as gas storage[3] and separations[4,5], imaging[6], sensing[7], catalysis[8], energy[9], analytical chemistry[10] and biomedicine[11]. Specially, the modulable porosity, tunable size and structure, and facile surface functionalization of MOFs make them become one of the most popular materials in biomedical field, of which drug delivery is promising with fast development.

Over the last decades, MOFs have found appliances in drug delivery systems (DDSs) and some novel designs and remarkable achievements using MOFs for drug delivery have been actualized. Similarly, articles about MOFs-based DDSs portray prevalent tendency over the past ten years (Fig. 1B). The well-defined porous crystalline MOFs showed additional advantages as compared to more conventional nanocarriers including liposomes[12], polymers[13], quantum dots[14], inorganic nanoparticles[15], allowing circumventing issues related to low drug loading, instability, systemic side effects and toxicities[16−18]. First and most importantly, as porous materials with large Brunauer−Emmett−Teller (BET) surface[19], MOFs have remarkable cargo loading capacities, a variety of cargos with various physico-chemical properties such as small drug molecules[20], peptides[21], and even biomacromolecules[22], can be loaded with efficiencies sometimes close to 100%[23]. Secondly, the porosities and compositions of MOFs can be adjusted by appropriately selecting the building blocks and metal ions to possess specific physical and chemical properties such as biodegradability, efficient drug loading and controlled release. In addition, MOFs can be conveniently surface-modified by using predesigning or post-synthetic strategies to achieve smart delivery using microrobots[24] or surface functionalities[25,26]. Moreover, it is noteworthy that the modification of MOFs' surfaces leads in most cases to no significant alteration of their physicochemical properties. Indeed, coating materials can be simply adsorbed from aqueous media onto the MOFs surface with high yields and good stabilities due to cooperative interactions[27] or polymerized onto the surfaces[28]. Alternatively, MOFs can be coated with lipid[29] or silica shells[30].

Thirdly, as the coordinative bonds in the structures of MOFs are weak interactions, the MOFs are prone to readily degrade in biological media, releasing their constitutive ligands. This leads to excellent biodegradability and biocompatibility after accomplishment of the intended mission[31,32]. Last but not least, several MOFs showed intrinsic properties favorable to combat cancer or infections. For example, specific Fe-based nanoMOFs showed: i) antibacterial properties, contributing together with their drug cargo, to fight intracellular infections[33] and ii) participations in improving radiation efficacy[23]. These studies lead the way for designing engineered nanoparticles (NPs) wherein each constituent plays a part in tumor remedy by radiotherapy or in the treatment of severe infections. In simple words, all these properties endow MOFs with promising potential in the field of DDSs.

In light of the expanding number of studies about MOFs over the past decades, several relevant reviews about the application of MOFs in biomedicine have appeared in the last few years on different aspects such as DDSs for cancer treatment[34] and cancer theranostics[35]. Owing to the tunability and facile functionalization of MOFs, efforts have been dedicated to developing MOFs-based stimuli-responsive systems and MOFs-composite materials for biomedical applications. Wang et al.[36] reviewed the growth of

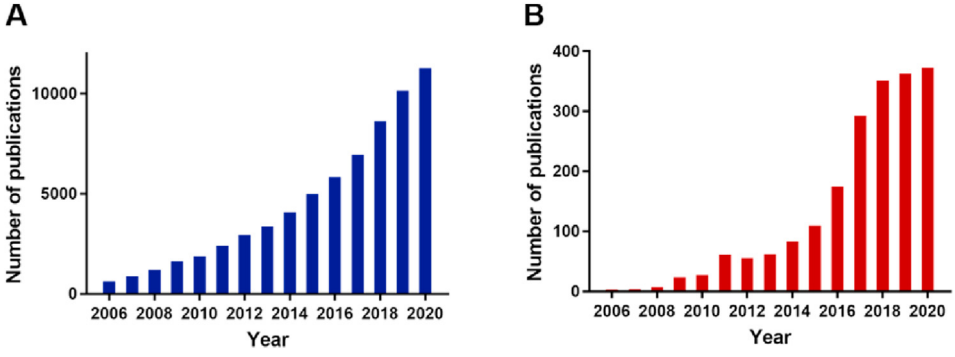

Figure 1 Publications in the period of 2006−2020 from Web of Science (A) "Metal organic framework" and (B) "metal organic framework and drug delivery".

MOF families and members, then summarized the mechanisms of drug release in accordance with the endogenous stimuli (*e.g.*, pH, glutathione, enzyme) and exogenous (*e.g.*, temperature, light). Similarly, Cai et al.[37] classified the MOFs-based stimuli-responsive systems into single or multiple stimuli. Differently, Giliopoulos et al.[38] introduced various types of polymer/MOF nanocomposites for drug delivery and imaging. What's more, MOF composites and surface functionalization for nanomedicine in cancer therapy and diagnostics were summarized as well[39,40]. Specially, biological MOFs (BioMOFs) composed of metal ions and biomolecular likers including nucleobases, cyclodextrin, amino acids, polypeptides and others for bio-applications were also summarized and discussed[41]. On the other side, a comparison between MOFs and other nanocarriers such as mesoporous silica nanoparticles and dendrimers as drug delivery systems was addressed[17].

By contrast, this review focuses on MOFs-based DDSs, instead of the bio-applications of MOFs. Firstly, a classification of MOFs for DDSs will be presented based on the type of both constitutive metals and ligands. Then, the methods for synthesis and characterizations of MOFs and MOFs-based DDSs are summarized. Next, the applications of MOFs-based DDSs are catalogued from three aspects. On the one hand, a perspective is given about the functions of MOFs-based DDS in pharmaceutics, including solubilization, increased stability, sustained release, etc. On the other side, practical applications of MOFs-based DDSs in the field of diseases are listed, including the treatment of infections, cancer, pulmonary and ocular diseases, etc. At the same time, the functionalization of MOFs-based DDSs for advanced applications is illustrated as well. Furthermore, the biopharmaceutics of MOFs and MOFs-based DDSs are stressed, which is rarely referred in previous reviews. Finally, the quality control and biosafety of MOFs-based DDS are presented, which are critical for clinical and industrial applications (Fig. 2).

2. Classification of MOFs

MOFs are built using diverse linkers and metals, which determine their polytropic structures and characteristics (Fig. 3). Besides, the linker and the metal cluster are congregated by frail coordination bonds, thereby enhancing biodegradability. However, a subtle balance between degradability and sufficient stability in biological media should be ensured. Specific applications can be reached by appropriately selecting both the metal ion and the organic linker, such as stimuli-responsiveness in drug delivery[34], toward pH-responsive[42], molecular-responsive[43], thermo-responsive[44], and pressure-responsive MOFs[45]. In this review, MOFs researched mostly for DDSs are classified based on the presence of specific components and features in their formulation.

2.1. *Classification by metal ions*

Since the choice of ligands and metal ions is practically infinite, varieties of metal ions and organic linkers have been designed and selected to synthesize thousands of MOFs. When MOFs are used in the field of DDSs, they must comprehensively premeditate the biocompatibility and toxicity properly, which are closely related to their compositions[46]. Both linkers and metals should be nontoxic.

The median lethal dose (LD_{50}) is usually used to assess the toxicity of metals[47]. Moreover, the recommended metals for DDSs with MOFs are, potassium, zinc, zirconium and iron with oral LD_{50} of 0.215, 0.35, 4.1 and 0.45 g/kg, respectively[48,49]. Nowadays, iron[50,51], zirconium[52,53], potassium[20,54] and zinc-based[55,56] MOFs remain the most employed for DDSs[48] and a variety of anticancer[57–59], antibiotics[33] and antiviral drugs[60,61] have been loaded in their porosities. Of note, drugs can be co-loaded in the MOF cages affording synergies to fight diseases[33,62]. Many other examples of MOFs as drug carriers have been reported in the pharmaceutical field, enabling reaching high drug payloads, increased drug solubility, improved stability, targeting abilities and better bioavailability. The MOFs for DDSs reported mostly so far are classified here according to their metal ions composition, as shown in Table 1[20,50,53,57,62–80].

2.1.1. *Cr-MOFs*

The testification of drug loading into MOFs has been given in 2006, using two model systems, chromium-based MOFs (Cr-MOFs), named MIL-100 (Cr) and MIL-101 (Cr) (MIL stands for Materials of Institut Lavoisier), which made up of trimers of metal octahedra and di- or tricarboxylic acids. MIL-100 (Cr) consisted of Cr (III) ions and 1,3,5-benzenetricarboxylic acid (BTC) or trimesic acid while MIL-101(Cr) consisted of 1,4-benzenedicarboxylic acid (BDC) or terephthalic acid and Cr (III)[81,82]. Ibuprofen (IBU), a common model drug, was loaded in Cr-MOFs, showing high drug loading capacity, reaching up to 1.4 g IBU of per gram of dehydrated MIL-101 (Cr), while MIL-100 (Cr) only adsorbed 0.35 g IBU.

2.1.2. *Fe-MOFs*

Due to the toxicity of Cr, the above-mentioned MOFs are not compatible for biomedical uses. Iron-based MOFs (Fe-MOFs) named MIL-53 (Fe) based on Fe (III) octahedra and terephthalate

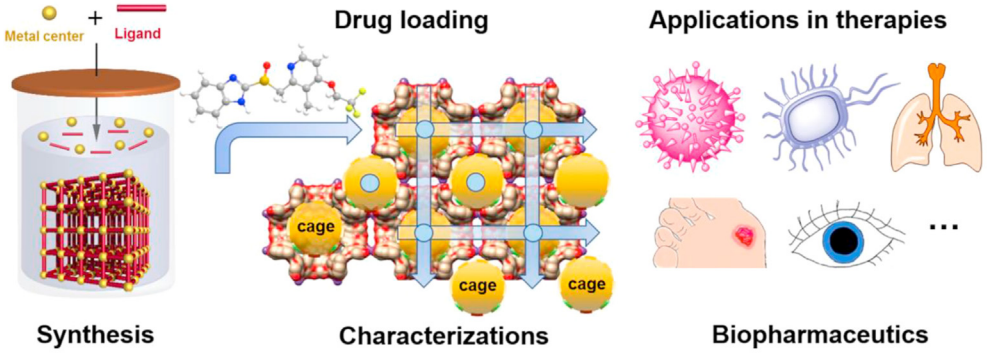

Figure 2 The graphical representation of MOFs in drug delivery.

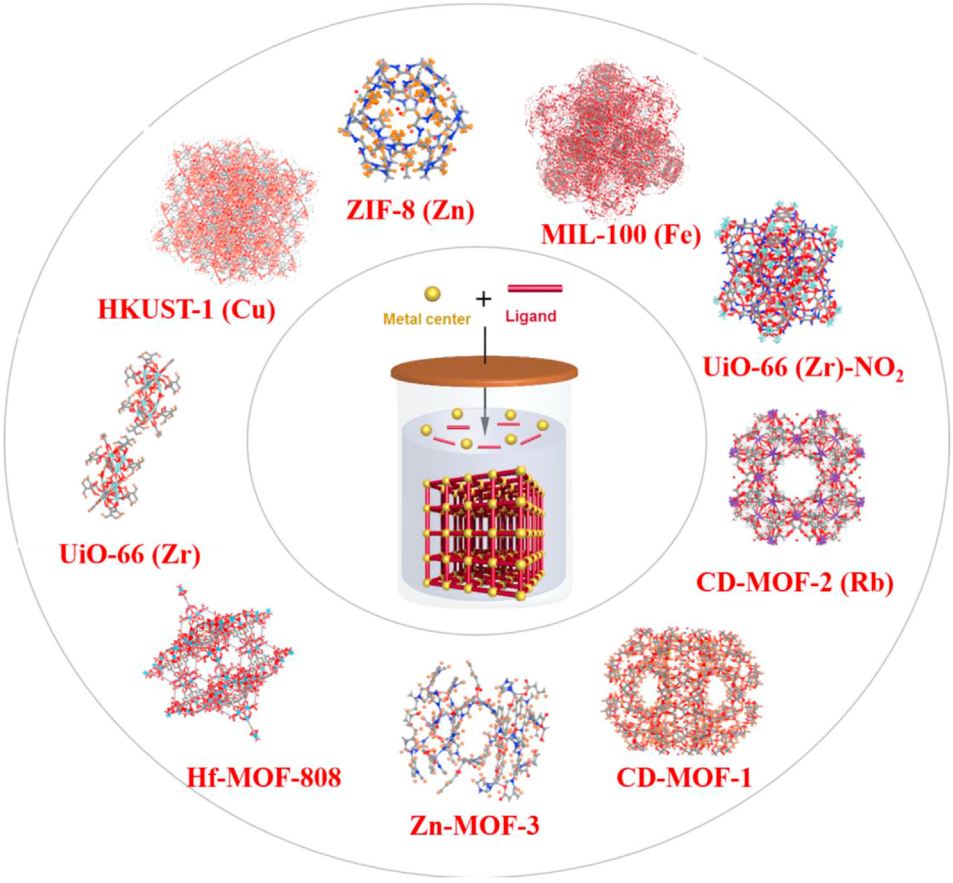

Figure 3 Representative MOFs crystal structures.

anions were synthesized soon after[63]. Because of low toxicity, configuration flexibility and biodegradability, they appeared as prospective candidates for drug delivery spontaneously. The first nanosized Fe-MOFs[57] were successfully utilized for loading anti-tumor or retroviral drugs and characterized *in vitro* and *in vivo* proving their degradability, biosafety and imaging properties. Owing to the flexibility of Fe-MOFs, Leng et al.[50] chose the non-toxic and biocompatible MIL-53 (Fe) to load anti-cancer drug oridonin, and the drug loading capacity could reach up to 56.25% (*w*/*w*), with a sustained release time more than 7 days. In addition, Fe-MOFs were researched for drug loading and magnetic/fluorescence imaging simultaneously[51]. The hollow Fe-MOFs-5-NH_2 with drug loading capacity as high as 35% (*w*/*w*) exhibited pH-controlled drug release property. Due to the existence of Fe (III) ions, the obtained MOFs displayed outstanding magnetic resonance imaging (MRI) performance. And after modification with folic acid (FA) and fluorescent reagent, targeted drug delivery and fluorescence imaging were realized.

Besides, MIL-100 (Fe) were used to co-encapsulate two active triphosphorylated nucleoside reverse transcriptase inhibitors, azidothymidine triphosphate and lamivudine triphosphate concomitantly for improving the efficacy of anti-human immunodeficiency virus (HIV)[62]. The azidothymidine triphosphate/lamivudine triphosphate ratio in MIL-100 (Fe) was equal to that among the currently commercialized triple therapy based on HIV prodrugs the overall drug loading was 9.6% (*w*/*w*). After freeze-drying, particles carried drugs could be preserved for 2 months, retaining similar physico-chemical properties.

2.1.3. *Zn-MOFs*

Zinc-based MOFs (Zn-MOFs) was developed by Rojas et al.[64] in 2016 as four zinc pyrazolate isoreticular MOFs ZnBDP_X composed of Zn (II) and functionalized organic linkers 1,4-bis(1*H*-pyrazol-4-yl)-2-X-benzene (H_2BDP_X; X = H, NO_2, NH_2, OH) for intravenous and oral administrations (<200 nm). This ZnBDP_X family presented tetragonal shape and square channels with a free pore aperture 11 Å. *In vitro* experiments demonstrated favorable structural and sticky durability in relevant biological conditions. Then, two kinds of antitumor drugs, namely, mitoxantrone and Ru (*p*-cymene) Cl_2 (1,3,5-triaza-7-phospaadamantane) (RAPTA-c) were enveloped within the pores of the ZnBDP_X, for the sake of investigating the effects of the different functional structure on the drug packaging and delivery.

For the purpose of increasing the aqueous stability and therapeutic activity of MOFs, Bag et al.[65] fabricated a sturdy bi-carboxylate ligand 4,4′-(9-H carbazole-3,6-diyl) dibenzoic acid (H_2CDDB) for constructing Zn-MOFs. Through the reaction of $Zn(NO_3)_2 \cdot 6H_2O$ and H_2CDDB in dimethylformamide (DMF), a porous MOF $[Zn_8(O)_2(CDDB)_6(DMF)_4(H_2O)]$ was fabricated, with an excellent loading ability of 53.3% (*w*/*w*) for 5-fluorouracil (5-FU). Furthermore, this MOF can keep stable up to three weeks in water and MTT assay against human hepatoblatoma cell line (HepG2) and human breast ductal carcinoma cell line (MDA-MB-435S) for 12 h incubation suggested the biosafety of this MOF.

Another Zn-MOFs named Zn-cpon-1 with 3D topological framework was prepared *via* employing ClO_4^- anion as template and 5-(4′-carboxyphenoxy) nicotinic acid (H_2cpon) as organic

Table 1 Classification of MOFs by metal ions and their molecular pore size for drug loading.

Genre	Naming	Organic linker	Pore size (Å)	Drug loading	Ref.
Fe-MOFs	MIL-89 (Fe)	Muconic acid	11	Ibuprofen, azidothymidine triphosphate	57
	MIL-88A (Fe)	Fumaric acid	6	Ibuprofen, cidofovir	57
	MIL-100 (Fe)	1,3,5-Benzenetricarboxylic acid	25, 29	Gemcitabine-monophosphate, topotecan, isoniazid, doxycycline, tetracycline, docetaxel, azidothymidine triphosphate, lamivudine triphosphate	57,62,68,70–72
	MIL-101_NH_2 (Fe)	Amino 1,4-benzenedicarboxylic acid	29, 34	Azidothymidine triphosphate, cidofovir, ethoxysuccinato-cisplatin	57,73
	MIL-53 (Fe)	1,4-Benzenedicarboxylic acid	8.6	Ibuprofen, oridonin	50,63
	MIL-101 (Fe)	2-Amino 1,4-benzenedicarboxylic acid	25−30	Ibuprofen, azidothymidine triphosphate	57
	MIL-127	3,3′,5,5′-Azobenzenetetracarboxylate	4	Caffeine	74
Zn-MOFs	Zn $(TATAT)_{2/3}$ $\cdot 3DMF \cdot H_2O$	TATAT = 5,5′,5″-(1,3,5-Triazine-2,4,6-triyl) Tris (azanediyl)triisophthalate	17, 21	5-Fluorouracil	75
	ZnBDP_X	1,4-Bis(1*H*-pyrazol-4-yl)-2-X-benzene (H_2BDP_X; X = H, NO_2, NH_2, OH)	11	Mitoxantrone	64
	Bio-MOFs	Azobenzene-4,4′-dicarboxylic acid and biphenyl-4,4′-dicarboxylic acid	8.3−26	Etilefrine hydrochloride	76
	$Zn_8(O)_2(CDDB)_6$ $(DMF)_4(H_2O)$	4,4′-(9-*H*-Carbazole-3,6-diyl) dibenzoic acid	28.1 × 23.17	5-Fluorouracil	65
	ZIF-8	2-Methylimidazolate	11.6	5-Fluorouracil, doxorubicin	77,78
Zr-MOFs	UiO-66	1,4-Benzenedicarboxylic acid	8	Caffeine, dichloroacetate	53,74
	UiO NMOFs	Amino-triphenyldicarboxylic acid	–	Cisplatin prodrug, siRNAs	79
	UiO-66-NH_2/NO_2	1,4-Benzenedicarboxylic acid	–	Ketoprofen	66
K-MOFs	CD-MOF-1	Cyclodextrins	4−17	Lansoprazole, azilsartan, budesonide, valsartan	20,67,68,80
Cu-MOFs	HKUST-1	1,3,5-Benzenetricarboxylic acid	14.67	Ibuprofen	69
	MOF-2/MOF-3	1,3,5-Benzenetricarboxylic acid and isophthalic acid	21.2/20.9	Ibuprofen, doxorubicin hydrochloride	69

–, not applicable.

linker[83]. This Zn-cpon-1 presenting a pH-responsive double stimulation behavior was an admirable drug delivery vessel, and the loading capacity of 5-FU in Zn-cpon-1 could reach 44.75% (*w*/*w*). Specially, the drug release behavior fitted well with the Weibull distribution model, which could be dual-irritated by pH and heating.

Zeolitic imidazolate frameworks (ZIFs), a sub-family of Zn-MOFs, connected by Zn(II) and imidazolate or its derivatives are widely used in DDSs[84–86]. Sun et al.[86] exploited ZIF-8 to pack the volatile and hydrophobic D-α-tocopherol succinate by one-pot process, and the drug loading ratio reached to 43.03% (*w*/*w*). The obtained D-α-tocopherol succinate@ZIF-8 would swiftly degrade in acidic environment on account of the pH-responsiveness of ZIF-8, resulting in on-demand drug release for tumor chemotherapy.

2.1.4. *Zr-MOFs*

Since the discovery of Zr_6 (μ_3-O)$_4$ (μ_3-OH)$_4$(BDC)$_6$ (UiO-66, UiO stands for the University of Oslo) with Zr_6(μ_3-O)$_4$ (μ_3-OH)$_4$(CO_2)$_{12}$ clusters and 1,4-benzene-dicarboxylate (BDC) by Cavka et al.[87] in 2008, zirconium-based MOFs (Zr-MOFs), mostly Zr(IV) carboxylates, have received increasing attentions. Owing to the exorbitant oxidation status of Zr(IV) in Zr-MOFs and intense coordination bonds between Zr(IV) and carboxylate ligands in the great majority of carboxylate-based Zr-MOFs, they own unparalleled stability, particularly hydrothermal stability[52]. Hence, a great many Zr-MOFs maintain stability in organic solvents and in water, even in acidic media. Moreover, Zr is considered suitable for biomedicine given its wide distribution in nature and low toxicity *in vivo* (oral lethal dose LD_{50} ~4.1 g/kg)[88].

Zr-MOFs are proverbially used in the realm of biomedicine. For example, Abánades et al.[53] found that synergistical delivery of dichloroacetate and 5-FU from Zr-MOFs to cancer cells can strengthen cytotoxicity *in vitro*. Adjusting the particle size, and most importantly, the surface chemistry can improve cytotoxicity by accelerating pit-mediated endocytosis and cytoplasmic drug delivery. In addition, Li et al.[66] introduced UiO-66 with $-NH_2$ and $-NO_2$ functional groups to study the difference of drug loading capacity and release behavior between them. Interestingly, results revealed that UiO-66–NH_2 had the maximal loading of ketoprofen and exhibited lowest release rate on account of the strong hydrogen bond ability and alkaline characteristics of $-NH_2$.

Another type of Zr-MOF, called Zr-fum, consists of an endogenous fumarate linker, and its structure is similar to UiO-66. Zr-fum could keep stable in aqueous solutions, with great potential as a DDS[89]. An anticancer molecule dichloroacetate was introduced into Zr-fum as a size-controlled modulator during fabrication process, with payloads of 20% (*w*/*w*)[90]. Contrast with UiO-66, Zr-fum shown enhanced biocompatibility in virtue of the endogenous fumarate linker, and transported the drug imitator calcein into HeLa cells more efficiently.

2.1.5. *K-MOFs*

Smaldone et al.[91] firstly reported a renewable, highly symmetric and porous, ultrahigh surface area, edible MOF, which was prepared only with edible ingredients: potassium (K) ions, alcohol (ethanol), and cyclodextrin, termed cyclodextrin-based metal-organic frameworks (CD-MOFs). Due to their inherently porous characteristics except for their water-soluble and non-toxic nature of CD-MOFs, it has extensive usages in the biomedical field[34,54], making this hotspot attracting a great deal of attentions and developing very rapidly. To date, by utilizing impregnation, grinding and co-crystallization, drugs have been successfully loaded into CD-MOFs[92]. For example, lansoprazole imbedded CD-MOFs were synthesized using an optimized co-crystallization method by the assemblage with γ-CD in the existence of K(I) ions with the drug loading up to 23.2% (*w*/*w*)[67]. Moreover, CD-MOFs can dramatically ameliorate the bioavailability and solubility of insoluble drugs. He et al.[20] reported that azilsartan (AZL) was loaded into CD-MOFs, and the bioavailability of AZL in Sprague−Dawley (SD) rats was increased by 9.7 times. Besides, compared with pure drugs, the apparent solubility of AZL/CD-MOF was increased by 340 times. Moreover, it is noteworthy that CD-MOFs have been proverbially used in oral, intravenous and even pulmonary DDSs[68,93,94].

2.1.6. *Cu-MOFs*

Copper-based MOFs (Cu-MOFs) have been explored as viable hosts for bio-oriented guest@MOF composite systems owing to the high accessibility of their coordinatively unsaturated metal sites in the structures, creating strong binding sites for guest cargos[95–97]. Sun et al.[69] devised mixed ligands Cu-MOFs, MOF-2 and MOF-3 for the delivery of IBU and doxorubicin hydrochloride (DOX), which were prepared by hydro-thermal method with reasonable alteration in the ratio of two ligands (BTC and isophthalic acid). They were nontoxic towards human normal cells, human embryonic kidney 293A cells (HEK 293A) and could load drug. Drug loading test showed that mixed ligand MOFs displayed better capacity in DDSs than single ligand MOFs, and MOF-2 with 40% BTC and 60% isophthalic acid had the best performance in drug delivery capability. By using the characteristics of amino-functionalized Cu-MOFs, a smartphone-based strategy for visual detection of alkaline phosphatase was designed by Hou et al.[98] which possessed oxidase mimic and fluorescence virtue. This fluorescent-based technique could be used for detecting alkaline phosphatase in serum samples, which opened up a wild prospect for the diagnosis of other biomarkers in clinical serum samples on the basis of alkaline phosphatase mediated enzyme-linked immunosorbent assay. Moreover, Cu-MOFs could be utilized for antibacterial therapy. For example, Cu-MOFs composed of glutaric acid and pyridine derivative performed superb antibacterial activities against different kinds of bacteria with very low minimal bactericidal concentration[99].

2.2. *Classification by organic ligands*

One of the primary merits of the MOFs is their variability in terms of compositions of both constitutive metals and organic linkers. In particular, the organic linkers perform a main part in the 3D supramolecular organization of the MOFs as well as their physicochemical properties. Carboxylates and other organic anions, including phosphonate, sulfonate, and heterocyclic compounds are the most common organic linkers. Actually, it has been highlighted that the choice of possible linkers is extremely wide[100,101]. Among them, MOFs composed of carboxylate ligands account for nearly half of all synthesized materials. In the case of MOFs for DDSs, the choice of the linker not only has a determinant part in the physical and chemical natures of the resulting MOFs, but also on their stability in biological media, degradability, bioavailability and toxicity.

Linker choice results in unique properties and MOF applications. For example, polycarboxylic acid or imidazole-based linkers are widely considered for MOFs preparation in reason of their relatively low toxicities, mainly on account of their strong polarity and metabolic clearance in physiological conditions[48]. Homologous iron carboxylates can be synthesized bio-safely[102]. Similarly, the drug payloads in MOFs and release patterns are affected by different organic linkers and functional groups[48,57,103]. Interestingly, active molecules were used as linkers to synthesize so-called BioMOFs. This strategy not only confers high drug payloads due to intrinsic self-assembly of active molecules, but also allows good biocompatibilities.

Indeed, a variety of biomolecules, including amino acid, nucleobases or sugars readily or naturally available can be used as building blocks[104]. As far as we know, Gramaccioli et al.[105] synthesized the first amino acid-based biocompatible 3D MOFs in 1966, by mixing Zn(II) and glutamate, an important neurotransmitter. However, the biomedical applications of BioMOFs have not been fully explored mainly because of the lack of studies to the stabilities in biological media of these systems. Only few examples report BioMOFs that can adsorb and release drugs[106]. Considering that many therapeutic molecules have multiple complex groups in their structures, there are many reports on the use of active ingredients to construct BioMOF. The first example of a drug-based BioMOF study was reported in 2,010,[107], which was composed of endogenous iron and therapeutically active vitamin B_3, with pellagra treatment, vasodilation and anti-lipid properties. Similarly, olsalazine, a generally employed agent in the therapy of ulcerative colitis and other gastrointestinal disorders, could be used as a ligand for fabrication of a series of new mesoporous MOFs, and exhibited the same coordinating functionality as the dihydroxyterephthalic acid used in the composite of the CPO-27/MOF-74 family[108]. Here, MOFs are catalogued according to their organic linkers, as shown in Table 2[43,57,67,69,74–77,82,107,109].

3. Synthesis of MOFs

3.1. Synthesis methods

Several methods have been exploited to synthesize all kinds of MOFs[110,111] (Fig. 4) for drug delivery, such as non-solvothermal synthesis, including direct precipitation and vapor diffusion synthesis[91], and solvothermal methods, microwave-assisted solvothermal synthesis[112,113], synthesis by reverse-phase microemulsions[114–116], electrochemical synthesis[117], dry-gel conversion methods[118], preparation using a microfluidics device[119], mechanochemical[120–122] or sonochemical synthesis[123], step-by-step synthesis[124] and high-throughput synthesis methods[125]. The advantages and disadvantages of various synthesis methods are summarized in Table 3.

3.1.1. Conventional synthesis

Conventional synthesis of MOF usually refers to reactions performed by heating at different temperatures, which is one of the most important parameters in MOFs synthesis. According to the temperature used, conventional synthesis is normally distinguished as nonsolvothermal synthesis (temperature below or at the boiling point was used) and solvothermal (where reactions taking place above the boiling point).

3.1.1.1. Nonsolvothermal synthesis. It can be further categorized as the ones taking place at room temperature or elevated temperatures. For example, precipitation reactions followed by recrystallization or vapor diffusion synthesis were reported. Some MOFs have been synthesized *via* direct precipitation method by simply mixing the starting materials at room temperature, such as HKUST-1 (HKUST stands for Hong Kong University of Science and Technology), MOF-5, MOF-177, MOF-74, or ZIF-8[126,127]. Some of these MOFs, such as ZIF-8, exhibited fine chemical and thermal stabilities.

The vapor diffusion method is the earliest synthetic method for CD-MOFs synthesis[91]. A variety of γ-CD-MOFs were synthesized combining γ-CD and K^+, Rb^+, Cs^+, Na^+ or Sr^+ by Stoddart's group[91,128]. Higher reaction temperature is also required in some CD-MOF synthesis to obtain good crystallinity and high yields. It was reported that the reaction time of γ-CD-MOFs synthesis was significantly reduced from days to 6 h[129] by raising the temperature from room temperature to 50 °C.

3.1.1.2. Solvothermal synthesis. A β-CD-MOF was synthesized by heating a mixture of methanol and water containing β-CD and sodium oxalate ($Na_2C_2O_4$) at 160 °C for 3 days[130]. Sha et al.[131] obtained a novel α-CD-MOF with a mixture of α-CD and KOH after heating at 160 °C for 4 days. MOF-5 was synthesized at 105 °C to have much higher yield than the ones obtained at room temperature[132].

Nonsolvothermal and solvothermal syntheses are limited to obtain MOFs in the laboratory. It is important to develop new

Table 2 Classification of MOFs by organic linkers.

Family of linkers	Organic linker	Drug loading	Ref.
Carboxylate ligands	1,3,5-Benzenetricarboxylate acid	Doxorubicin	69
	4,4′,4″-Benzene-1,3,5-triyl-tribenzoate	Ibuprofen	82
	5,5′,5″-(1,3,5-Triazine-2,4,6-triyl) tris(azanediyl)triisophthalate	5-Fluorouracil	75
	Biphenyl-4,4′-dicarboxylic acid	Hydrochloride	76
	Azobenzene-4,4′-dicarboxylic acid	Etilefrine	76
Pyrazolate ligands	Bis (pyrazolate) ligand (1,4-bis(1*H*-pyrazol-4-yl)-2-X-benzene (H_2BDP_X; X = H, NO_2, NH_2, OH)	Mitoxantrone	74
Imidazolate	2-Methylimidazolate	5-Fluorouracil	77
Polysaccharide	Cyclodextrin	Lansoprazole	67
	Other polysaccharides (agar, dextran)	Procainamide	43
BioMOFs	Nicotinic acid	Vitamin B_3	107
	Succinic acid	Cisplatin	109
	Fumarate ligands	Doxorubicin	57

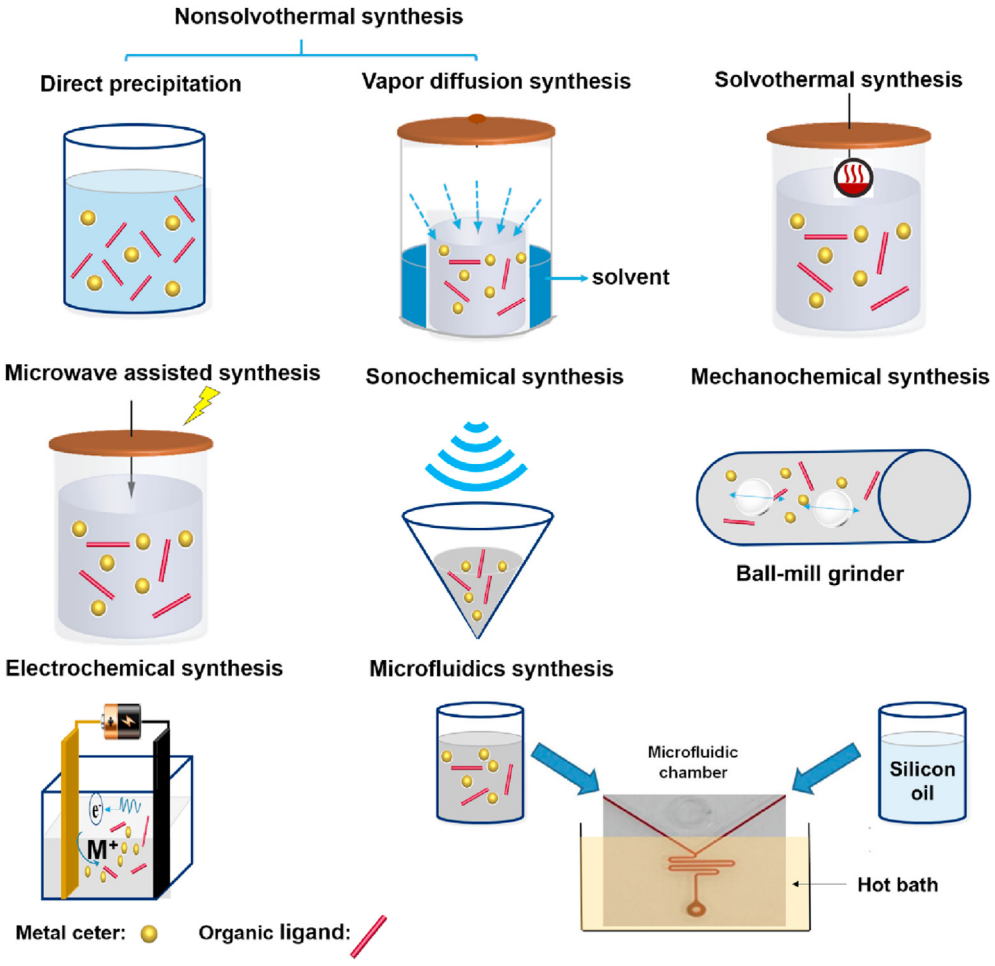

Figure 4 Overview of MOFs synthesis methods.

Table 3 Synthesis methods of MOFs.

Method	Advantage	Disadvantage
Nonsolvothermal synthesis	• Under ambient pressure • Simplifier synthetic requirements	• Long reaction time • Low yield • Large particle size
Solvothermal synthesis	• Higher yield than nonsolvothermal synthesis • Smaller and more homogeneous crystals than non-solvothermal synthesis	• Long reaction time
Microwave assisted solvothermal synthesis	• Environment-friendly rapid synthesis • Morphology and size control • High yield • Good monodispersity	• Specific device
Sonochemical synthesis	• Easy and environment-friendly rapid synthesis • Good monodispersity	• Further sonication led to decomposition of the crystals • Low yield
Mechanochemical synthesis	• Solvent-free • Low-cost and high-throughput production	• Energy and materials consumption • Potential structure change
Electrochemical synthesis	• Prepare a higher solids content	• Specific device

synthetic routes towards MOFs production at industrial scale. For CD-MOFs, Ding et al.[133] reported a novel production strategy based on crystal transformation to industrialization, which helped the productivity yield increase dozen times in comparison of reported synthesis methods.

3.1.2. *Microwave assisted solvothermal synthesis*

It has been widely applied for MOFs synthesis under microwave assisted hydrothermal conditions, due to many potential advantages such as environment-friendly rapid synthesis, high yield[134], and morphology[135] and size control[136]. The first reported MOFs obtained by microwave assisted solvothermal synthesis was MIL-100[137]. MIL-100 (Cr) synthesized at 220 °C in 4 h by microwave was reported to have similar physicochemical properties to the ones synthesized at 220 °C for 4 days using conventional heating. MIL-100 (Fe) synthesized at 130 °C for 6 min was shown to be well crystalized nanoparticles (NPs) with narrow particle size distribution, faceted morphology, and high porosity[138].

Among different MOF preparation methods, microwave assisted synthesis allowed to achieve the best results in terms of high yields, small sizes (<100 nm) and monodispersed NPs[139]. "Green" synthesis allowed produced fluorine-free MIL-100 (Fe) within minutes opening the way to synthesize large-scale nanoMOFs for biomedical applications[138]. Microwave assisted solvothermal synthesis were also applied recently to synthesize Hf, Zr, Zn and Ca based nanoMOFs for drug delivery[140–143].

Liu et al.[144] obtained γ-CD-MOFs within 10 min using the microwave-assisted method. By optimizing the reaction temperature, time, and solvent ratios, both micro- and nanometer-sized crystals were prepared. In addition, it was found to be a method of choice for fast crystallization of HKUST-1[145], MIL-53 (Fe)[73], MIL-101-NH2 (Fe)[136], ZIF-8[146] and MIL-100[147].

3.1.3. *Sonochemical synthesis*

Sonochemical method is an easy and environmentally friendly pathway for rapid synthesis of MOFs. When high-energy ultrasound interacts with liquids, bubbles form and collapse in the solution, which is the so-called acoustic cavitation, leading to the production of very high local temperatures up to 5000 K and the pressures could reach 1000 bar[148]. This contributes to terrifically fast heating and cooling rates (>1010 K/s), favorable to fine crystal growth[110]. HKUST-1 was obtained using a mixture of DMF/ethanol/water in an ultrasonic bath[149]. The nanocrystalline NPs (10−40 nm) formed after only 5 min sonication. Increasing the sonication time resulted in larger crystals (50−200 nm), but further sonication led to the decomposition of the crystals. Sonochemical method was also employed to prepare well crystallized MOF-5 (5−25 μm)[150], MOF-74 (Mn) (0.6 μm)[151], PCN-6 (4.5−6.0 μm), IRMOF-9 (5−20 μm), PCN-6 (1.5−2.0 μm) and IRMOF-10 (5−20 μm)[152]. Ultrasound led to very tiny monodisperse MIL 88A nanoMOFs[139], however, the yields were low.

3.1.4. *Mechanochemical synthesis*

Mechanochemistry, known as using mechanical force to induce and conduct chemical transformations, demonstrates the most evident benefit of providing a solvent-free or very small amounts of solvents synthetic path compared to conventional synthesis based on solution or microwave. Additionally, mechanochemical method has been affirmed to be a practical and environmentally friendly way to achieve high-throughput and low-cost production of MOFs. Different research groups recently reported that mechanochemical synthesis by planetary mill possessed substantial improvements in energy efficiency[153,154]. For MOFs mechanosynthesis, the oxide-based chemistry at room temperature with low-solvent and low-energy routes developed by Friščić et al.[154] could avoid large energy and materials expenses. This facile method was also reported to the irreversible ball milling-[155], pressure-[156] and thermal-induced[157] amorphous ZIFs synthesis.

3.1.5. *Other methods*

Other than the methods mentioned above, electrochemical synthesis was first reported in 2005 using metal ions continuously supplied through anodic dissolution, which reacted with the dissolved linker molecules[158]. This route is possible to prepare a higher solids content compared with batch reactions[110]. A variety of MOFs were synthesized by this method, including HKUST-1[158], MIL-53 (Al), MIL-100 (Al), ZIF-8, and MIL-53-NH2 (Al)[159]. In addition, dry-gel conversion methods[118], and preparation using a microfluidics device[119] were also reported.

3.2. *Particle size and shape control*

Control of particle size and shape is of importance for biomedical applications, because the particle size dictates the interactions of the particles with cells, organs and biomolecules. It also plays a major role in several chemical and physical properties including rheology, surface reactivity towards biomolecules, external surface properties, packing, stability, etc.[48,160–164], which are essential for drug loading capacity, surface modification for targeting and the administration routes. Consequently, it is very important to prepare homogeneous, monodispersed, and stable NPs. Whatever the synthesis method is, it remains challenging to control the crystallization process with controlled shapes and monodispersed size distribution. Primary strategies to actualize this goal composed of controlling composition and process parameters, adding additives, applying nanoscale templates, and downsizing the particles employing mechanical or mechanochemical methods.

3.2.1. *Compositional and process parameters*

Compositional parameters include the nature of solvents, pH, metal source, reactant concentration and molar ratios. As an example, the fabrication of aluminium-based MOFs utilizing trimesic acid as an organic liker is dependent on the pH (Fig. 5A)[165]. The pH of the reactant [$Al(NO_3)_3 \cdot 9H_2O$, BTC and cetyltrimethyl ammonium bromide (CTAB)] was reported as 2.1, where MIL-100 formed after heating at 120 °C for 12 h using a mixture of ethanol and water as solvent. While keeping the reactant composition, MIL-100 started to form at higher pH values (2.3−2.5). At pH 2.6, a mixture of both MIL-96 and MIL-100 was produced, with the relative amount of the former growing when the pH was 2.7. When water alone was used as solvent, MOFs were obtained at different pH values: MIL-110 at acidic pH (both the range of 0−0.3, and 4), MIL-100 in a narrow acidic pH range (0.5−0.7), MIL-96 at pH 1−3. The topologies of the particles were significantly different with or without ethanol.

Process parameters consist of temperature, heating source, reaction time, and pressure. Generally, both microwave-assisted and sonochemical synthesis produce smaller and more homogeneous crystals than conventional synthesis. For instance, various

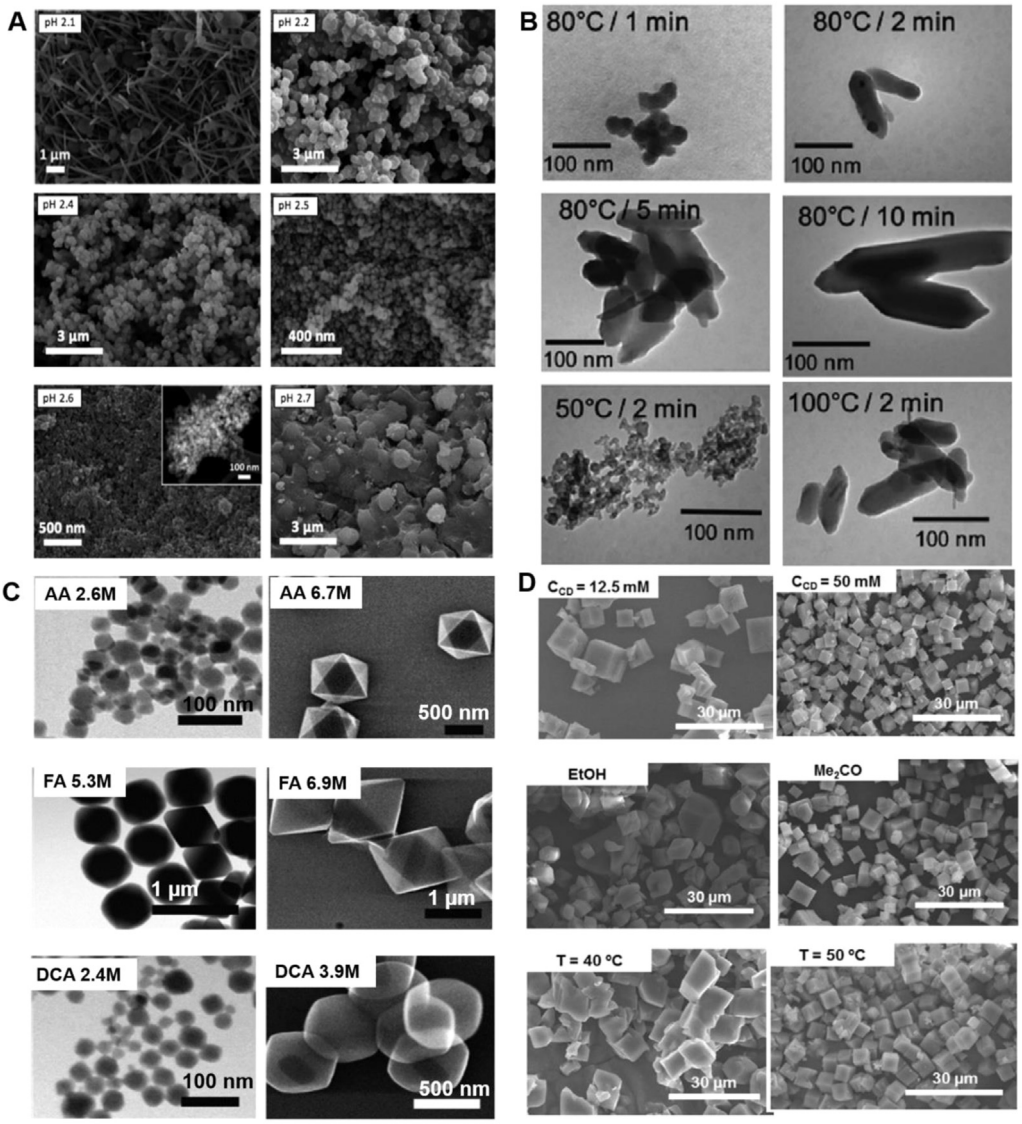

Figure 5 SEM images of MOFs with different sizes and morphologies synthesized by synthetic parameters optimization (A) pH (B) reaction temperature and time (C) role of modulators (D) compositional and process parameters (A) Different aluminium trimesate MOFs synthesized at different pH: the particles obtained were MIL-110 (at pH of 2.1), MIL-100 (pH 2.2), MIL-100 (pH 2.4), mixture of MIL-100 and MIL-110 (pH 2.5) and mixture of MIL-100 and MIL-96 (pH of 2.6 and 2.7). Inset: TEM image acquired for the MIL-100 sample obtained at pH 2.6. Reprinted with permission from Ref. 165. Copyright © 2015, The Royal Society of Chemistry (B) Synthesis of MIL-88 by microwave assisted hydrothermal methods at different heating temperature and time. Reprinted with permission from Ref. 139. Copyright © 2011, The Royal Society of Chemistry (C) Role of modulators on the UiO-66 synthesis (AA: acetic acid; FA: formic acid; DCA: dichloroacetic acid. Reprinted with permission from Ref. 167. Copyright © 2017, American Chemical Society (D) Synthesis of CD-MOFs at different CD concentrations, using different solvents, and at different temperature. Reprinted with permission from Ref. 129. Copyright © 2016 Elsevier.

methods[139] were used to synthesize nano-MIL-88A, including conventional synthesis, microwave-assisted hydrothermal synthesis, and sonochemical method. Optimized reaction conditions yielded crystals with varied size using different methods: around 250 nm by conventional hydrothermal synthesis; 100 nm by sonochemical synthesis; smaller than 100 nm with good monodispersity for microwave assisted synthesis. Even using the same synthesis methods, the reaction temperature and time played important roles on both the crystal size and shape (Fig. 5B)[139]. Similarly, the size of $Zn_3(BTC)_2 \cdot 12H_2O$ MOFs decreased from 900 nm to less than 100 nm by reducing the reaction time from 90 to 10 min[166]. Among many influencing factors, solvents, pH, temperature and reaction time are four crucial parameters mostly reported in terms of crystal size and shape.

3.2.2. *Additives*

Modulators are the linkers that can coordinate with the metal ions, therefore competing with the organic linkers during crystal growth. Therefore, the diameters and morphology of the crystals are highly affected by modulators. Modulators, *e.g.*, acetic acid, formic acid, dichloroacetic acid, and trifluoroacetic acid, were systematically investigated in the synthesis of UiO-66 MOFs (Fig. 5C)[167], showing a size difference from 20 nm to 1 µm with various modulators. In addition, other molecules such as amino acid[168],

polyoxometalates[169], benzoic acid[170], polyacids[171] and water[172] have been used. Recently, multivariate modulation of the UiO-66 for defect-controlled combination anticancer drug delivery was reported[173], which was developed as a new strategy to incorporate up to three drugs in UiO-66 nanoMOFs by defect-loading.

Blocking agents or inhibiting additives, such as acetic acid, hydroxybenzoic acid and pyridine, have been shown to reduce the crystal growth. For example, the diameter of MIL-89 (Fe) was decreased to 30 nm by adding acetate ions in the synthesis process[174]. Luminescent terbium benzenedicarboxylate nanoMOFs with sizes of only 4−5 nm formed by adaption of a previous method[175] utilizing a poly (vinylpyrrolidone) as inhibitors[176]. Besides, pyridine was used as inhibitors for synthetizing indium terephthalate MOF particles[177], which was hexagonal rods of around 16.3 μm length and 1.75 μm width. After adding pyridine, the width and length were reduced to 0.43 and 0.97 μm, respectively. Not only the size but the morphology of the particles would be influenced by the inhibitor.

3.2.3. *Nanoscale templates*

The template approach is also a promising strategy to synthesize MOFs with controlled size distribution. For instance, MOF-66 (Gd) NPs formed in reverse microemulsions obtained from a mixture of 1-hexanol, isooctane, CTAB, and water. The size and shape of nanoscale templates were easily controlled by altering the constituents of the system[178,179].

3.2.4. *Downsizing*

The size of nano-MOFs could also be controlled by mechanochemical synthesis as reported in 2006[121]. It induced a mechanical disruption of intramolecular bonds leading to a chemical transformation. Advantageously, this reaction occurred at room temperature[180] under solvent-free conditions[120] in the case of HKUST-1 NPs. Mechanochemical synthesis of nano-MOFs was also reviewed[181].

In some cases, strategies can be combined to synthesize MOFs with controlled size distribution and morphologies. For instance, intense efforts have been made to prepare γ-CD-MOFs with narrow size distributions. Using conventional vapor diffusion method, only large crystals of γ-CD-MOFs were obtained in the range of 200−400 μm. After addition of CTAB[182] to decrease the crystal growth, CD-MOFs were formed with uniform size of around 1−10 μm. Interestingly, Furukawa et al.[182] successfully achieved to obtain nano γ-CD-MOFs (200−300 nm) by adding both CTAB and methanol. However, it still took more than one day for the synthesis. Liu et al.[129] shortened the reaction time to 6 h using increased reaction temperature of 50 °C. The size of the resulting CD-MOFs was well controlled by addition of CTAB and/or methanol (about 6 μm with CTAB and around 600 nm with CTAB and methanol, Fig. 5D)[129]. However, the disadvantage of CTAB lies in its potential toxicity and it is difficult to be removed from the MOF particles. Recently, a seed-mediated method was employed to produce this CD-MOF using short-chain starch NPs instead of CTAB to have crystals with monodispersed size about 2 μm[183]. However, this method was not able to scale-down the particles to the nano-regime. Finally, the most efficient method was reported as microwave assisted method[144]. CD-MOF particles were obtained in 10 min, with monodispersed size distribution for different sizes (200 nm−300 μm) by adjusting the compositional and process parameters.

3.3. *Physicochemical characterizations of MOFs*

The synthesized MOFs need to be fully characterized with a set of complementary techniques to determine their physicochemical properties, including MOFs' crystallinity, morphology, porosity, size distribution, colloidal stability, degradation patterns, drug loading capacity and drug release patterns. Various characterization techniques of MOFs are summarized in Table 4.

4. Drug loading and characterizations

4.1. *Methods for drug loading*

MOFs possess the unique characteristics of highly ordered structure and large surface area. Drugs can be embedded on the outer surface, or encapsulated into inter pores *via* diverse loading methods. Two kinds of widely applied loading strategies, namely, one-step method and two-step method are summarized here (Fig. 6).

4.1.1. *One-step*

One-step method is the most convenient loading strategy to incorporate drugs into MOFs, which is achieved either during the MOFs synthesis or by directly using drug molecules as MOF linkers.

4.1.1.1. Co-crystallization. It is widely used for drug loading in laboratory research or manufacturing. Under mild reaction conditions, drug could co-crystallize with MOFs and form a 3D supramolecular structure integrating the active molecules. More importantly, co-crystallization does not alter the physicochemical properties of the drug, which can be advantageously exploited to improve the loading efficiency and enhance the drugs solubility. As an example, poorly soluble drugs, such as IBU[184], lansoprazole[67], leflunomide[93] and methotrexate (MTX)[185] were successfully embedded in γ-CD-MOFs using the co-crystallization method and the drug loading was equal to or higher than that by an impregnation method.

4.1.1.2. One-pot method. It is an economic method for loading drug during MOFs synthesis, which not only shortens reaction time and reduces the waste, but also overcomes the limitations of MOFs' small pore window. In this method, drug molecules could be loaded in MOFs matrix by insertion inside MOFs crystal or coating onto the surface. In addition, the pore sizes of some MOFs are too small for the drugs to penetrate inside the crystalline matrix. For example, the diameter of the pore cavity of ZIF-8 is 11.6 Å, many bulky molecules including high-molecular weight drugs, nucleic acid or proteins cannot diffuse into the MOFs' porosity. Nevertheless, successful encapsulations had been achieved for drugs as DOX[84], camptothecin[186], and 3-methyladenine[187] *via* mixing with reactants through one-pot method. Similarly, 5-FU[188] also could be loaded on zinc glutamate MOF coated cotton fabric using one-pot synthesis method. Besides, enzymes embedded in MOFs by this method were prevented from degradation. As a *in situ* loading strategy, organic linkers and inorganic metal ions simultaneously contributed to the efficient incorporation of the enzyme in one-pot method. The protein molecules induced the formation of MOFs and facilitated their crystallization. Cytochrome *c* (Cyt *c*) was directly immobilized in ZIF-8 utilizing one-pot method[189]. The peroxidase activity of Cyt *c*@ZIF-8 was 10-fold better than free enzyme. Similarly, Wu et al.[190] also designed a ZIF-8 based multi-enzymatic system

Table 4 MOF characterization techniques.

Technique	Property
Powder/single-crystal X-ray diffraction (XRD)	Crystallinity: crystal structure, crystalline parameters
Small- and wide-angle scattering (SAXS/WAXS)	Monitor the crystallization of MOFs
X-ray photoelectron spectroscopy (XPS)	Surface characterization: electronic structure, oxidation states, elemental composition, coating material binding
X-ray absorption spectroscopy (XAS)	Element-specifical investigation of chemical state and interatomic distances of species
Energy dispersive X-ray spectroscopy/spectroscopy (EDX/EDS)	Quantitatively determine elemental composition of MOFs
Porosimetry	Porosity: BET surface area and deep insight of pore size, volume and distribution of MOFs
Scanning electron microscopy (SEM)	Size and morphology
Transmission electron microscopy (TEM)	Size and morphology
Scanning transmission electron microscope (STEM)	Combined with high-angle annular dark field (HAADF) detector and EDX for investigation of morphology, elemental composition, and crystal structure
Raman microscopy	Homogeneity on composition and morphology
Atomic force microscope (AFM)	Size and shape in 3D mode, evaluate surface modification, localization of MOFs in cells or other matrices
Dynamic light scattering (DLS)	Hydrodynamic diameter
Nanoparticle tracking analysis (NTA)	Hydrodynamic diameter, particle concentration, individual particle tracking
Zeta potential	Surface charge
Fourier-transform infrared spectroscopy (FT-IR)	MOF degradation, drug loading, surface modification, structural defects
Ultrafast 2D IR spectroscopy	Structural dynamics inside a functionalized MOF
Nuclear magnetic resonance spectroscopy (NMR)	Interaction between the drug and MOF crystals, the precise drug localization, as well as catechizing the metal center and probing the linker molecules
Mössbauer spectroscopy	Investigation of chemical environment of Mössbauer nuclei (such as Fe atoms) in the sample, including the oxidation state, surface spins, and symmetry, etc.
Ultraviolet−visible spectroscopy (UV−Vis)	Optical properties, size, concentration
Inductively coupled plasma mass spectrometry (ICP-MS)	Elemental composition, intracellular MOFs quantification
Thermogravimetric analysis (TGA)	Thermal decomposition of MOFs

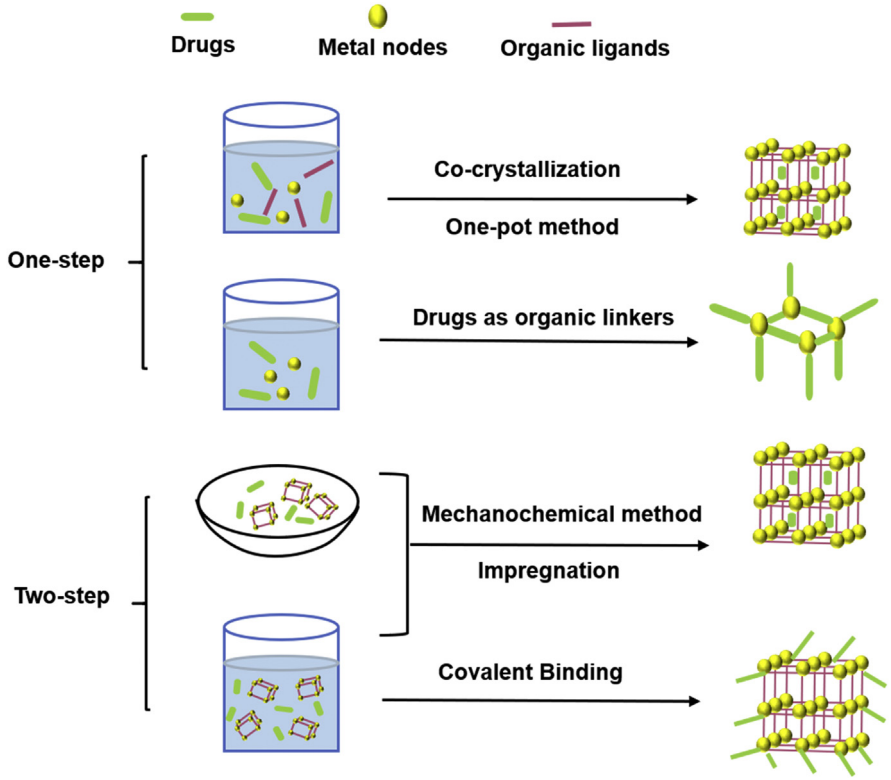

Figure 6 Two kinds of drug-loading strategies for MOFs.

utilizing the same approach. Glucose oxidase (GOx) and horseradish peroxidase (HRP) were mixed with the zinc nitrate solution to prepare GOx&HRP@ZIF-8. Catalytic tests demonstrated that GOx&HRP@ZIF-8 composite displayed better catalytic efficiency than GOx@ZIF-8 or HRP@ZIF-8.

4.1.1.3. Drugs as organic linkers for MOFs. In addition to MOFs as reservoirs, drug or their prodrug can be as organic linkers to form MOFs, by coordination between the available coordinated functions of drugs and specific metal nodes. Employing biologically-acceptable ions Ca (II) and Mg (II) as metal ions and anti-osteoporosis bisphosphonate model drugs (*e.g.*, etidronate, pamidronate, alendronate and neridronate) as organic linkers, a phosphonate MOF-based DDS was prepared that exhibited variable release rate pattern[191].

4.1.2. Two-step

The two-step strategy immerses loading drugs with the MOFs in a drug-solution or in grinding MOFs together with the drugs.

4.1.2.1. Impregnation. The MOFs were immersed in drug solution to allow drug molecules to diffuse into MOFs through the porosity. Usually, interactions between drugs and MOFs include van der Waals interaction, π-π interaction and hydrogen bonding. The pore size, window dimension, chemical composition and flexibility of MOFs were key parameters to ensure a successful drug incorporation[57]. MOFs were applied for caffeine loading *via* impregnation[192]. Similarly, Javanbakht et al.[193] immersed porous Cu-MOFs into an IBU solution to embed the drug into the 2D channels. The supercritical carbon dioxide ($scCO_2$) assisted impregnation method could introduce poor-soluble drug honokiol into the CD-MOFs cavity with a high drug loading around 40.78% (*w*/*w*)[194]. In addition, this strategy reached almost 100% efficiency in the case of phosphate drug owing to the intense coordination between phosphates groups and Fe ions. Gemcitabine monophosphate (GEM) was encapsulated into MIL-100(Fe) with satisfied drug loading capacity of 30% (*w*/*w*) and exceptional encapsulation efficacy rates of >98%[195].

4.1.2.2. Mechanochemical method. It is a solvent-free, green, and economical drug loading technique, mechanically mixing drug powder and MOFs together in solid status. Drugs such as 5-FU, caffeine, p-aminobenzoic acid and benzocaine were caged into MOFs by grinding method, reaching high drug loading amount and sustained release[196].

4.1.2.3. Covalent binding. Although the appeal method incorporates various drugs into MOFs, the relatively weak interaction force between the cargos and MOFs usually leads to slow leaching problems of the drugs. Thus, it is necessary to adopt a solution of covalent bonding and immobilization. Generally, the surface of MOFs presents various active groups (*e.g.*, carboxyl, amino, and hydroxyl) which can be used to mold covalent bond with reactive groups of active drugs[197]. Morris et al.[198] exhibited the DNA-MOF conjugate, which was formed by a click reaction between azide-functionalized UiO-66 and dibenzylcyclooctyne-functionalized DNA. The DNA@UiO-66 conjugate was reported to have increased colloidal stability and improved cellular transfection capabilities in comparison to nonfunctionalized UiO-66. Additionally, enzymes also can be successfully immobilized onto MOFs by covalent binding. Cao et al.[199] reported efficiently immobilization of soybean epoxide hydrolase onto the prepared surface of UiO-66-NH_2 MOF *via* cross-linking approach. Compared with free soybean epoxide hydrolase, the synthesized soybean epoxide hydrolase@UiO-66-NH_2 conjugates manifested high loading capacity, excellent enzyme−substrate binding affinity and enhanced catalytic efficiency.

4.2. Characterizations of drug-loaded MOFs

Drug loading efficiency following in Eq. (1) and encapsulation efficiency following in Eq. (2) are significant factors that are closely related to the pore size and surface property of MOFs. The drug can be physically adsorbed on the surface of the MOFs by the impregnation method when the size of the loaded drug is larger than the pore diameter of the MOFs. Typically, applying the one-step strategy can effectively encapsulate the large sized drugs to the inside of the MOFs for improving the drug loading and encapsulation efficiency[84]. In addition, changing the structure of MOFs may favor a higher drug loading level *via* improving the interactions (hydrogen bonding or van der Waals) between drugs and MOFs[65]. The determination of drug loading and encapsulation efficiency mostly adopts direct or indirect methods, that is, dissolving drug loaded MOFs in a solvent to determine the drug content, and calculating the loaded drug content by measuring the content of unloaded drugs supernatant. Moreover, the determination of the content of adsorbed drugs in MOFs also can be indirectly analyzed by TGA, since a mass loss step within a certain temperature range[200].

$$\text{Loading efficiency}\ (\%) = \frac{\text{Mass of loaded drug}}{\text{Mass of drug loaded MOFs}} \times 100 \quad (1)$$

$$\text{Encapsulation efficiency}\ (\%) = \frac{\text{Mass of loaded drug}}{\text{Mass of total drug}} \times 100 \quad (2)$$

Various strategies were developed to characterize drug@MOFs particle. The morphology of drug@MOFs was usually studied by SEM and TEM. Zeta potential might indicate the drug location in MOF, while the crystalline structure of drug@MOFs can be identified by Powder XRD for the crystallinity might be altered by drug loading. The reduced nitrogen adsorption of drug@MOFs was used to verify the occupation by drug in the pore and cavity of the MOFs. Lastly, adsorption isotherm was employed to evaluate loading capabilities of MOFs, and TGA to give information of drug loading and stability in the MOF matrix.

In addition, the state and interaction between drugs and MOFs may help to deepen knowledge of drug loading mechanism. DSC measurement for the melting point of the binary system of MOFs and drug was applied to explore the form of the cargo in MOFs and evaluate the interaction between them. FTIR spectroscopy was applied to investigate the interaction between host and guest. Differences in absorption frequency and chemical bond type were strong evidence to prove the relationship between drug and MOFs. The host/drug interactions were indicated by ultrafast magic-angle spinning (MAS) and NMR. Dielectric relaxation spectroscopy (DRS) was used to understand the molecular mobility of MOFs skeleton caused by the presence of drugs. Molecular simulation was helpful to analyze the interaction between drug and carrier, and the drug loading mechanism. For example, molecular

simulation was applied to investigate how γ-CD-MOFs enhanced the solubility of insoluble drugs and a dual-molecule loading mechanism of complexation and clusterization was established[20].

5. Applications of MOFs in therapy and drug delivery

5.1. MOF systems for disease therapies

On account of their advantageous features in drug delivery, MOFs have been explored as favorable DDSs for plenty of diseases, including infections, lung disease, diabetes mellitus, ocular disease and tumors, which have made prominent advance in the past few years.

5.1.1. Anti-bacterial applications

Smart delivery of antibacterial agent is of great interest in light of the bacteria resistance and bacterial infection in injury and surgical process. Inorganic carriers[201] and organic polymer carriers[202] have been proposed for targeting antibacterial DDSs, but their instability, poor biocompatibility and uncontrolled release behaviors limit their applications in anti-bacteria. Recently, MOFs combining the hybrid organic and inorganic framework have been studied for anti-bacteria therapy. Owing to good chemical stability in acidic environment, MOF-53(Fe) constituted of iron ions and BDC was explored as a carrier for antibacterial agents by Lin et al.[203] (Fig. 7A). The glycopeptide macromolecule antibiotics, vancomycin was incorporated into MOF-53(Fe) NPs by physical absorption. And the drug loading of vancomycin could reach up to 20% (*w*/*w*). Moreover, MOF-53(Fe) showed a slower and controllable drug release profile with 99.3% antibacterial efficiency against *Staphylococcus aureus* under bacterial infection condition (pH = 5.5). Meanwhile, MOF-53 (Fe)@vancomycin exhibited an ideal chemical stability with excellent biocompatibility *in vitro*.

Intracellularly bacterial infections are hard to treat in particular, as pathogens can hide inside the cell components, thereby avoiding the surveillance of the immune system. Gallis et al.[204] utilized ZIF-8 to load ceftazidime, a third-generation broad-spectrum cephalosporin (Fig. 7D). And successful loading of ceftazidime in ZIF-8 was probed by high resolution STEM-EDS elemental mapping. Drug release test in PBS revealed that about 70% of the ceftazidime released at pH 5.0, while 50% for pH 7.0 during the first day. Antibacterial capabilities of pristine ZIF-8 and ceftazidime@ZIF-8 particles were measured against Gram-negative *E. coli.* Interestingly, no difference was noted between them after 24 h, but ceftazidime@ZIF-8 displayed nearly entire growth inhibition of *E. coli* at 50 μg/mL while the pristine ZIF-8 didn't present any antibacterial effect after 72 h incubation, suggesting the antibacterial effectiveness was relied on the degradation of ceftazidime@ZIF-8. In addition, cell internalization of particles was visualized directly by confocal microscopy, which

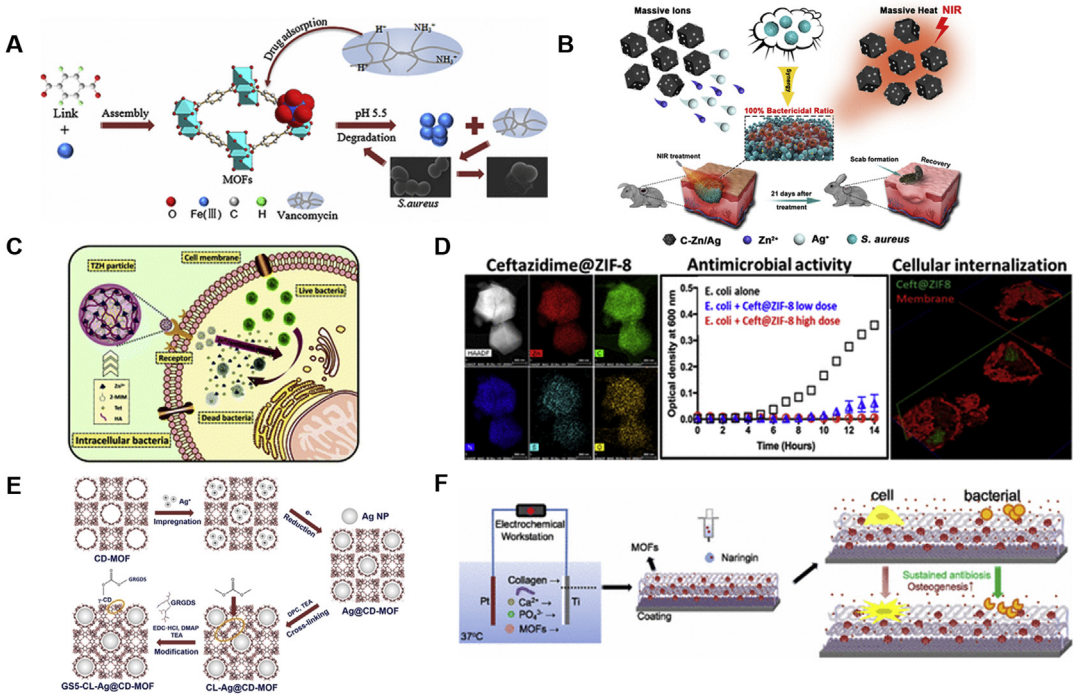

Figure 7 Applications of MOFs in anti-bacteria (A) MOF-53 (Fe) structure and the process of MOF packing vancomycin for killing bacteria. Reprinted with permission from Ref. 203. Copyright © 2017, American Chemical Society (B) MOF/Ag-derived nanocomposite with forceful photothermal conversion capability and metal-ion-releasing ability for synergistic sterilization. Reprinted with permission from Ref. 211. Copyright © 2020, American Chemical Society (C) Elimination of intracellular bacteria by TZH particles. Reprinted with permission from Ref. 205. Copyright © 2019, The Royal Society of Chemistry (D) The antibacterial properties and internalization of ceftazidime@ZIF-8 particles. Reprinted with permission from Ref. 204. Copyright © 2019, American Chemical Society (E) Schematic diagram of CD-MOF template guided synthesis of Ag NPs for anti-bacteria and hemostasis. Reprinted with permission from Ref. 210. Copyright © 2019, WILEY-VCH (F) Naringin-loaded MOF NPs for coating mineralized collagen to promote osseointegration and prevent bacterial infection. Reprinted with permission from Ref. 207. Copyright © 2017, American Chemical Society.

qualified that this system can be applied for intracellular bacterial killing.

Another ZIF-8 application for anti-bacteria was reported by Zhang et al[205]. During the synthesis of ZIF-8, tetracycline was encapsulated in MOF through one-step. Moreover, hyaluronic acid (HA) was decorated on tetracycline@ZIF-8 *via* coordination for active-targeting of bacteria within the cell (Fig. 7C)[205]. This tetracycline@ZIF-8@HA nanocomposite (TZH) could realize a pH-responsive antibiotic release. More importantly, Zn(II) and antibacterials released from ZIF-8 could reach a synergistic antibacterial effect. In addition, with the help of HA, TZH could eliminate intracellular bacteria more efficiently and decrease the antibiotic dosage remarkably. Finally, clearance rate of intracellular bacteria by TZH was over 98%.

Hitherto, the mainly investigated MOFs in anti-bacterial field as drug carriers, few studies discussed that diameter, shape and surface modification of MOFs affected their cellular internalization. Guo et al.[206] explores MIL-88 (A) and MIL-100 (Fe) particles both incorporated with mannose for active targeting, which were designed with rod-like and spherical shapes respectively, as a promising bacteria-mimicking delivery strategy for intramacrophagic-based infections. The shape of MIL-88 (Fe) was rod with a long-axis size of 3628 ± 573 nm and the aspect ratio was 1:5, while the diameter of spherical MIL-100 (Fe) was 103.9 ± 7.2 nm. Cell internalization test displayed that MIL-100 (Fe) NPs were internalized quicker, however, the mannosylation did not enhance the uptake of MIL-100 (Fe), because its rate and extent of uptake were high enough, whereas cellular uptake of MIL-88A (Fe) were highly increased. Moreover, micropinocytosis/phagocytosis proved to be the primary internalized pathway in MOF particle uptake.

Prevention of infection and promotion of osseointegration are two important goals in orthopedics. Yu et al.[207] designed naringin-loaded MOF NPs for coating mineralized collagen. With the help of MOF NPs, the release kinetics of naringin could be controlled to boost osseointegration and avoid bacterial infection (Fig. 7F)[207]. Results showed an outstanding performance of the coating for mesenchymal stem cells including the attachment, proliferation, osteogenic differentiation, and mineralization. Meanwhile, the antibacterial effectiveness against *S. aureus* was also enhanced which confirmed the potential application of this orthopedic coating for implants.

Numerous studies have revealed that ultrafine silver (Ag) NPs are promising antimicrobial agent because the release of Ag(I) ions and generation of reactive oxygen species (ROS)[208]. However, ultrafine Ag NPs are usually unstable and easily to aggregate[209]. Shakya et al.[210] reported a template-assisted synthesis of ultrafine Ag NPs with size about 2 nm by utilizing the mesoporosity of γ-CD-MOFs in one pot, achieving stability enhancement of Ag NPs. Further, the Ag@CD-MOFs were cross-linked and surface modified with GRGDS peptide for improvement of hemostasis in the wound area. The anti-bacteria test as well as the hemostasis test proved that the obtained GS5-CL-Ag@CD-MOFs were a fine strategy to combine hemostasis with antibiosis (Fig. 7E)[210].

Owing to the limited antibacterial efficiency, high-dose use and slow sterilization rate of single-model bactericidal method are usually used, and it's urgent to develop a dual bactericidal system. Yang et al.[211] synthesized an MOF/Ag-derived nanocomposite consisting of metallic Zn and a cgraphitic-like carbon framework with preeminent metal-ion-releasing ability and forceful photothermal conversion capability for synergistic sterilization (Fig. 7B)[211]. When exposed to near-infrared irradiation, massive heat was generated to destroy bacterial membranes, at the same time, bacterial intracellular substances would be damaged by abundant released Zn(II) and Ag(I) ions from MOF-derived nanocarbon. Moreover, the nanocomposite exhibited less cytotoxicity with an excellent antibacterial effect in systematic antibacterial experiments.

5.1.2. *Lung disease therapy*

Pulmonary delivery of drugs can achieve high efficiently targeted drug therapy for lung disease, like asthma, respiratory tract infections, chronic obstructive pulmonary disease and lung cancer. Owing to the tunable structure and porosity, inhalable size, MOFs can be used as carriers for pulmonary drug delivery. Recently, Hu et al.[68] utilized γ-CD-MOF to load budesonide which were modified with cholesterol (CHO) and leucine poloxamer for dry power inhaler (Fig. 8A)[68]. Particle size distribution showed that more than 90% particles were within the suitable diameter of 1−5 μm for the inhalation administration. Moreover, modification with CHO could successfully improve the flowability and aerodynamic properties of CD-MOF *in vitro*. Most importantly, *in vivo* animal experiments demonstrated that the CHO-CD-MOF based dry power inhaler may be a promising pulmonary delivery carrier.

Another research reported by Mohamed et al.[212] utilized MIL-89 and PEGylated MIL-89 (MIL-89 PEG) as carriers for pulmonary arterial hypertension delivery. Both of them had particulate sizes, within 50−150 nm, with a majority particle size of 100 ± 38 nm. After PEGylation, MIL-89 PEG expressed enhanced homogeneity of shape and improved stability. Cell experiments demonstrated that both MIL-89 and MIL-89 PEG was nontoxic to endothelial cells. Moreover, both of them showed anti-inflammatory effect in macrophages. Besides, *in vivo* experiments revealed that MIL-89 was well-tolerated in short period and accumulated in lungs, which may be suitable carriers for pulmonary arterial hypertension drugs.

The treatment of tuberculosis needs the combination of drug delivery and imaging to achieve a better control and personalized therapy. For preventing massive systemic exposure and side effects, pulmonary delivery of anti-tuberculosis drug is an ideal strategy to maintain local therapeutically effective concentrations. Thus, Fe−MIL-101−NH_2 NPs were used as carriers for controlling release of isoniazid (INH) and MRI contrast agent by Wyszogrodzka et al.[213,214] (Fig. 8B). *In vitro* cytotoxicity experiments confirmed the safety of Fe-MIL-101-NH_2 and cell internalized studies supported the potential application in tuberculosis treatment. For improving the aerodynamic properties of INH-loaded MOF (INH-MOF), hydrophobic poly (lactide-*co*-glycolide) (PLGA) microparticles were utilized to load INH-MOF *via* spray-drying, then mixed with spray-dried INH-MOF-loaded D-leucine (LC) microparticles. Finally, the obtained INH-MOF-loaded PLGA/LC expressed excellent aerodynamic properties, controlled release of INH and good internalization into the macrophages. Moreover, the Fe ions in INH-MOF could be MRI contrast agent for tracking particles after inhalation.

In addition, Simon-Yarza et al.[195] discovered that Fe(III) polycarboxylate based nanoMOFs were capable of targeting lung tissue, due to their unique pH- sensitiveness and reversible aggregation properties (Fig. 8C)[195]. After intravenous administration, under the neutral pH in blood, the nanoMOFs formed microaggregates which were detained in the lung capillaries. During 24 h, the agglomerates disaggregated and started to degrade,

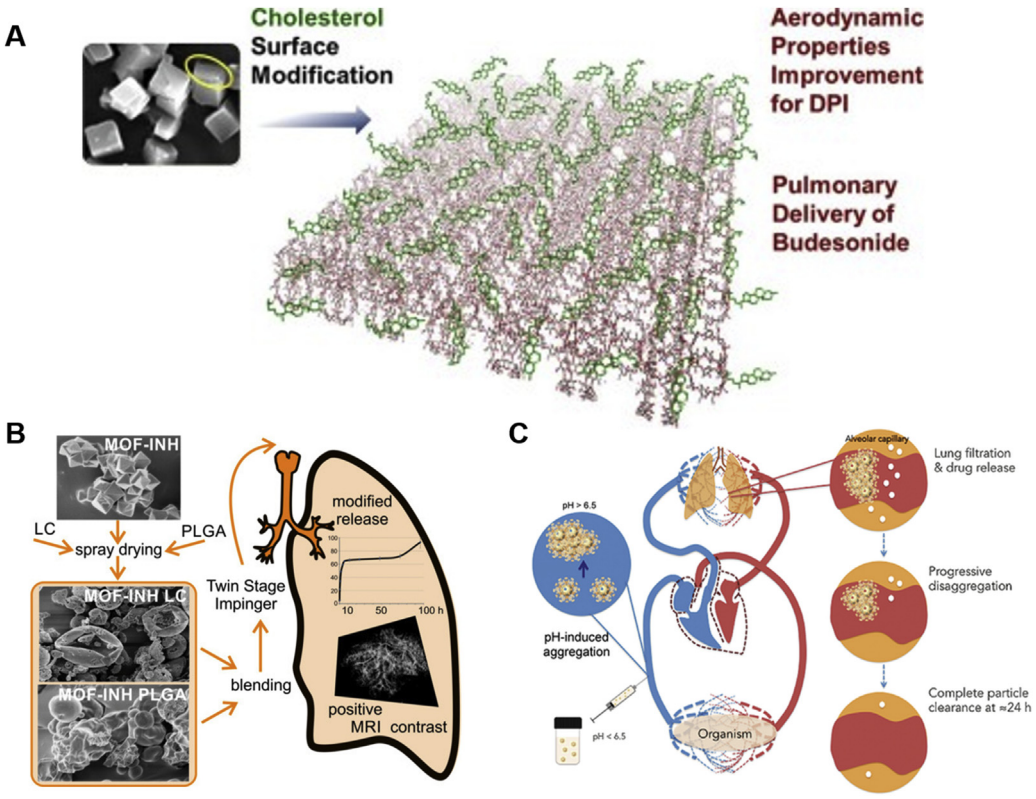

Figure 8 Applications of MOFs in lung disease (A) Cholesterol modification of CD-MOF to improve aerodynamic properties for pulmonary delivery of budesonide. Reprinted with permission from Ref. 68. Copyright © 2019, Elsevier (B) INH-loaded MOF combined with PLGA and LC microparticle for pulmonary delivery of anti-tuberculosis drug. Reprinted with permission from Ref. 214. Copyright © 2019, MDPI(OA) (C) Graphical mechanism of nano-MOF-based particle lung retention after i.v. administration. Reprinted with permission from Ref. 195. Copyright © 2017, WILEY-VCH.

leading to drug release with improved therapeutic effect as compared to free drug and metastasis reduction. Particularly, the appropriate timing of reversible aggregation/disaggregation was compatible with tissue physiology, avoiding of toxicity issues.

5.1.3. *Diabetes therapy*

Diabetes mellitus still remains a serious health problem around the world. The management of type 1 diabetes needs continual insulin injection to maintain euglycemia. Developing an efficacious and advanced insulin delivery system is of great significance. The most studied insulin delivery systems are based on GOx for realizing glucose responsiveness, which are usually modified with pH-responsive materials. Duan et al.[215] investigated a simple one-pot approach for construction an advanced glucose-responsive insulin delivery system, where insulin-GOx/ZIF-8 was self-assembled by the mixture of Zn(II), 2-methylimidazole, GOx and insulin (Fig. 9A)[215]. When the blood glucose level was higher than normal, GOx catalyzed glucose to gluconic acid, then the local pH change led ZIF-8 decompose and thus caused insulin release. Moreover, when glycemic level reached to normoglycemic conditions, insulin release from the ZIF-8 decreased, avoiding hypoglycemia.

Recently, a novel strategy was designed by Yang et al.[216], using multi-enzyme Co-ZIF-8 embodied insulin and GOx as repertories to integrate with microneedles for transdermal insulin delivery (Fig. 9B)[216]. Co(I) ions in ZIF-8 MOFs were designed as a biomimetic catalase to decompose the excessive H_2O_2 for avoiding the conceivable damage to normal tissue. Meanwhile, free Co(I) ions can be chelated by ethylene diamine tetraacetic acid modified SiO_2 NPs in microneedles, then removed by peeling microneedles off. Results showed that the obtained MOF-based microneedles exhibited good insulin release performance depending on glucose concentration without leakage of H_2O_2 and Co(I).

Diabetic foot ulcers are a serious problem for people with diabetes, and there are no effective therapies. Xiao et al.[97] developed FA modified Cu-MOFs (F-HKUST-1) for the therapy of chronic nonhealing wounds (Fig. 9C)[97]. FA was added when synthesizing HKUST-1 to slow the release of Cu(II) ions, resulting in improved wound healing rates and reduced toxicity. *In vivo* experiments revealed that F-HKUST-1 could induce angiogenesis, promote collagen deposition and re-epithelialization and increase wound healing speed.

5.1.4. *Ocular disease therapy*

The ophthalmic drugs formulated as eye drops are usually removed fast from the eyes, thus limiting their ocular bioavailability, which to usually less than 5%. Therefore, Kim et al.[217] utilized NH_2—MIL-88 (Fe) for sustained release of brimonidine to enhance its ocular bioavailability (Fig. 10A)[217]. Brimonidine was incorporated *via* physical absorption into the large internal pores of NH_2—MIL-88 (Fe). Besides, due to the amino groups and hydrogen-rich organic ligands in this MOF, hydrogen bonds were formed with the hydroxyl groups and intrinsic carboxyl of mucin chains, then generating mucoadhesive properties and thus increasing the retention of drugs in preocular. *In vitro* test showed a sustained release manner of encapsulated drug in NH_2—MIL-88

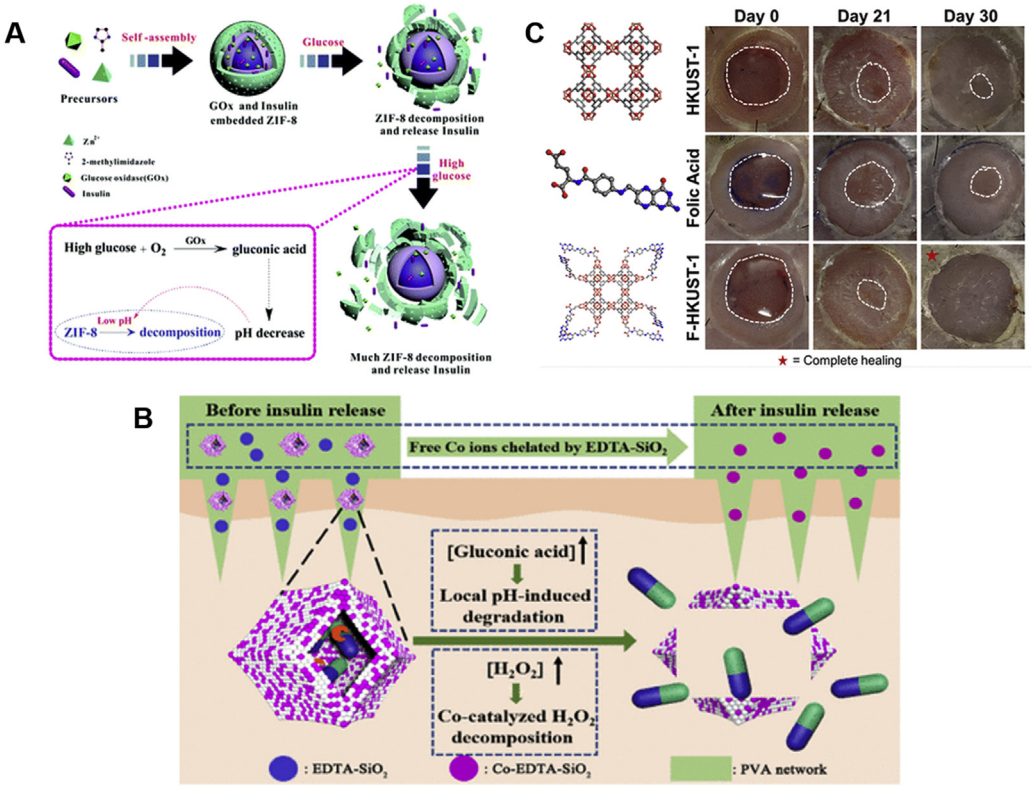

Figure 9 Applications of MOFs in diabetes therapy (A) glucose-responsive insulin release from the MOF-based nanosystem. Reprinted with permission from Ref. 215. Copyright © 2018, The Royal Society of Chemistry (B) Microneedles containing Co-ZIF-8 embodied insulin and GOx for transdermal insulin delivery. Reprinted with permission from Ref. 216. Copyright © 2020, American Chemical Society (C) FA modified Cu-MOFs (F-HKUST-1) for the therapy of chronic nonhealing wounds. Reprinted with permission from Ref. 97. Copyright © 2018, American Chemical Society.

(Fe). Moreover, in comparison with the marketed product of brimonidine (Alphagan-P), the bioavailability of brimonidine was enhanced in NH_2−MIL-88 (Fe) in the *in vivo* test. Worthily, although this MOF can be fully degraded into Fe(III) and 2-amino BDC in physiological fluid during half a day, the long-term existence of Fe(III) may be threat for eye safety.

Another research utilizing Zr-based UiO-67 loaded brimonidine tartrate and polyurethane nanocomposite films as novel ocular therapeutics was developed by Gandara-Loe et al[218]. This functional MOFs-based ocular polymeric device exhibited excellent adsorption and release performance for brimonidine tartrate owing to large tetrahedral and octahedral cages of UiO-67 and realized a controllable and extended drug release in glaucoma therapy (Fig. 10B)[218].

5.1.5. *Anti-tumor applications*

Developing novel DDSs to improve the effectiveness of chemotherapy and diminish the adverse reactions is of significant sense for the treatment of tumors. As nanocarriers with high drug loadings and easy modification, MOFs have been exploited to enhance the accumulation of drugs into tumors. In order to conquer the multidrug resistance effect, Zhang et al.[219] utilized ZIF-8 to co-deliver chemotherapeutic drugs DOX and P-glycoprotein (P-gp) inhibitor verapamil hydrochloride (VER), realizing increased drug concentrations in multidrug resistance tumor cells (Fig. 11A)[219]. DOX and VER were co-incorporated into ZIF-8 through one-pot strategy, then (DOX + VER)@ZIF-8 was functionalized with poly (ethylene glycol)-folate (PEG-FA) by coordination for realizing prolong circulations and active targeting, which displayed increased therapeutic efficiencies and much safer properties than free DOX.

GOx-based cancer starving therapy has been regarded as a promising strategy for tumor therapy. However, the low GOx delivery efficacy and self-limiting curative effect have restricted its application. Therefore, Zhang et al.[220] exploited ZIF-8 as the carriers to embody GOx and prodrug tirapazamine, then packaged with an erythrocyte membrane to develop biomimetic nanoreactor tirapazamine-GOx-ZIF-8@erythrocyte membrane (Fig. 11B)[220]. The large cavities of ZIF-8 would reach to a high loading efficacy of GOx, protecting GOx from leaching, aggregation and loss of catalytic activity. Erythrocyte membrane could help escape immunity and prolong blood circulation, then assisting the delivery of GOx to tumor cells for exhausting intracellular glucose and O_2. The resulting tumor hypoxia further initiated the activation of tirapazamine for strengthened colon tumor therapy. In another study reported by Jiang et al.[221], ZIF-8 was used to co-deliver quercetin as an antitumor drug and CuS NPs as a photothermal therapy (PTT) agent for enhanced synergistic tumor treatment (Fig. 11C)[221]. Using ZIF-8 to incorporate quercetin which is a promising anticancer agent with poor water solubility and chemical instability could greatly overcome the drawback of quercetin.

Owing to its minimal invasiveness and high selectivity, PTT has attracted tremendous attention. In this field, Huang et al.[222]

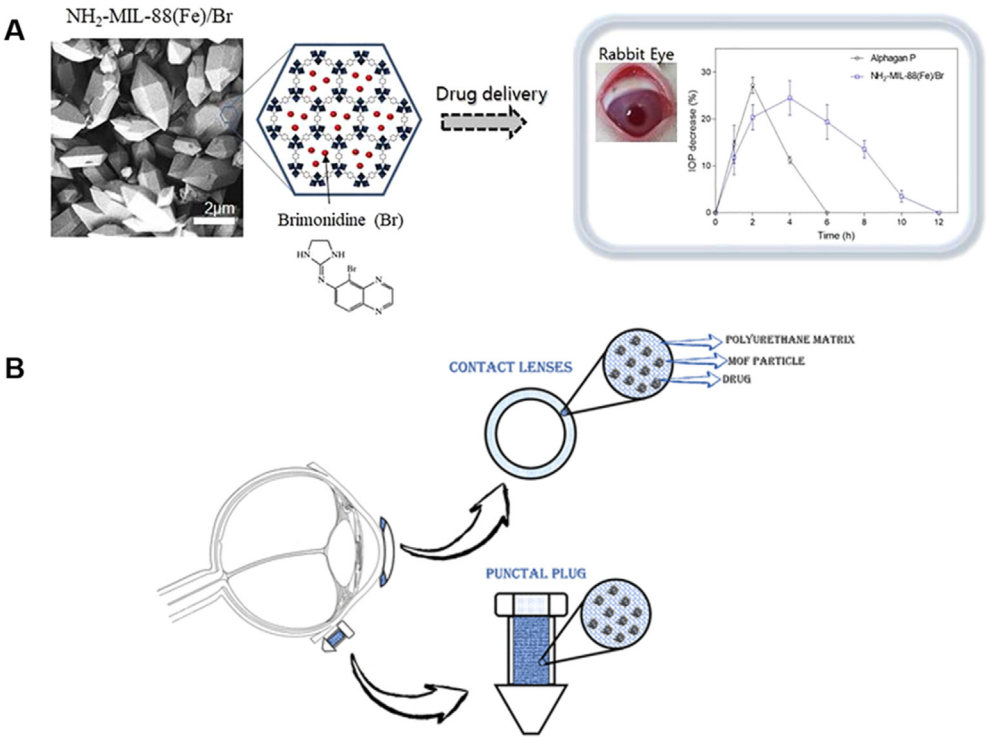

Figure 10 Applications of MOFs in ocular disease therapy (A) NH_2−MIL-88 (Fe) for sustained release of brimonidine to enhance its ocular bioavailability. Reprinted with permission from Ref. 217. Copyright © 2018, Elsevier (B) Zr-based UiO-67 loaded brimonidine tartrate and polyurethane nanocomposite films as novel ocular therapeutics. Reprinted with permission from Ref. 218. Copyright © 2020, American Chemical Society.

explored *in situ* fabrication of nanocomposites made of MIL-53 (Fe) taking advantage of the oxidation of the pyrrole monomer in the cage to generate polypyrrole NPs (Fig. 11D)[222]. After polymerization, the large surface area, porosities and initial structure of MIL-53 were unchanged, which allowed it to load DOX for chemotherapy. Meanwhile, the Fe ions in MIL-53 would act as a T2 MRI contrast agent for tracking the distribution of the composites. Results showed that the obtained PPy@MIL-53/DOX with high drug loading capability and photothermal effect exhibited good therapeutic synergism.

In addition to chemotherapy and PTT, photodynamic therapy (PDT) with the ability to generating cytotoxic singlet oxygen ($^1O_2$) by photosensitizers (PS) is also a promising strategy for management of malignant tumor. However, oxygen consumption induced by PDT treatment would lead to irreversible tumor metastasis and drug resistance. Therefore, developing novel O_2-generating materials to supply O_2 in tumor microenvironment would greatly enhance the efficiency of PDT against hypoxia tumor. The tunable MOFs pore sizes, high distinctive surface area and porous framework endow them with good capacity for gas storage. Inspired by these, Gao et al.[223] developed a biomimetic O_2-evolving PDT nanoplatform (O_2@UiO-66@ICG@RBC), using UiO-66 as a depot for O_2 storage, then conjugating with indocyanine green (ICG) (Fig. 11F)[223]. Finally, a coating with red blood cell (RBC) membranes was achieved to allow immunologic escape. When exposed to 808 nm laser irradiation, $^1O_2$ generated from ICG degraded the RBC membrane and facilitated O_2 release from UiO-66, and thus improved the PDT effects. In response to the intracellular damage induced by $^1O_2$, the concentration of GSH, a vital intracellular antioxidant, was decreased for maintaining the redox homeostasis. It was noteworthy that GSH consumption was relevant to ferroptosis which is an Fe-dependent cell death, generally different from other cell death. In another study, Meng et al.[224] designed an MOF-based nanocarrier for integrating PDT with ferroptosis, by using disulfide-containing imidazole as organic ligand and Zn(II) as corresponding coordination metal ions, then encapsulating a photosensitizer chlorin e6 (Fig. 11E)[224]. Upon light irradiation, GSH depletion caused by chlorin e6-loaded MOF through the disulfide-thiol reaction resulted in the inactivation of glutathione peroxide 4 which was attributed to ferroptosis, finally, obtaining an enhancement of antitumor PDT by the MOF nanocarrier.

Another study combining PDT with anti-angiogenesis therapy, utilizing porphyrinic MOF nanostructure as antiangiogenic drug delivery carrier and PDT agent was reported by Min et al.[225], which was decorated with MnO_2 layer to neutralize excessive GSH in tumor for enhancement of PDT therapy, then endowed by mouse breast cancer cells (4T1) membrane to achieve tumor-targeting ability (Fig. 11G)[225]. After intravenous administration, the multi-functionalized porphyrin Zr-MOF would selectively accumulate in tumor through homologous targeting mediated by tumor cell membrane camouflage, then, enhanced PDT by GSH consumption and release of antiangiogenic drug apatinib cooperatively improved tumor therapy. Besides, the released Mn(II) from MnO_2 could be used for *in vivo* tumor imaging as its MRI contrast property.

Very recently, Haddad et al.[226] developed a mitochondria targeting DDS based on MOF for cancer therapy, using UiO-66 as carriers to load anti-cancer drug dichloroacetate, then, conjugating with triphenylphosphonium for mitochondria targeting. Super-

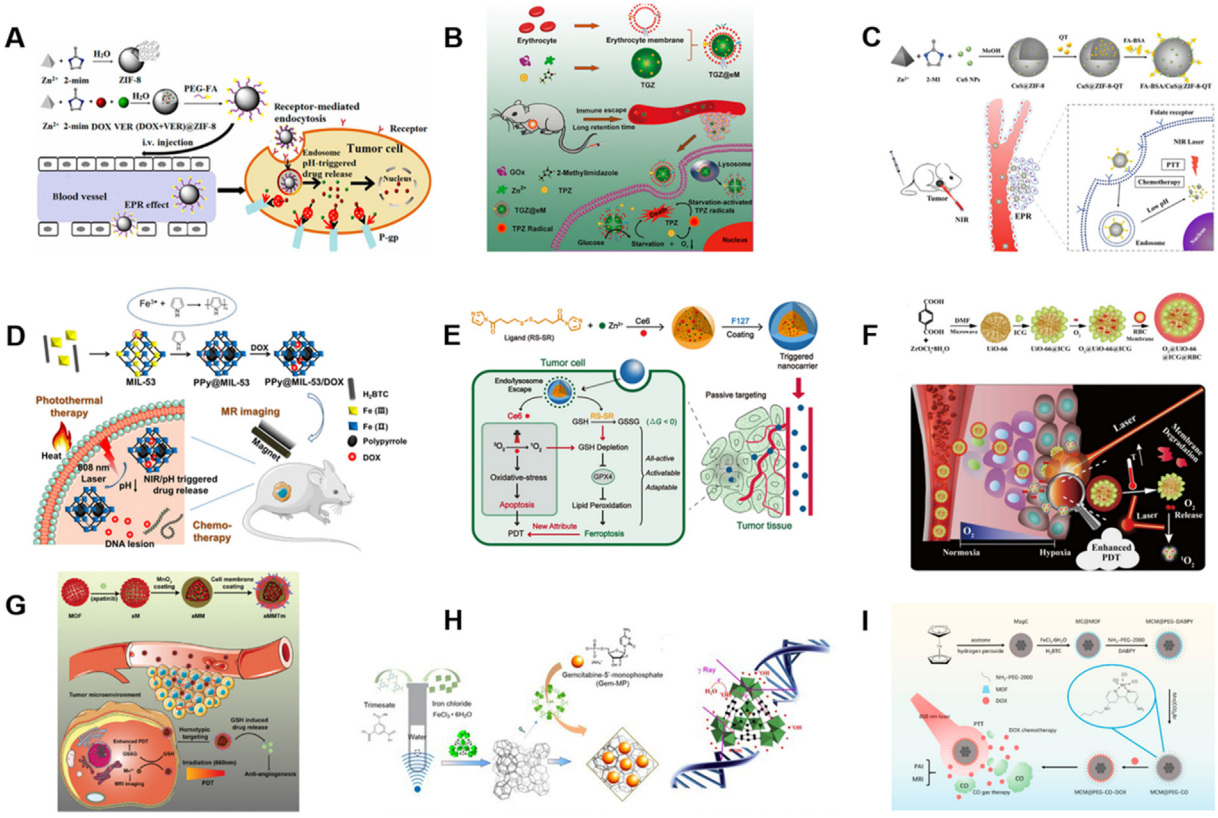

Figure 11 Applications of MOFs in anti-tumor therapy (A) pH-responsive ZIF-8 as codelivery vehicles of DOX/VER for efficient anticancer effect. Reprinted with permission from Ref. 219. Copyright © 2017, American Chemical Society (B) Preparation of erythrocyte membrane cloaked MOF biomimetic nanoreactor for starvation therapy. Reprinted with permission from Ref. 220. Copyright © 2018, American Chemical Society (C) Illustration of ZIF-8 to co-deliver quercetin as an anticancer agent and CuS NPs as a photothermal therapy agent for enhanced synergistic tumor treatment. Reprinted with permission from Ref. 221. Copyright © 2018, American Chemical Society (D) Fabrication of nanocomposites made of MIL-53 (Fe) for chemotherapy-photothermal and MRI of tumors. Reprinted with permission from Ref. 222. Copyright © 2018, American Chemical Society (E) Illustration of MOF based nanocarriers for integrating PDT with ferroptosis. Reprinted with permission from Ref. 224. Copyright © 2019, American Chemical Society (F) Illustration of a biomimetic O2-evolving PDT nanoplatform O2@UiO-66@ICG@RBC using UiO-66 for NIR-triggered O2 releasing and improved PDT therapy. Reprinted with permission from Ref. 223. Copyright © 2018, Elsevier (G) Preparation of aMMTm for combination therapy of antiangiogenesis and PDT. Reprinted with permission from Ref. 225. Copyright © 2019, WILEY-VCH (H) Illustration of nano MOF preparation and Gem-MP encapsulation for enhanced radiotherapy. Reprinted with permission from Ref. 23. Copyright © 2019, WILEY-VCH (I) Preparation of Mn carbonyl modified PEGylated Fe (III)-based nanoMOFs for NIR-responded DOX-CO combination therapy. Reprinted with permission from Ref. 227. Copyright © 2019, Elsevier.

resolution microscopy experiments directly displayed that human breast carcinoma cell lines MCF-7 cells treated with the obtained MOF revealed mitochondrial morphological transformation followed with autophagy and cell death. Moreover, whole transcriptome analysis showed that cellular gene expression was widely changed when treated with the targeted MOF, indicating the valuable strategy of this targeting MOFs towards mitochondria.

As it is well known, carbon monoxide (CO) is harmful to people because of its greater affinity towards hemoglobin than oxygen, which can be used for malignant tumor treatment in combination with chemotherapy and PTT. It is noteworthy that intracellular delivery of CO and on-demand release are vital owing to its toxicity. For realizing near infrared spectroscopy light-responded CO gas therapy and chemotherapy combination, a novel protocol was proposed by Yao et al.[227] by utilizing Mn carbonyl modified PEGylated Fe(III)-based nanoMOFs (MIL-100) enwrapped magnetic carbon NPs (MCM@PEG-CO) (Fig. 11I)[227]. In this strategy, $Mn(CO)_5Br$ was selected as the CO source whereas MIL-100 nano MOFs allowed high drug loading capacity of DOX. In the meantime, MIL-100 modified with 4,4′-diamino-2,2′-bipyridine (DABPY) would immobilize $Mn(CO)_5Br$ firmly for controlled release of CO. Moreover, the appearance of magnetic carbon core not only could execute PTT therapy by near infrared spectroscopy irradiation, but also enhanced T_2 MRI which endued MCM@PEG-CO with capability of tumor dual-mode imaging, including photoacoustic imaging and MRI.

More recently, a study showed the first application of radio-enhancers made of MIL-100 carried with a radiosensitizing anti-cancer drug, GEM[23]. The MIL-100 regular porous framework with oxocentered Fe trimers detached by around 5 Å (trimesate linkers) was able to disperse the electrons emitted from nano-MOFs owing to activation of γ radiation. In turn, this provoked water radiolysis and emergence of hydroxyl radicals, creating harm to cancer cells. Moreover, MIL-100 carried their GEM inside cancer cells. By exhibiting different mechanisms of action, both MIL-100 and GEM contributed to enhance radiation effect synergistically (Fig. 11H)[23]. This study opened new avenues

toward the project of engineered NPs wherein each constituent played a part in tumor therapy by radiotherapy.

5.2. *Applications in pharmaceutics*

5.2.1. *Enhancement of drug solubility and bioavailability*

In drug discovery, almost 70% of new drug candidates show poor water solubility, which may limit their clinical applications for poor absorption[228]. In virtue of the highly porous structure, MOFs have boundlessly potential loading capacity to poorly soluble drugs, proving to be effective carriers for aqueous solubility and bioavailability improvement of certain hydrophobic drugs. A drug might immediately release if the particles quickly collapse in aqueous environment. Compared with leflunomide, the use of porous γ-CD-MOFs as a drug container to load leflunomide could significantly increase the solubility of leflunomide by 80 times[93]. The γ-CD-MOFs could load poorly soluble drugs including AZL (Fig. 12A)[20], valsartan[80], and FA[229], increasing the solubility up to 340, 39.5 and 1453 times respectively, and for bioavailability 9.7, 1.9 and 1.5 times were reached, respectively. Similarly, the pharmacokinetics results exhibited that the IBU@CD-MOF can increase the uptake rate of IBU with a maximal plasma concentration within 20 min, and had a longer half-life in blood when compared to potassium salt of IBU[230].

5.2.2. *Improvements of drug stability*

Poor stability restricts the development, storage, and application of drugs. Many drugs are sensitive to acids, alkalis, heat, light, oxygen, and moisture, and cause oxidation, polymerization, degradation and crystallization. A number of studies have shown that MOFs can be used to improve the stability of drugs.

It is well known that curcumin is unstable under neutral and alkaline conditions. In order to solve this problem, curcumin was incorporated into the cavity of γ-CD-MOFs. Contrast to free curcumin and curcumin/γ-CD inclusion complex, the stability of curcumin at pH 11.5 was significantly improved by γ-CD-MOFs at least 3 times[231]. On the other hand, γ-CD-MOFs could also be used as vehicles to prevent drug degradation and crystallization during long-term storage. Lansoprazole degrades rapidly in humid environments and has a strong tendency to crystallize. Li et al.[67] encapsulated lansoprazole during the synthesis of γ-CD-MOFs, which could be stored for up to two years and retained its spectral characteristics. γ-CD-MOFs also could be employed as carrier for the unstable vitamin A palmitate. Stability tests showed that γ-CD-MOFs improved the stability of encapsulated vitamin A palmitate without any antioxidant, the stability was better than the commercially available BASF vitamin A powder, and the half-life of vitamin A palmitate was extended up to 1.6 times[232].

The pharmaceutical applications of enzymes are hampered because of their poor stability at high temperature and extreme pH conditions. Recently, MOFs for immobilization of enzymes have great attention that extremely improve chemical/thermal stability of enzymes. He et al.[233] had encapsulated thermophilic lipase within ZIF-8 by a self-assembly approach which improved the chemical stability and preserve catalytic activity of lipase (Fig. 12C)[233]. Compared to lipase@ZIF-8 with no trypsin treatment, lipase@ZIF-8 could still preserve 91% of catalytic activity after trypsin treatment. Higher stability of lipase also be detected in the pH tolerance test, wherein lipase@ZIF-8 could maintain 90% of catalytic activity after incubation at 5.0, 7.0 and 9.0 for 200 min. Liang et al.[234] studied the stability of urease embedded in ZIF-8 by one-pot strategy. Results showed that over a range of 23−80 °C, urease@ZIF-8 offered significant improvement of the initial reaction rate by comparing free enzyme.

5.2.3. *Control of drug release*

MOFs control drug release by avoiding the "burst effect" and prolong drug retention time. Diclofenac sodium (DS) encapsulated in MOFs allowed a sustained release behavior. DS@ZJU-800 compacted with different pressures were suitable candidates

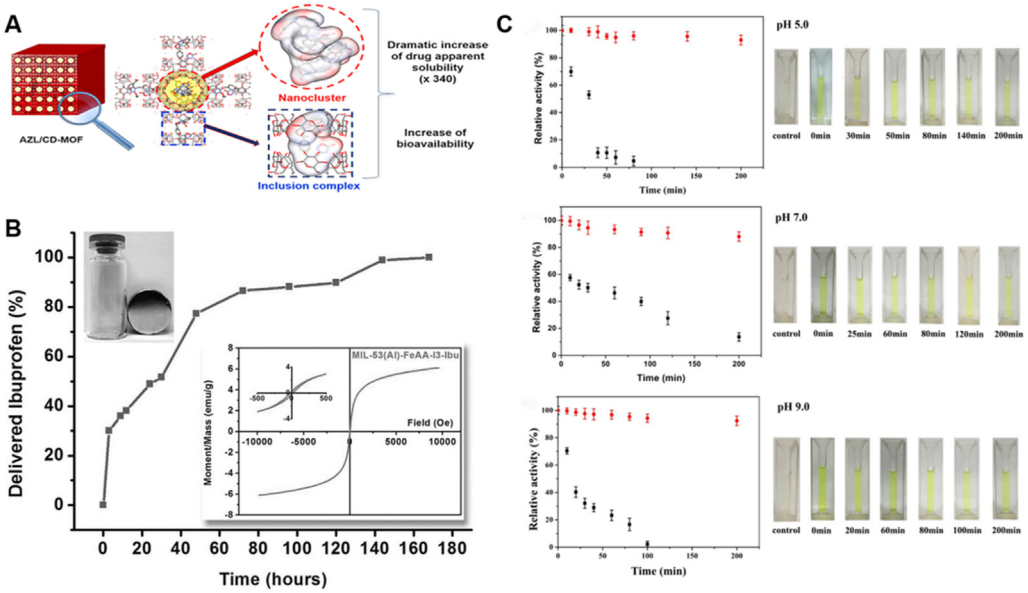

Figure 12 Applications of MOFs in pharmaceutics (A) CD-MOFs significantly improve the solubility and bioavailability of Azilsartan. Reprinted with permission from Ref. 20. Copyright © 2019, Elsevier (B) Fe_2O_3@MIL-53(Al) exhibits excellent controlled release behavior of IBU. Reprinted with permission from Ref. 236. Copyright © 2014, WILEY-VCH (C) PH tolerance of lipase@ZIF-8 (red) and free lipase QLM (black) at pH 5.0, 7.0, and 9.0 for different time. Reprinted with permission from Ref. 233. Copyright © 2016, American Chemical Society.

for drug delivery. Compared with the release kinetics of DS@ZJU-800 lasting 2 days in PBS (pH = 7.4), the drug release could be extended to 5 and 8 days when the pressure was increased to 10 and 30 MPa, respectively[45]. What's more, γ-CD-MOFs can also control DS release under simulated physiological conditions of the gastrointestinal tract (pH = 1.2). DS@γ-CD-MOF released about 20% of DS in the first 2 h. In contrast, free DS showed burst release, with more than 70% of the drug released within the first 0.5 h[235].

In addition, MOFs were also excellent carriers for controlled release of IBU (Fig. 12B)[236]. After Fe_2O_3@MIL-53(Al) encapsulated IBU, the release behavior in saline was divided into three stages: first, around 30% of IBU was released fast in the first 3 h; then, 50% of IBU was released within 2 days; last, the remainder 20% of drug was released slowly over 5 days. MIL-100, MIL-101 and MIL-53 also presented better controlled release to IBU[236]. The release kinetics indicated that an entire release of IBU from MIL-100 happened after 3 days, from MIL-101 after 6 days[82], and from MIL-53 after 21 days[63].

The Fe(III) based non-toxic MOFs have the potential for controlled drug release[61,62]. The phosphorylated drug, azidothymidine triphosphate, was encapsulated into the biocompatible MIL-100. The gradual release of azidothymidine triphosphate from MIL-100(Fe) NPs was mainly triggered by the phosphate ion in the incubation medium. The release kinetics showed three different steps: a few percent of drug was released in 4 h; then, about 90% azidothymidine triphosphate was released to the PBS (pH = 7.4) with 10% FBS within 3 days; last, the remaining 10% of drug was slowly released in 3 days[62]. Interestingly, topotecan can aggregate into the cages of MIL-100 by stacking interactions following a "ship in a bottle" strategy, the drug was not released until the system was submitted to a two-photon excitation[62]. Besides, porous MIL-100 was utilized as a nanocarrier of DOX, with payload of 9% (*w/w*) and entire release within 14 days[62].

5.3. *Functionalization of MOFs and design of advanced systems using MOFs*

5.3.1. *Surface functionalization of MOFs*

Some MOFs are excellent drug carriers without any surface modification, whilst some MOFs need to be modified to perform special functions. Surface or interior functionalization of MOFs can doubtlessly promote the applications of MOFs in biomedicine. Herein, the functionalizations of MOFs were summarized as targeted therapy of cancer, preparation of stimulus-responsive carriers, hemostatic systems, antibacterial systems and improvement of the encapsulation capability (Fig. 13).

5.3.1.1. Targeted therapy of cancer. FA is often used for tumor targeting because of the ability to specifically recognize tumor cells. Hollow Fe−MOFs (MIL-53(Fe)-5−NH_2) was grafted with FA to increase drug loading and confer targeting abilities for specific drug delivery[51]. Meanwhile, NH_2−MIL-101(Fe) modified with pegylated folate significantly enhanced the validity of drug delivery to tumor cells[237]. By PEGulation on the appearance of the NH_2−MIL-101(Fe), the circulation time of the carrier *in vivo* was prolonged, meanwhile the phagocytosis of the carrier by the cells was reduced. Furthermore, RGD-grafted camptothecin@zeolitic imidazolate framework-8 (RGD@CPT@ZIF-8) was constructed as a neoteric particle on the basis of hydrophobic DDS for targeted and improved cancer treatment[238]. In addition to linear peptides, cyclic peptides were also frequently used in the functionalization

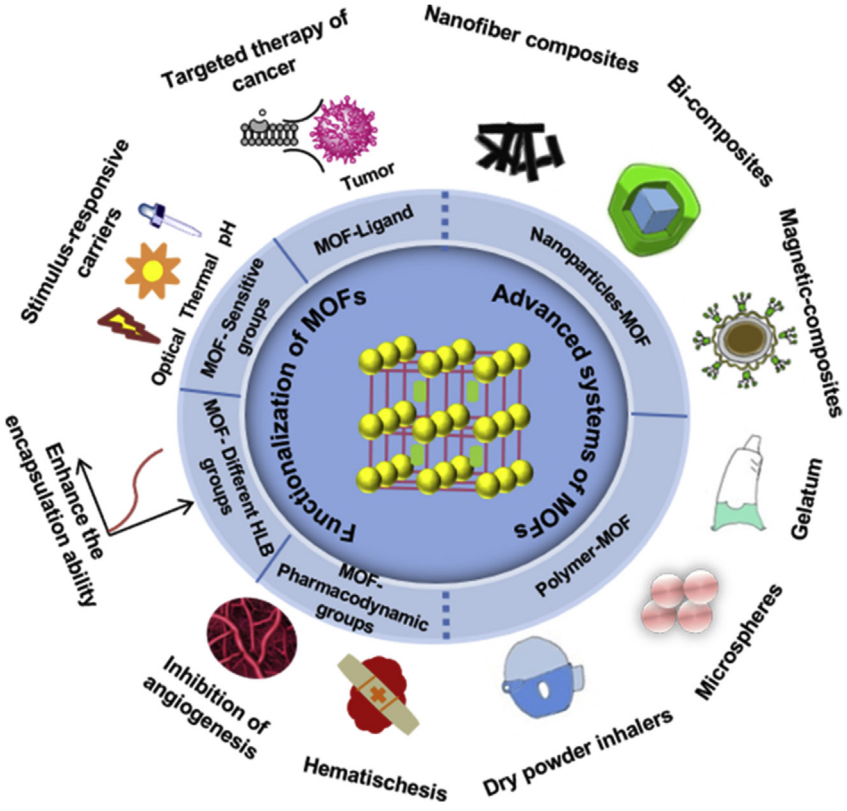

Figure 13 Overview the functionalization of MOFs and design of advanced systems using MOFs.

of MOFs. NMOF@SiO_2 nanoparticles conjugated with a tumor-targeting peptide c (RGDyK) was prepared with a high binding affinity toward integrin $\alpha v\beta 3$. Therefore, targeted therapy of tumor was achieved[239].

5.3.1.2. Stimulus-responsive carriers. Stimulus-responsive carriers realize the thermal, optical and pH responsiveness *via* modification of functional groups to MOFs. Azobenzene is a typical photosensitive material, which could couple with the surface of MOFs to form a supramolecular complex with β-CD named UiO-68-azo. The UiO-68-azo compound showed favorable stimuli-responsive without any premature drug release[240]. Based on the low pH of micro-environment in tumor, the pH responsive poly dimethacrylate was grafted by surface reaction to manufacture the PEGMA@GQDs@γ-CD-MOF which provided a platform for valid DOX delivery and neoplasm growth suppression both *in vitro* and *in vivo*[241]. Furthermore, high temperatures facilitate drug released[242]. However, it's unrealistic to release drugs in the body at a high temperature, which will cause tissue burns. A thermal sensitive drug carrier (ZIF-8, EuxTby)@AuNP, was synthesized successfully to control the drug release at temperatures close to 37 °C[243].

5.3.1.3. Hemostatic or antibacterial systems. In addition, MOFs coupled with polypeptide GRGDS have been shown to be effective in hematischesis and angiogenesis. CD-MOF by crosslinking and surface decoration with GRGDS became a particle with hemostatic function which realized the clustering of activated platelets and highly targeting to impaired vessels[94]. Furthermore, crosslinking CD-MOF grafted with GRGDs and loaded with Ag NPs possessed hemostatic and antibacterial functions[210].

5.3.1.4. Improvement of the encapsulation capability. Modification of MOFs can enhance their encapsulation ability. The hydrophilic–lipophilic balance value of organic linker had a huge influence on drug loading. For example, caffeine loading in UiO-66 was increased because the organic ligand had a high octanol–water partition coefficient and possessed limited hydrogen bond acceptors. Nevertheless, the IBU entrapment was improved while the organic ligand contained active groups with a bulky solvent surface and free volume, and lesser degree hydrogen bond acceptor capabilities[200].

5.3.2. Advanced systems made of MOFs

In addition to functional modification, MOFs can be combined with other carriers and materials to prepare nanoparticles-MOF, polymer-MOF, non-biological-MOF composites and biomolecule-MOF composites[39], greatly expanding the application space of MOF as composites. Herein, the nanoparticles-MOF and polymer-MOF composites are discussed.

5.3.2.1. Nanoparticles-MOF composites. There were numerous combinations of NPs and MOFs[244,245]. Fe-MOFs and nanofibrous polycaprolactone were used to fabricate nanofiber composites by electrospinning technique. Polycaprolactone-MIL-53(Fe) offered proper surface and mechanical performance such as cellular biocompatibility, high porosity, stability, cell viability, and proliferation[244]. Bimetallic organic framework NP was prepared *via* parceling the inner MOFs with an outer MIL-100(Fe) *via* a layer-by-layer approach. The d-MOFs NPs regarded as a T_1–T_2 dual-modal MRI contrast and fluorescence imaging agent as a result of the being of inner MOFs and outer MIL-100(Fe) MOFs, which showed a great potential in the treatment of tumors[245]. Furthermore, the magnetic Fe_3O_4@silica@MIL-100Fe/β-CD as a drug nanocarrier was studied for the drug loading and controlled release of cefalexin. It was found that the carrier could achieve zero-order release on specific locations[246].

5.3.2.2. Polymer-MOF composites. Polymers modified with MOFs were engineered for applications as antibacterial gels, microspheres dry powder inhalers and so on. As a semisolid dosage form, medical gel is of great significance in antibacterial activities. Cu-MOFs embedded hydrogels were fabricated by UV light-mediated thiolene photopolymerization. The activities of hydrogels were tested against the gram-negative bacterium *E. coli* and the gram-positive bacterium *S. aureus* showing good antibacterial activities[247]. The niflumic acid and 2-methylimidazole were incorporated to the sodium alginate composite material as a ligand for Zn(II) which had strong antibacterial property and processed sustained release behavior of Zn(II) and high drug loading effect[248]. Furthermore, the mixture of CD-MOFs and polyacrylic acid (PAA) were fabricated by a solid in oil-in-oil (s/o/o) emulsifying solvent evaporation method, which presented a favorable dispersion of drug loaded CD-MOF nanocrystals (IBU and lansoprazole) mixed with PAA matrices and the uniform distribution of the drug molecules within these crystals. Meanwhile, the composite microspheres could significantly reduce the cytotoxicity and prolong the drug release time[184].

Polymer@MOFs were also employed in pulmonary inhaled DDS. CHO and leucine were applied to embellish CD-MOF particles with loading of budesonide for pulmonary inhalation. To have enhanced the fluidity and optimize aerodynamics deposition by the modifications to the carrier using cholesterol, the distribution abundance in the lungs was significantly improved in rats compared with that of CD-MOF[68].

6. Biopharmaceutics of MOFs and MOFs-based DDSs

It is of great significance for the pharmacokinetics investigation of MOFs for the sake of design and development of MOFs as pharmaceutical excipients. The pore sizes (micro- or mesopores), pore shapes (cages, channels, etc.), rigid or flexible frameworks, and the functional groups allow MOFs carriers to carry drugs with high capacities, controlled release kinetics, enhanced amphiphilic internal microenvironment, modulated biological interactions and penetration to overcome the gastrointestinal or the blood–brain barrier in a controllable manner[40,101]. MOFs carriers exhibited various merits such as increasing drug concentration at a local position, minimizing drug degradation and clearance, targeting specific cell, and creating drug-delivery formulation[249]. These all converge towards goals to improve the efficacy and decrease the toxicity of the therapy[250].

Currently, improving the pharmacokinetic profile of MOFs carriers is a primary drug delivery strategy to optimize drug targeting toward diseased tissues or cells. A great number of studies[20,185] focused on the capability to improve drug bioavailability and biodistribution. The absorption, distribution, metabolism and excretion (ADME) processes differ in MOFs and then have consequences on the pharmacokinetic profile of the loaded drugs[57,251–253]. An understanding of these pharmacokinetic characteristics is elemental to ensure effective therapy in MOF nanomedicine as an integral step to clinical application. However,

very little is known about the pharmacokinetics of MOFs as relatively new drug carriers. The purpose of this part is to summarize what we can learn from the available data so far on the ADME of MOFs and the pharmacokinetic characteristics of drugs loaded in MOFs *in vivo* or in cells.

6.1. Pharmacokinetic characteristics of MOFs as drug carriers

In consideration of the hybrid nature of MOFs as drug carriers, their pharmacokinetic profiles were assessed by quantifying the components, the organic ligand and the ion cation of the MOFs in simulated physiological conditions, in cells and *in vivo*.

6.1.1. Studies in simulated physiological conditions

The physicochemical properties such as colloidal and chemical stability of nanomaterials strongly impact their efficacy and biodistribution[254]. Some researchers explored the biodegradability of MOFs under physiological conditions[48,255,256]. For instance, nanoMOFs of the MIL family progressively degraded in PBS after incubation at 37 °C[57,257] as well as in cell culture media[61]. In all these studies, it was highlighted that the specific interaction between the MOFs and the phosphate groups in PBS that governed the progressive degradation of the NPs. Interestingly, it was discovered that degradation led to an amorphous material without significant changes of the initial size of the crystals[258]. In particular, the biodegradability of MIL-100(Fe) potentially relied on their physicochemical surface and the media composition. Furthermore, the excess phosphate ions in buffer decomposed the Zr-MOFs quickly leading to a rapid drug release[74]. In contrast, the NU-1000 degraded slowly and released its cargo gradually when exposed to simulated blood solution with a high concentration of phosphate ions[259]. Differently, the procainamide HCl released from the bio-MOF-1 in PBS showing a steady profile over 20 h while completed release within 72 h[43].

6.1.2. In vitro experiments

Recently, studies have focused on the interaction between MOF particles and cells, which were assessed by cell viability, metabolism, penetration, and excretion[57,253,260]. For instance, the cytotoxicity of MIL-100(Fe), MIL-101(Cr), and Zr-fum MOF NPs of different sizes on primary gingiva fibroblasts as effector cells for dental implants were accessed[249]. Additionally, the cell uptake of the MIL-100(Fe) was pivotal to deliver cargos[261]. NanoMOFs like other drug carriers efficiently internalized in macrophages and degraded in their inner compartments[33]. Orellana-Tavra et al.[262] revealed the internalization processes of UiO-66 MOF particles by the caveolae-mediated pathway, which could avoid to deliver the cargo in other intracellular location without the lysosomal acidic degradation. Besides, cellular internalization of UiO-66 into HeLa cells was depended on the particle size of the solids, and the uptake of larger UiO-66 (260 nm) particles were more efficient compared with smaller UiO-66 (150 nm). This difference is critical when lysosome activity may prevent the MOF action from pre-degradation for MOFs-based DDSs.

6.1.3. In vivo evaluations

One of the major issues with administration of the MOFs as drug carriers *in vivo* is their pharmacokinetic properties. The efficient drug delivery of MOFs is mainly depended on host−guest interactions, diffusion and their degradation in the body fluid. As an example, nano MIL-100(Fe) degraded to be compatible with biomedical applications *in vivo*[31,32]. In this study, the pharmacokinetics of MIL-100 were evaluated by intravenous administration in mice in short term (up to 24 h) (Fig. 14B)[32]. When MIL-100 arrived into the blood, phosphates replaced the carboxylate linkers, releasing the metal ions and the organic linker. Another criterion is closely related to their solubility, the release of solubilized metal ions, crystal parameters such as particle size and subsequent cellular uptake.

Besides, the biocompatible MIL-127 was used for oral drugs detoxification *in vivo*. Except for slight absorption in the intestine, the intact MIL-127 was remained along the gastrointestinal (GI) tract and then excreted in the feces after oral administration in rats (Fig. 14A)[263]. The large particle size, high structural and chemical stability, and low intestinal permeation of both MIL-127 and its constitutive ligand potentially led to the lack of intestinal absorption. Moreover, the multimodal cancer therapy nanocomposite, Fe_3O_4/ZIF-8-Au25[264] and Fe_3O_4@PAA/AuNCs/ZIF-8 NPs[265] were administrated by injection into the tumor-bearing mice for accessing the biocompatibility and synergistic therapeutic effect. More efforts should be made to fabricate good biocompatible MOFs to ensure the biosafety of MOFs *in vivo*. The accumulation took place mainly in the liver and spleen and then degraded into their constituent of ions and ligands, and excreted through urine and feces without any metabolization.

6.2. Pharmacokinetic characteristics of drug-loaded MOFs

Bioavailability is a combinative result of physicochemical properties, mucosal penetration, gastric pH, drug-metabolizing enzymes, and drug transporters, whilst the extensive first pass metabolism is a major impediment to clinical application of a therapeutic agent[266,267]. Plenty of efforts have been dedicated to the improvement of drug solubility using CD-MOF[230]. Kritskiy et al.[185] reported enhanced bioavailability of MTX loaded in γ-CD-MOF with increased dissolution of MTX and the decreased drug permeability through the lipophilic membrane. At the same time, the γ-CD-MOF was suitable for long-term administration due to its elimination with a longer time ($T_{1/2}$ = 4.5 h) than that of MTX ($T_{1/2}$ = 1.5 h). However, the unknown biodistribution and aqueous instability might limit their practical use. Hence, it is of sense to understand the mechanism of bioavailability enhancement to the insoluble drug in CD-MOFs. He et al.[20] fabricated CD-MOF with molecular cages confined with nano cluster of AZL and its CD complexation. The AZL/CD-MOF and raw AZL were orally administrated to SD rats at a dose of 1 mg/kg. The plasma drug level of AZL in CD-MOF increased quickly and achieved maximal concentration at 1.5 h after oral administration, and the AUC_{0-24h} of 30.65 ± 14.24 μg/mL·h was almost nearly 9.7 times higher than that of free AZL, which intensively displayed that AZL/CD-MOF enhanced the absorption and bioavailability of AZL (Fig. 14C)[20]. The mechanism of the AZL distribution inside the CD-MOF by molecular docking suggested that the drug nanoclusters with uniform and tiny size immediately released from CD-MOF could temporarily improve the apparent solubility of AZL in water. Additionally, further studies should be paid to the mechanism of distribution, metabolism and excretion.

Overcoming the barriers of the GI system to provide sufficient bioavailability following oral administration is vital for MOFs potential clinical usages. A number of research groups have explored the bioavailability with controlled and pH specific release behaviors without burst effects[84,193,268,269]. For instance, PCN-221 with MTX loading demonstrated that about 40% of MTX was released at the pH of stomach after 3 days, whereas

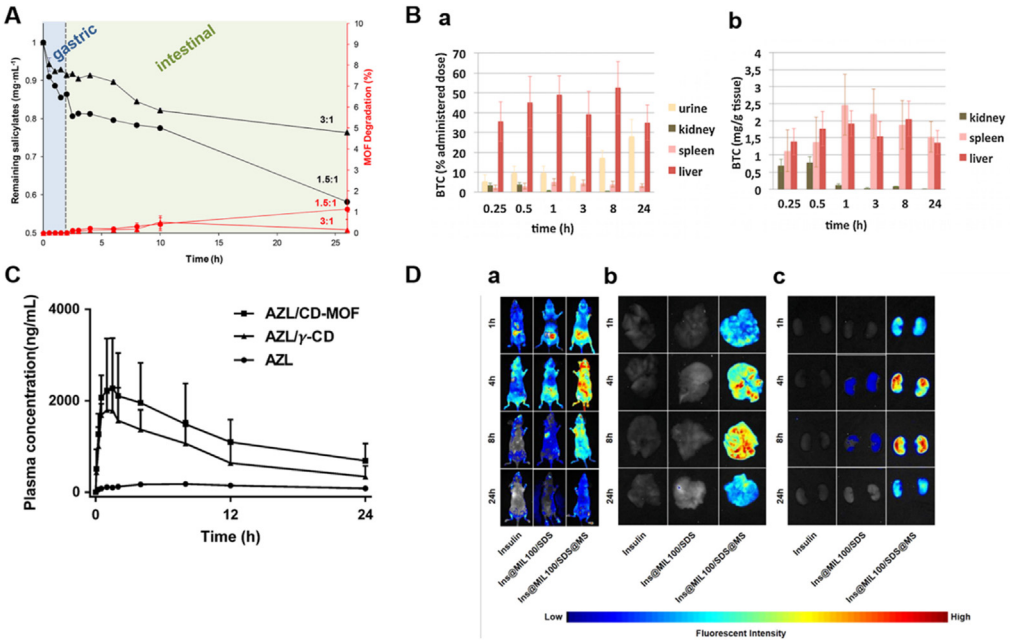

Figure 14 Pharmacokinetic characteristic of MOFs (A/B) and drugs loaded in MOFs(C/D) (A) Assessment of salicylate elimination (black) and MIL-127 matrix degradation (red) under simulated GI environment. Different acetylsalicylic acid: MIL-127 ratios were studied: 3:1 (triangles) and 1.5:1 (circles). Reprinted with permission from Ref. 263. Copyright © 2018, American Chemical Society (B) Biodistribution. (a) Levels of BTC in major organs and urine (b) mg of BTC per g of major organ. Reprinted with permission from Ref. 32. Copyright © 2016, Elsevier (C) Plasma concentration−time curves of AZL in rats after oral administration. Reprinted with permission from Ref. 20. Copyright © 2019, Elsevier (D) Biodistribution of RhoB-labeled insulin in the bodies of the mice (a), livers (b), kidneys (c) after the oral administration at different time points. Reprinted with permission from Ref. 273. Copyright © 2020, American Chemical Society.

100% was released at the intestinal[270]. Besides, the challenges to protect MOFs from enzymatic degradation in the GI condition and low permeation across the intestinal epithelium remain to be solved. Hidalgo et al.[271] showed an increased penetration of chitosan coated MIL-100(Fe) NPs across the intestinal barrier as compared to uncoated NPs. Chen et al.[272] found that acid stable MOF capsules named NU-1000 could effectively prevent insulin from degrading under simulated physiological conditions.

What's more, Zhou et al.[273] studied insulin loaded microspheres named Ins@MIL100/SDS@MS, which showed resistance to the stomach acid environment while absorption and transportation at intestinal after oral administration *in vivo*. The distribution of insulin in major organs suggested that the microsphere potentially circulated through the portal veins to the liver then into the heart, finally metabolized *via* the kidneys (Fig. 14D)[273]. From pharmacokinetic parameter analysis, the peak level of BALB/c nude mice plasma insulin was emerged at 4 h and remained over 8 h. Moreover, contrast to the subcutaneous insulin injection, the relatively lagged absorption of oral system was likely due to the absorption process of GI tract.

Until now, the intravenous injection is the most preferred administration route for MOF nanomedicines to prevent the nanomedicines from being degraded in advance[36]. Intravenously administered the porous Fe(III) nanoMOFs in rats were quickly captured by the liver and spleen, then further biodegraded and directly removed in urine or feces. The BTC ligands were gradually eliminated in urine[31]. Pan et al.[274] explored relatively comprehensive pharmacokinetic characteristics of 5-FU enveloped in Mn-ZIF-8. The Mn-ZIF-8 (30 mg/kg) was injected intravenously into U87-MG tumor bearing mice were, which indicated the accumulation of Mn-ZIF-8 from peaking at 12 h to slightly decrease at 24 h. For *in vivo* biodistribution and metabolism, the tumor bearing mice were administered intravenously with Mn-ZIF-8 (30 mg/kg) solution, the biological distribution of the NPs in the major organs and tumor were observed. The amount of Mn(II) ions exhibited high levels of accumulation in the liver and spleen. And the retained Mn(II) ions in major organs reduced quickly over time, suggesting that Mn-ZIF-8 may efficiently be removed from mice after gradual decomposition into small molecules and ions in a relatively rapid way, to have minor side effects on the functions of vital organs.

The bone targeting immunostimulatory MOF (BT-is MOF) NPs can effectively target tumor bone tissues through blood circulation and enhanced tumor penetration[275]. The specific deposition and accumulation of BT-is MOF on bone tissues were detected after sequential injection to C57BL/6 mice. Also, the *in vivo* distribution was largely deposited in bone and liver tissues but not in the kidney after vein injection.

Moreover, latest study show that the bioavailability and therapeutic efficacy of GEM encapsulated in the MIL-100(Fe) were improved in comparation to the GEM[276]. In this study, the Wistar rats were given i.v. dose as 40 mg/kg of GEM for MIL100-GEM and GEM solution. The plasma drug level of MIL100-GEM was 5 times higher than the GEM, while the GEM had a wider distribution in major organs, which indicated that encapsulating of GEM into MIL-100 restricted drug distribution in systemic circulation while elongating its distribution half-life. Further, MIL100-GEM exhibited a much slower removal ($t_{1/2\beta}$ = 173.25 min) compared to GEM ($t_{1/2\beta}$ = 11.17 min). Namely, MIL-100-GEM showed enhanced stability and durable release profile, leading to improved therapeutic effect at target site.

Zn is an essential trace element in human body, which was revealed to gather the highest content in brain compared with other organs[277]. Du et al.[277] constructed a coordination strategy by ion-exchange for controlling release of drug molecules, and the topological types of MOF-In1 and MOF-In2 were selected to illustrate the strategy. With the increase of node connectivity and the capture of guest OH anions, 5-Fu is preferentially loaded into MOF-In1. Meanwhile, the Zn(II) concentration was also elevated along with the enhanced controlled release of 5-FU.

6.3. *Future prospects*

The complex *in vivo* fate of MOFs as well as their passengers loaded inside should be clarified. Currently, MOFs biodistribution (bio-adhesion, stealth, targeting, etc.) and their stability can be both improved by surface modification and functionalization. However, plenty of challenges remain to be exploited before these materials can reach to the market as drug carriers. First of all, very little data of the MOFs *in vivo* are available. The degradation mechanism of the MOF particles is difficult to be mimicked *in vitro,* as body fluids contain huge number of different ions, proteins, and cells which all potentially interact with MOF particles. Optimizing the route and dosage of administration is necessary to identify the appropriate animal model such as orthotopic tumor models, syngeneic mouse tumor models for the *in vivo* test or the utilization of 3D *in vitro* preclinical evaluation[101]. Indeed, potentially interesting pharmaceutical preparations such as pellets, thin films, gels, ocular, etc. have been developed using MOFs. Nevertheless, most studies mainly focused on bioavailability and biodistribution of drugs after intravenous/oral administration and there is a lack of a comprehensive MOFs pharmacokinetics mechanism as the whole ADME process. For the case of bioavailability, it is indispensable to pay more attention to enzymatic degradation (*e.g.*, CYP450) and the efflux transporters (*e.g.*, P-gp), which hinder the absorption and permeation of therapeutics from the body[278].

7. Quality control of MOFs-based DDSs

For pharmaceutical applications, not only the toxicological compatibility but also the quality, especially the purity of MOFs should be well controlled by established methodologies. Powder XRD is the most commonly used technique to measure the crystalline purity of MOFs, such as the crystallinity, phase purity and crystal phases inside materials[279,280]. Pure-phase crystalline or multiphase MOFs materials could be identified by powder XRD. However, this technique is limited to analyze detect weakly crystalline and even amorphous impurities. Through the elements of MOFs by EDS, nanosized MOF-5 was confirmed to be homogeneous and highly pure[281]. But for the starting materials as impurities in MOFs which share the same elements as MOFs, they could not be distinguished by techniques like EDS. The surface area analysis was also used to the phase purity confirmation of MOFs. The expected surface area will not be reached if MOFs have not been thoroughly made free of solvent, starting materials or by-products from the synthesis. In more specific cases, other technique like photoluminescence spectroscopy can complement these characterizations[282]. Nevertheless, the above measurements are limited to the qualitative evaluation on MOFs, lack of quantitative analysis. As the starting materials and structural compositions of MOFs, quantitative determination of the free or residual uncoordinated organic linkers as impurities is of difficulty, such as γ-CD and free ions in CD-MOFs. It is estimated that quantitative quality control strategies for contents of MOF and limit of starting materials as impurities are the primary concerns in the aspect of developing MOFs as pharmaceutical excipients or drug delivery carriers.

8. Conclusions and perspectives

Combining molecular functional building blocks into an advanced porous multifunctional system, it is expected that the MOFs will find increasing conceivable utilizations in drug delivery. In last decades, significant advance has been realized in MOF-based DDSs, though most of the researches remain in the proof-of-concept phase, partially due to the difficulty to achieve the consistency of the drug release under *in vitro* and *in vivo* conditions spatiotemporally. Moreover, developing MOFs with optimized pore/channel size, surface properties (charge, hydrophilicity and presence of grafted ligands for targeting purposes) for therapeutic cargos delivery without disrupting their activity still has a long way to go. Furthermore, the underlying mechanisms of drug release *in vivo* in MOFs-based DDSs are still to be fully unraveled whilst extremely vital, and most of the studies contain hypothesis to be confirmed[283–285]. In addition, the majority of MOFs-based DDSs were administrated intravenously, the design of MOFs-based DDSs given by other administration routes should be more thoroughly investigated. Similarly, the applications of MOFs-based DDSs are expected to be broadened, close attention should be paid to other diseases except for cancer to fully take advantages of the MOFs.

In simple words, an overall perspective of MOFs-based DDSs has been reviewed, from the classification, synthesis, characterization to application. In particular, the biopharmaceutical characteristics and biosafety of MOFs-based DDSs were highlighted. To develop an efficient DDSs using MOFs, toxicity is the first and most important consideration in exploring their applications. Besides, the quality control of MOFs-based DDSs was put forward as well. The requirements of MOFs for DDSs are much stricter than non-biomedical applications, and biomedical applications of MOFs are still confronted with many challenges. Thus, the particle size, morphology, drug loading efficacy, stability and toxicology of the MOFs must be comprehensively characterized. Future continuative efforts should be endeavored to the biostability, biosafety, biopharmaceutics and manufacture to achieve the application of MOFs-based DDSs in clinic (Table 5).

8.1. *Balance between degradability and stability of MOFs in vivo*

Some MOFs are unstable in physiological conditions, which may cause serious issues, such as decomposition of MOFs, short circulation time and premature drug release, limiting their biomedical application significantly. The stability of MOFs depends on the intensity of the coordination bond between the metal ions and the ligands, which is a significant factor to be taken into consideration during the fabrication of MOFs for application in aqueous environments. The main reason why some MOFs are unstable in biological media is that water molecules, ions and other molecules in the environment compete with the linkers for the interaction with metal ions or clusters, resulting in the collapse or the degradation of the framework. Other factors such as high

Table 5 Current challenges and potential suggestions for MOFs-based DDS.

Challenge	Suggestion
In vivo fates of MOFs and drugs loaded inside are unclear	• Choosing the appropriate animal model as preclinical evaluation • Optimizing the preparations and administration routes
Current researches are limited to qualitative evaluation of MOFs	• Paying attention to quantitative quality control strategies for contents of MOFs • Limiting starting materials for impurities control
Some MOFs are unstable in physiological conditions	• Surface functionalization of MOFs • Combination with other more stable materials
Lack of systematic biosafety evaluation to MOFs	• Selecting metal ions and organic linkers with favorable biocompatibility • Highlighting the pharmacokinetics mechanism as the whole ADME process
No established standard for MOFs classification and nomenclature	• Unifying the naming rules of MOFs

hydrophobicity and poor crystallinity can affect the stability of MOFs in water as well. In addition, the pH and temperature of the environment are also key factors. Surface functionalization of the MOFs or their combination with other more stable materials may improve the colloidal stability for biomedical applications. On one hand, the stability and biodegradability of MOFs are vital factors that should be emphasized. One the other hand, the collapse of MOFs at a targeted organ or tissue is preferable to avoid endogenous accumulation and toxicity.

8.2. *Systematic biosafety evaluation to MOFs*

The biosafety of MOFs carriers is pivotal to determine whether an MOF carrier can enter clinical studies or not. However, the evaluation of the *in vivo* long-term toxicity for MOFs-based DDSs needs further studies. Currently, while numerous studies deal with the *in vitro* toxicity of MOFs, there is still a lack on *in vivo* studies. Moreover, it is well known that *in vitro* cell experiments can hardly simulate the *in vivo* environments. Only very few researches have reported the *in vivo* toxicity of MOFs. Thus far, MOFs-based DDSs for *in vivo* therapy have emerged, but far away to clinical studies. Hence, selecting metal ions and organic linkers with favorable biocompatibility needs careful deliberation and more efforts should be made to evaluate the acute and chronic toxicities of MOFs. Nevertheless, toxicity is a complex topic to deal with, as not only the MOF composition, but their size distribution, degradation behaviors, aggregation, interaction with biomolecules etc. can make a great difference to their biosafety.

8.3. *Comprehension of the biopharmaceutics of MOFs in vivo*

To unveil the *in vivo* fate of MOFs which is essential to reach the clinical stage, further efforts should be dedicated to exploring the metabolic mechanisms and metabolites of MOFs *in vivo*. What's more, a comprehensive investigation of the mechanism of ADME is indispensable. Although most of the synthesized MOFs for drug delivery have been tested *via in vitro* experiments for their biosafety, the ADME mechanism of MOFs-based DDSs has not been well-established. Particle size and polydispersity strongly influences the ADME of MOFs-based DDSs, as NPs with sizes less than 30 nm tend to be eliminated by renal excretion while larger ones are prone to accumulate in liver, spleen and lungs. Therefore, the kinetics of MOFs-based DDSs *in vivo* is of great importance to deeply understand their biopharmaceutics *in vivo* and promote clinical translation of MOFs-based DDSs.

8.4. *Nomenclature*

Series of MOFs have been reported, but there is no established standard for MOFs classification and nomenclature until now. MOFs are named based on the following four sides: (1) material composition; (2) structure; (3) laboratory/institution; (4) function. In most cases, the members in the same MOF families are named with identical letters in the front, while disparate in the last numbers for distinguishing diverse individuals. Hence, it's of urgency to unify the naming rules of MOFs.

Acknowledgments

This work was financially supported by the National Key R&D Program of China (No. 2020YFE0201700), National Nature Science Foundation of China (No. 81773645) and a public grant overseen by the French National Research Agency (ANR), France as part of the "Investissements d'Avenir" program (Labex Nano-Saclay: ANR-10-LABX-0035, France).

Author contributions

Siyu He, Li Wu, Xue Li, Hongyu Sun, Ting Xiong, Jie Liu, Chengxi Huang and Huipeng Xu wrote the manuscript. Huimin Sun, Weidong Chen, Ruxandra Gref and Jiwen Zhang revised the manuscript. All of the authors have read and approved the final manuscript.

Conflicts of interest

The authors have no conflicts of interest to declare.

References

1. Hoskins BF, Robson R. Infinite polymeric frameworks consisting of three dimensionally linked rod-like segments. *J Am Chem Soc* 1989; **111**:5962−4.
2. Furukawa H, Cordova KE, O'Keeffe M, Yaghi OM. The chemistry and applications of metal-organic frameworks. *Science* 2013;**341**: 1230444.

3. Connolly BM, Madden DG, Wheatley AEH, Fairen-Jimenez D. Shaping the future of fuel: monolithic metal-organic frameworks for high-density gas storage. *J Am Chem Soc* 2020;**142**:8541−9.
4. Ding N, Li H, Feng X, Wang Q, Wang S, Ma L, et al. Partitioning MOF-5 into confined and hydrophobic compartments for carbon capture under humid conditions. *J Am Chem Soc* 2016;**138**:10100−3.
5. Bloch ED, Queen WL, Krishna R, Zadrozny JM, Brown CM, Long JR. Hydrocarbon separations in a metal-organic framework with open iron(II) coordination sites. *Science* 2012;**335**:1606−10.
6. Wang D, Zhao C, Gao G, Xu L, Wang G, Zhu P. Multifunctional $NaLnF_4$@MOF-in nanocomposites with dual-mode luminescence for drug delivery and cell imaging. *Nanomaterials* 2019;**9**:1274.
7. Kumar P, Deep A, Kim KH. Metal organic frameworks for sensing applications. *Trends Anal Chem* 2015;**73**:39−53.
8. Li GD, Zhao SL, Zhang Y, Tang ZY. Metal-organic frameworks encapsulating active nanoparticles as emerging composites for catalysis: recent progress and perspectives. *Adv Mater* 2018;**30**:e1800702.
9. Li X, Yu J, Gosztola DJ, Fry HC, Deria P. Wavelength-dependent energy and charge transfer in MOF: a step toward artificial porous light-harvesting system. *J Am Chem Soc* 2019;**141**:16849−57.
10. Wang X, Ye N. Recent advances in metal-organic frameworks and covalent organic frameworks for sample preparation and chromatographic analysis. *Electrophoresis* 2017;**38**:3059−78.
11. Luo Z, Fan S, Gu C, Liu W, Chen J, Li B, et al. Metal-organic framework (MOF)-based nanomaterials for biomedical applications. *Curr Med Chem* 2019;**26**:3341−69.
12. Allen TM, Cullis PR. Liposomal drug delivery systems: from concept to clinical applications. *Adv Drug Deliv Rev* 2013;**65**:36−48.
13. Ulbrich K, Holá K, Šubr V, Bakandritsos A, Tuček J, Zbořil R. Targeted drug delivery with polymers and magnetic nanoparticles: covalent and noncovalent approaches, release control, and clinical studies. *Chem Rev* 2016;**116**:5338−431.
14. Matea CT, Mocan T, Tabaran F, Pop T, Mosteanu O, Puia C, et al. Quantum dots in imaging, drug delivery and sensor applications. *Int J Nanomed* 2017;**12**:5421−31.
15. Sayed E, Haj-Ahmad R, Ruparelia K, Arshad MS, Chang MW, Ahmad Z. Porous inorganic drug delivery systems—a review. *AAPS PharmSciTech* 2017;**18**:1507−25.
16. Abdelaziz HM, Gaber M, Abd-Elwakil MM, Mabrouk MT, Elgohary MM, Kamel NM, et al. Inhalable particulate drug delivery systems for lung cancer therapy: nanoparticles, microparticles, nanocomposites and nanoaggregates. *J Control Release* 2018;**269**:374−92.
17. Wuttke S, Lismont M, Escudero A, Rungtaweevoranit B, Parak WJ. Positioning metal-organic framework nanoparticles within the context of drug delivery—a comparison with mesoporous silica nanoparticles and dendrimers. *Biomaterials* 2017;**123**:172−83.
18. Li Z, Ye E, David Lakshminarayanan R, Loh XJ. Recent advances of using hybrid nanocarriers in remotely controlled therapeutic delivery. *Small* 2016;**12**:4782−806.
19. Zhou HC, Kitagawa S. Metal-organic frameworks (MOFs). *Chem Soc Rev* 2014;**43**:5415−8.
20. He Y, Zhang W, Guo T, Zhang G, Qin W, Zhang L, et al. Drug nanoclusters formed in confined nano-cages of CD-MOF: dramatic enhancement of solubility and bioavailability of azilsartan. *Acta Pharm Sin B* 2019;**9**:97−106.
21. Bonnefoy J, Legrand A, Quadrelli EA, Canivet J, Farrusseng D. Enantiopure peptide-functionalized metal-organic frameworks. *J Am Chem Soc* 2015;**137**:9409−16.
22. Chu C, Su M, Zhu J, Li D, Cheng H, Chen X, et al. Metal-organic framework nanoparticle-based biomineralization: a new strategy toward cancer treatment. *Theranostics* 2019;**9**:3134−49.
23. Li X, Porcel E, Menendez-Miranda M, Qiu J, Yang X, Serre C, et al. Highly porous hybrid metal-organic nanoparticles loaded with gemcitabine monophosphate: a multimodal approach to improve chemo- and radiotherapy. *ChemMedChem* 2020;**15**:274−83.
24. Wang X, Chen XZ, Alcântara CCJ, Sevim S, Hoop M, Terzopoulou A, et al. Mofbots: metal-organic-framework-based biomedical microrobots. *Adv Mater* 2019;**31**:e1901592.
25. Wang S, McGuirk CM, d'Aquino A, Mason JA, Mirkin CA. Metal-organic framework nanoparticles. *Adv Mater* 2018;**30**:e1800202.
26. Agostoni V, Horcajada P, Noiray M, Malanga M, Aykaç A, Jicsinszky L, et al. A "green" strategy to construct non-covalent, stable and bioactive coatings on porous mof nanoparticles. *Sci Rep* 2015;**5**:7925.
27. Aykaç A, Noiray M, Malanga M, Agostoni V, Casas-Solvas JM, É Fenyvesi, et al. A non-covalent "click chemistry" strategy to efficiently coat highly porous mof nanoparticles with a stable polymeric shell. *Biochim Biophys Acta Gen Subj* 2017;**1861**:1606−16.
28. Giménez-Marqués M, Bellido E, Berthelot T, Simón-Yarza T, Hidalgo T, Simón-Vázquez R, et al. Graftfast surface engineering to improve MOF nanoparticles furtiveness. *Small* 2018;**14**:e1801900.
29. Wuttke S, Braig S, Preiß T, Zimpel A, Sicklinger J, Bellomo C, et al. MOF nanoparticles coated by lipid bilayers and their uptake by cancer cells. *Chem Commun* 2015;**51**:15752−5.
30. Guerrero-Martínez A, Pérez-Juste J, Liz-Marzán LM. Recent progress on silica coating of nanoparticles and related nanomaterials. *Adv Mater* 2010;**22**:1182−95.
31. Baati T, Njim L, Neffati F, Kerkeni A, Bouttemi M, Gref R, et al. In depth analysis of the *in vivo* toxicity of nanoparticles of porous iron(III) metal-organic frameworks. *Chem Sci* 2013;**4**:1597−607.
32. Simon-Yarza T, Baati T, Neffati F, Njim L, Couvreur P, Serre C, et al. In *vivo* behavior of MIL-100 nanoparticles at early times after intravenous administration. *Int J Pharm* 2016;**511**:1042−7.
33. Li X, Semiramoth N, Hall S, Tafani V, Josse J, Laurent F, et al. Compartmentalized encapsulation of two antibiotics in porous nanoparticles: an efficient strategy to treat intracellular infections. *Part Part Syst Char* 2019;**36**:180360.
34. Wu MX, Yang YW. Metal-organic framework (MOF)-based drug/cargo delivery and cancer therapy. *Adv Mater* 2017;**29**:1606134.
35. He L, Liu Y, Lau J, Fan W, Li Q, Zhang C, et al. Recent progress in nanoscale metal-organic frameworks for drug release and cancer therapy. *Nanomedicine* 2019;**14**:1343−65.
36. Wang Y, Yan J, Wen N, Xiong H, Cai S, He Q, et al. Metal-organic frameworks for stimuli-responsive drug delivery. *Biomaterials* 2020;**230**:119619.
37. Cai W, Wang J, Chu C, Chen W, Wu C, Liu G. Metal-organic framework-based stimuli-responsive systems for drug delivery. *Adv Sci* 2019;**6**:1801526.
38. Giliopoulos D, Zamboulis A, Giannakoudakis D, Bikiaris D, Triantafyllidis K. Polymer/metal organic framework (MOF) nanocomposites for biomedical applications. *Molecules* 2020;**25**:185.
39. Osterrieth JWM, Fairen-Jimenez D. Metal-organic framework composites for theragnostic and drug delivery applications. *Biotechnol J* 2020:e2000005.
40. Liu Y, Zhao Y, Chen X. Bioengineering of metal-organic frameworks for nanomedicine. *Theranostics* 2019;**9**:3122−33.
41. Cai H, Huang YL, Li D. Biological metal-organic frameworks: structures, host−guest chemistry and bio-applications. *Coord Chem Rev* 2019;**378**:207−21.
42. Gao PF, Zheng LL, Liang LJ, Yang XX, Li YF, Huang CZ. A new type of pH-responsive coordination polymer sphere as a vehicle for targeted anticancer drug delivery and sustained release. *J Mater Chem B* 2013;**1**:3202−8.
43. An J, Geib SJ, Rosi NL. Cation-triggered drug release from a porous zinc-adeninate metal-organic framework. *J Am Chem Soc* 2009;**131**:8376−7.
44. Nagata S, Kokado K, Sada K. Metal-organic framework tethering pnipam for on-off controlled release in solution. *Chem Commun* 2015;**51**:8614−7.
45. Jiang K, Zhang L, Hu Q, Zhao D, Xia T, Lin W, et al. Pressure controlled drug release in a Zr-cluster-based MOF. *J Mater Chem B* 2016;**4**:6398−401.

46. Nel AE, Parak WJ, Chan WC, Xia T, Hersam MC, Brinker CJ, et al. Where are we heading in nanotechnology environmental health and safety and materials characterization?. *ACS Nano* 2015;**9**:5627−30.
47. Rojas S, Devic T, Horcajada P. Metal organic frameworks based on bioactive components. *J Mater Chem B* 2017;**5**:2560−73.
48. Horcajada P, Gref R, Baati T, Allan PK, Maurin G, Couvreur P, et al. Metal-organic frameworks in biomedicine. *Chem Rev* 2012;**112**:1232−68.
49. Dongmei L, Zhiwei W, Qi Z, Fuyi C, Yujuan S, Xiaodong L. Drinking water toxicity study of the environmental contaminant—bromate. *Regul Toxicol Pharmacol* 2015;**73**:802−10.
50. Leng X, Dong X, Wang W, Sai N, Yang C, You L, et al. Biocompatible Fe-based micropore metal-organic frameworks as sustained-release anticancer drug carriers. *Molecules* 2018;**23**:2490.
51. Gao X, Cui R, Song L, Liu Z. Hollow structural metal-organic frameworks exhibit high drug loading capacity, targeted delivery and magnetic resonance/optical multimodal imaging. *Dalton Trans* 2019;**48**:17291−7.
52. Zhang M, Chen YP, Bosch M, Gentle T, Wang K, Feng D, et al. Symmetry-guided synthesis of highly porous metal-organic frameworks with fluorite topology. *Angew Chem Int Ed Engl* 2014;**53**:815−8.
53. Abánades Lázaro I, Abánades Lázaro S, Forgan RS. Enhancing anticancer cytotoxicity through bimodal drug delivery from ultrasmall Zr MOF nanoparticles. *Chem Commun* 2018;**54**:2792−5.
54. Inoue Y, Nanri A, Murata I, Kanamoto I. Characterization of inclusion complex of coenzyme Q10 with the new carrier CD-MOF-1 prepared by solvent evaporation. *AAPS PharmSciTech* 2018;**19**:3048−56.
55. Schnabel J, Ettlinger R, Bunzen H. Zn-MOF-74 as pH-responsive drug-delivery system of arsenic trioxide. *ChemNanoMat* 2020;**6**:1229−36.
56. Alsaiari SK, Patil S, Alyami M, Alamoudi KO, Aleisa FA, Merzaban JS, et al. Endosomal escape and delivery of CRISPR/-CAS9 genome editing machinery enabled by nanoscale zeolitic imidazolate framework. *J Am Chem Soc* 2018;**140**:143−6.
57. Horcajada P, Chalati T, Serre C, Gillet B, Sebrie C, Baati T, et al. Porous metal-organic-framework nanoscale carriers as a potential platform for drug delivery and imaging. *Nat Mater* 2010;**9**:172−8.
58. Chalati T, Horcajada P, Couvreur P, Serre C, Ben Yahia M, Maurin G, et al. Porous metal organic framework nanoparticles to address the challenges related to busulfan encapsulation. *Nanomedicine* 2011;**6**:1683−95.
59. Anand R, Borghi F, Manoli F, Manet I, Agostoni V, Reschiglian P, et al. Host-guest interactions in Fe(III)-trimesate MOF nanoparticles loaded with doxorubicin. *J Phys Chem B* 2014;**118**:8532−9.
60. Agostoni V, Chalati T, Horcajada P, Willaime H, Anand R, Semiramoth N, et al. Towards an improved anti-HIV activity of NRTI *via* metal-organic frameworks nanoparticles. *Adv Healthc Mater* 2013;**2**:1630−7.
61. Agostoni V, Anand R, Monti S, Hall S, Maurin G, Horcajada P, et al. Impact of phosphorylation on the encapsulation of nucleoside analogues within porous iron(III) metal-organic framework MIL-100(Fe) nanoparticles. *J Mater Chem B* 2013;**1**:4231−42.
62. Marcos-Almaraz MT, Gref R, Agostoni V, Kreuz C, Clayette P, Serre C, et al. Towards improved HIV-microbicide activity through the co-encapsulation of NRTI drugs in biocompatible metal organic framework nanocarriers. *J Mater Chem B* 2017;**5**:8563−9.
63. Horcajada P, Serre C, Maurin G, Ramsahye NA, Balas F, Vallet-Regí M, et al. Flexible porous metal-organic frameworks for a controlled drug delivery. *J Am Chem Soc* 2008;**130**:6774−80.
64. Rojas S, Carmona FJ, Maldonado CR, Horcajada P, Hidalgo T, Serre C, et al. Nanoscaled zinc pyrazolate metal-organic frameworks as drug-delivery systems. *Inorg Chem* 2016;**55**:2650−63.
65. Bag PP, Wang D, Chen Z, Cao R. Outstanding drug loading capacity by water stable microporous MOF: a potential drug carrier. *Chem Commun* 2016;**52**:3669−72.
66. Li Z, Zhao S, Wang H, Peng Y, Tan Z, Tang B. Functional groups influence and mechanism research of UiO-66-type metal-organic frameworks for ketoprofen delivery. *Colloids Surf B Biointerfaces* 2019;**178**:1−7.
67. Li X, Guo T, Lachmanski L, Manoli F, Menendez-Miranda M, Manet I, et al. Cyclodextrin-based metal-organic frameworks particles as efficient carriers for lansoprazole: study of morphology and chemical composition of individual particles. *Int J Pharm* 2017;**531**:424−32.
68. Hu X, Wang C, Wang L, Liu Z, Wu L, Zhang G, et al. Nanoporous CD-MOF particles with uniform and inhalable size for pulmonary delivery of budesonide. *Int J Pharm* 2019;**564**:153−61.
69. Sun K, Li L, Yu X, Liu L, Meng Q, Wang F, et al. Functionalization of mixed ligand metal-organic frameworks as the transport vehicles for drugs. *J Colloid Interface Sci* 2017;**486**:128−35.
70. Simon MA, Anggraeni E, Soetaredjo FE, Santoso SP, Irawaty W, Thanh TC, et al. Hydrothermal synthesize of hf-free MIL-100(Fe) for isoniazid-drug delivery. *Sci Rep* 2019;**9**:16907.
71. Taherzade SD, Soleimannejad J, Tarlani A. Application of metal-organic framework nano-MIL-100(Fe) for sustainable release of doxycycline and tetracycline. *Nanomaterials* 2017;**7**:215.
72. Rezaei M, Abbasi A, Varshochian R, Dinarvand R, Jeddi-Tehrani M. NanoMIL-100(Fe) containing docetaxel for breast cancer therapy. *Artif Cells Nanomed Biotechnol* 2018;**46**:1390−401.
73. Taylor-Pashow KM, Della Rocca J, Xie Z, Tran S, Lin W. Post-synthetic modifications of iron-carboxylate nanoscale metal-organic frameworks for imaging and drug delivery. *J Am Chem Soc* 2009;**131**:14261−3.
74. Cunha D, Ben Yahia M, Hall S, Miller SR, Chevreau H, Elkaim E, et al. Rationale of drug encapsulation and release from biocompatible porous metal-organic frameworks. *Chem Mater* 2013;**25**:2767−76.
75. Sun CY, Qin C, Wang CG, Su ZM, Wang S, Wang XL, et al. Chiral nanoporous metal-organic frameworks with high porosity as materials for drug delivery. *Adv Mater* 2011;**23**:5629−32.
76. Oh H, Li T, An J. Drug release properties of a series of adenine-based metal-organic frameworks. *Chemistry* 2015;**21**:17010−5.
77. Sun CY, Qin C, Wang XL, Yang GS, Shao KZ, Lan YQ, et al. Zeolitic imidazolate framework-8 as efficient pH-sensitive drug delivery vehicle. *Dalton Trans* 2012;**41**:6906−9.
78. Gao H, Zhang Y, Chi B, Lin C, Tian F, Xu M, et al. Synthesis of 'dual-key-and-lock' drug carriers for imaging and improved drug release. *Nanotechnology* 2020;**31**:445102.
79. He C, Lu K, Liu D, Lin W. Nanoscale metal-organic frameworks for the co-delivery of cisplatin and pooled sirnas to enhance therapeutic efficacy in drug-resistant ovarian cancer cells. *J Am Chem Soc* 2014;**136**:5181−4.
80. Zhang W, Guo T, Wang C, He Y, Zhang X, Li G, et al. MOF capacitates cyclodextrin to mega-load mode for high-efficient delivery of valsartan. *Pharm Res (N Y)* 2019;**36**:117.
81. Férey G, Mellot-Draznieks C, Serre C, Millange F. Crystallized frameworks with giant pores: are there limits to the possible?. *Acc Chem Res* 2005;**38**:217−25.
82. Horcajada P, Serre C, Vallet-Regí M, Sebban M, Taulelle F, Férey G. Metal-organic frameworks as efficient materials for drug delivery. *Angew Chem Int Ed Engl* 2006;**45**:5974−8.
83. Xing K, Fan R, Wang F, Nie H, Du X, Gai S, et al. Dual-stimulus-triggered programmable drug release and luminescent ratiometric pH sensing from chemically stable biocompatible zinc metal-organic framework. *ACS Appl Mater Interfaces* 2018;**10**:22746−56.
84. Zheng H, Zhang Y, Liu L, Wan W, Guo P, Nyström AM, et al. One-pot synthesis of metal-organic frameworks with encapsulated target molecules and their applications for controlled drug delivery. *J Am Chem Soc* 2016;**138**:962−8.
85. Wu Q, Niu M, Chen X, Tan L, Fu C, Ren X, et al. Biocompatible and biodegradable zeolitic imidazolate framework/polydopamine nanocarriers for dual stimulus triggered tumor thermo-chemotherapy. *Biomaterials* 2018;**162**:132−43.

86. Sun Q, Bi H, Wang Z, Li C, Wang X, Xu J, et al. Hyaluronic acid-targeted and pH-responsive drug delivery system based on metal-organic frameworks for efficient antitumor therapy. *Biomaterials* 2019;**223**:119473.
87. Cavka JH, Jakobsen S, Olsbye U, Guillou N, Lamberti C, Bordiga S, et al. A new zirconium inorganic building brick forming metal organic frameworks with exceptional stability. *J Am Chem Soc* 2008;**130**:13850−1.
88. Lee DB, Roberts M, Bluchel CG, Odell RA. Zirconium: biomedical and nephrological applications. *Asaio J* 2010;**56**:550−6.
89. Röder R, Preiß T, Hirschle P, Steinborn B, Zimpel A, Höhn M, et al. Multifunctional nanoparticles by coordinative self-assembly of his-tagged units with metal-organic frameworks. *J Am Chem Soc* 2017;**139**:2359−68.
90. Abánades Lázaro I, Haddad S, Rodrigo-Muñoz JM, Marshall RJ, Sastre B, Del Pozo V, et al. Surface-functionalization of Zr-fumarate MOF for selective cytotoxicity and immune system compatibility in nanoscale drug delivery. *ACS Appl Mater Interfaces* 2018;**10**:31146−57.
91. Smaldone RA, Forgan RS, Furukawa H, Gassensmith JJ, Slawin AM, Yaghi OM, et al. Metal-organic frameworks from edible natural products. *Angew Chem Int Ed Engl* 2010;**49**:8630−4.
92. Han Y, Liu W, Huang J, Qiu S, Zhong H, Liu D, et al. Cyclodextrin-based metal-organic frameworks (CD-MOFs) in pharmaceutics and biomedicine. *Pharmaceutics* 2018;**10**:271.
93. Kritskiy I, Volkova T, Surov A, Terekhova I. γ-Cyclodextrin-metal organic frameworks as efficient microcontainers for encapsulation of leflunomide and acceleration of its transformation into teriflunomide. *Carbohydr Polym* 2019;**216**:224−30.
94. He Y, Xu J, Sun X, Ren X, Maharjan A, York P, et al. Cuboidal tethered cyclodextrin frameworks tailored for hemostasis and injured vessel targeting. *Theranostics* 2019;**9**:2489−504.
95. McKinlay AC, Morris RE, Horcajada P, Férey G, Gref R, Couvreur P, et al. BioMOFs: metal-organic frameworks for biological and medical applications. *Angew Chem Int Ed Engl* 2010;**49**:6260−6.
96. Li Y, Li X, Guan Q, Zhang C, Xu T, Dong Y, et al. Strategy for chemotherapeutic delivery using a nanosized porous metal-organic framework with a central composite design. *Int J Nanomed* 2017;**12**:1465−74.
97. Xiao J, Zhu Y, Huddleston S, Li P, Xiao B, Farha OK, et al. Copper metal-organic framework nanoparticles stabilized with folic acid improve wound healing in diabetes. *ACS Nano* 2018;**12**:1023−32.
98. Hou L, Qin Y, Li J, Qin S, Huang Y, Lin T, et al. A ratiometric multicolor fluorescence biosensor for visual detection of alkaline phosphatase activity *via* a smartphone. *Biosens Bioelectron* 2019;**143**:111605.
99. Jo JH, Kim HC, Huh S, Kim Y, Lee DN. Antibacterial activities of Cu-MOFs containing glutarate and bipyridyl ligands. *Dalton Trans* 2019;**48**:8084−93.
100. Lu W, Wei Z, Gu ZY, Liu TF, Park J, Park J, et al. Tuning the structure and function of metal-organic frameworks *via* linker design. *Chem Soc Rev* 2014;**43**:5561−93.
101. Simon-Yarza T, Mielcarek A, Couvreur P, Serre C. Nanoparticles of metal-organic frameworks: on the road to *in vivo* efficacy in biomedicine. *Adv Mater* 2018;**30**:e1707365.
102. Bala S, Bhattacharya S, Goswami A, Adhikary A, Konar S, Mondal R. Designing functional metal-organic frameworks by imparting a hexanuclear copper based secondary building unit (sbu) specific properties: structural correlation with magnetic and photocatalytic activity. *Cryst Growth Des* 2014;**14**:6391−8.
103. Gimenez-Marques M, Hidalgo T, Serre C, Horcajada P. Nanostructured metal-organic frameworks and their bio-related applications. *Coord Chem Rev* 2016;**307**:342−60.
104. Xu H, Cai J, Xiang S, Zhang Z, Wu C, Rao X, et al. A cationic microporous metal-organic framework for highly selective separation of small hydrocarbons at room temperature. *J Mater Chem* 2013;**1**:9916−21.
105. Gramaccioli CM. The crystal structure of zinc glutamate dihydrate. *Acta Crystallogr* 1966;**21**:600−5.
106. Imaz I, Rubio-Martínez M, An J, Solé-Font I, Rosi NL, Maspoch D. Metal-biomolecule frameworks (MBioFs). *Chem Commun* 2011;**47**:7287−302.
107. Miller SR, Heurtaux D, Baati T, Horcajada P, Grenèche JM, Serre C. Biodegradable therapeutic MOFs for the delivery of bioactive molecules. *Chem Commun* 2010;**46**:4526−8.
108. Levine DJ, Runčevski T, Kapelewski MT, Keitz BK, Oktawiec J, Reed DA, et al. Olsalazine-based metal-organic frameworks as biocompatible platforms for H_2 adsorption and drug delivery. *J Am Chem Soc* 2016;**138**:10143−50.
109. Rieter WJ, Pott KM, Taylor KM, Lin W. Nanoscale coordination polymers for platinum-based anticancer drug delivery. *J Am Chem Soc* 2008;**130**:11584−5.
110. Stock N, Biswas S. Synthesis of metal-organic frameworks (MOFs): routes to various MOF topologies, morphologies, and composites. *Chem Rev* 2012;**112**:933−69.
111. Kumar S, Jain S, Nehra M, Dilbaghi N, Kim KH. Green synthesis of metal-organic frameworks: a state-of-the-art review of potential environmental and medical applications. *Coord Chem Rev* 2020;**420**:213407.
112. Jhung SH, Lee JH, Forster PM, Férey G, Cheetham AK, Chang JS. Microwave synthesis of hybrid inorganic-organic porous materials: phase-selective and rapid crystallization. *Chemistry* 2006;**12**:7899−905.
113. Mendes RF, Rocha J, Paz FAA. *Microwave synthesis of metal-organic frameworks. Metal-organic frameworks for biomedical applications*. Amsterdam: Elsevier; 2020. p. 159−76.
114. Rieter WJ, Taylor KM, An H, Lin W, Lin W. Nanoscale metal-organic frameworks as potential multimodal contrast enhancing agents. *J Am Chem Soc* 2006;**128**:9024−5.
115. Sun CY, Qin C, Wang XL, Su ZM. Metal-organic frameworks as potential drug delivery systems. *Expet Opin Drug Deliv* 2013;**10**:89−101.
116. Taylor KM, Jin A, Lin W. Surfactant-assisted synthesis of nanoscale gadolinium metal-organic frameworks for potential multimodal imaging. *Angew Chem Int Ed Engl* 2008;**47**:7722−5.
117. Sun Y, Zhou HC. Recent progress in the synthesis of metal-organic frameworks. *Sci Technol Adv Mater* 2015;**16**:054202.
118. Das AK, Vemuri RS, Kutnyakov I, McGrail BP, Motkuri RK. An efficient synthesis strategy for metal-organic frameworks: dry-gel synthesis of MOF-74 framework with high yield and improved performance. *Sci Rep* 2016;**6**:28050.
119. Juan-Alcaiz J, Gascon J, Kapteijn F. Metal-organic frameworks as scaffolds for the encapsulation of active species: state of the art and future perspectives. *ChemInform* 2012;**22**:10102−18.
120. Pichon A, James SL. An array-based study of reactivity under solvent-free mechanochemical conditions—insights and trends. *CrystEngComm* 2008;**10**:1839−47.
121. Pichon A, Lazuen-Garay A, James SL. Solvent-free synthesis of a microporous metal-organic framework. *CrystEngComm* 2006;**8**:211−4.
122. Lee YR, Kim J, Ahn WS. Synthesis of metal-organic frameworks: a mini review. *Kor J Chem Eng* 2013;**30**:1667−80.
123. Carné A, Carbonell C, Imaz I, Maspoch D. Nanoscale metal-organic materials. *Chem Soc Rev* 2011;**40**:291−305.
124. Shekhah O, Wang H, Kowarik S, Schreiber F, Paulus M, Tolan M, et al. Step-by-step route for the synthesis of metal-organic frameworks. *J Am Chem Soc* 2007;**129**:15118−9.
125. Banerjee R, Phan A, Wang B, Knobler C, Furukawa H, O'Keeffe M, et al. High-throughput synthesis of zeolitic imidazolate frameworks and application to CO_2 capture. *Science* 2008;**319**:939−43.

126. Tranchemontagne DJ, Hunt JR, Yaghi OM. Room temperature synthesis of metal-organic frameworks: MOF-5, MOF-74, MOF-177, MOF-199, and IRMOF-0. *Tetrahedron* 2008;**64**:8553−7.
127. Cravillon J, MüNzer S, Lohmeier SJ, Feldhoff A, Huber K, Wiebcke M. Rapid room-temperature synthesis and characterization of nanocrystals of a prototypical zeolitic imidazolate framework. *Chem Mater* 2009;**21**:1410−2.
128. Forgan RS, Smaldone RA, Gassensmith JJ, Furukawa H, Cordes DB, Li Q, et al. Nanoporous carbohydrate metal-organic frameworks. *J Am Chem Soc* 2012;**134**:406−17.
129. Liu B, Li H, Xu X, Li X, Lv N, Singh V, et al. Optimized synthesis and crystalline stability of γ-cyclodextrin metal-organic frameworks for drug adsorption. *Int J Pharm* 2016;**514**:212−9.
130. Lu HJ, Yang XN, Li SX, Zhang Y, Sha JQ, Li CD, et al. Study on a new cyclodextrin based metal-organic framework with chiral helices. *Inorg Chem Commun* 2015;**61**:48−52.
131. Sha J, Yang X, Sun L, Zhang X, Li S, Li J, et al. Unprecedented α-cyclodextrin metal-organic frameworks with chirality: structure and drug adsorptions. *Polyhedron* 2017;**127**:396−402.
132. Eddaoudi M, Kim J, Rosi N, Vodak D, Wachter J, O'Keeffe M, et al. Systematic design of pore size and functionality in isoreticular mofs and their application in methane storage. *Science* 2002;**295**:469−72.
133. Ding HY, Wu L, Guo T, Zhang ZY, Garba BM, Gao G, et al. CD-MOFs crystal transformation from dense to highly porous form for efficient drug loading. *Cryst Growth Des* 2019;**19**:3888−94.
134. John NS, Scherb C, Shöâeè M, Anderson MW, Attfield MP, Bein T. Single layer growth of sub-micron metal-organic framework crystals observed by *in situ* atomic force microscopy. *Chem Commun* 2009: 6294−6.
135. Bang JH, Suslick KS. Applications of ultrasound to the synthesis of nanostructured materials. *Adv Mater* 2010;**22**:1039−59.
136. Ni Z, Masel RI. Rapid production of metal-organic frameworks *via* microwave-assisted solvothermal synthesis. *J Am Chem Soc* 2006; **128**:12394−5.
137. Jhung SH, Lee JH, Chang JS. Microwave synthesis of a nanoporous hybrid material, chromium trimesate. *Bull Kor Chem Soc* 2005;**26**: 880−1.
138. Agostoni V, Horcajada P, Rodriguez-Ruiz V, Willaime H, Couvreur P, Serre C, et al. 'Green' fluorine-free mesoporous iron(III) trimesate nanoparticles for drug delivery. *Green Mater* 2013;**1**:209−17.
139. Chalati T, Horcajada P, Gref R, Couvreur P, Serre C. Optimisation of the synthesis of MOF nanoparticles made of flexible porous iron fumarate MIL-88A. *J Mater Chem* 2011;**21**:2220−7.
140. Thi Dang Y, Hoang HT, Dong HC, Bui K-BT, Nguyen LHT, Phan TB, et al. Microwave-assisted synthesis of nano Hf- and Zr-based metal-organic frameworks for enhancement of curcumin adsorption. *Microporous Mesoporous Mater* 2020;**298**:110064.
141. Fu C, Zhou H, Tan L, Huang Z, Wu Q, Ren X, et al. Microwave-activated mn-doped zirconium metal-organic framework nanocubes for highly effective combination of microwave dynamic and thermal therapies against cancer. *ACS Nano* 2018;**12**:2201−10.
142. Ranjbar M, Pardakhty A, Amanatfard A, Asadipour A. Efficient drug delivery of β-estradiol encapsulated in Zn-metal-organic framework nanostructures by microwave-assisted coprecipitation method. *Drug Des Dev Ther* 2018;**12**:2635−43.
143. George P, Das RK, Chowdhury P. Facile microwave synthesis of Ca-BDC metal organic framework for adsorption and controlled release of curcumin. *Microporous Mesoporous Mater* 2019;**281**:161−71.
144. Liu BT, He YP, Han LP, Singh V, Xu XN, Guo T, et al. Microwave-assisted rapid synthesis of gamma-cyclodextrin metal-organic frameworks for size control and efficient drug loading. *Cryst Growth Des* 2017;**17**:1654−60.
145. Schlesinger M, Schulze S, Hietschold M, Mehring M. Evaluation of synthetic methods for microporous metal-organic frameworks exemplified by the competitive formation of $[Cu_2(btc)_3(H2O)_3]$ and $[Cu_2(btc)(OH)(H_2O)]$. *Microporous Mesoporous Mater* 2010;**132**: 121−7.
146. Park HJ, Jeong DH, Noh SG, Lim HJ, Park JY. Identification of secondary chemistry teachers' ability to carry-out experimentation. *J Kor Chem Soc* 2009;**53**:765−73.
147. Aguiar LW, Otto GP, Kupfer VL, Fávaro SL, Silva CTP, Moisés MP, et al. Simple, fast, and low-cost synthesis of MIL-100 and MIL-88B in a modified domestic microwave oven. *Mater Lett* 2020;**276**: 128127.
148. Jones WD, Kosar WP. Carbon-hydrogen bond activation by ruthenium for the catalytic synthesis of indoles. *J Am Chem Soc* 1986;**108**: 5640−1.
149. Li ZQ, Qiu LG, Xu T, Wu Y, Wang W, Wu ZY, et al. Ultrasonic synthesis of the microporous metal-organic framework $Cu_3(BTC)_2$ at ambient temperature and pressure: an efficient and environmentally friendly method. *Mater Lett* 2009;**63**:78−80.
150. Son WJ, Kim J, Kim J, Ahn WS. Sonochemical synthesis of MOF-5. *Chem Commun* 2008:6336−8.
151. Yang DA, Cho HY, Kim J, Yang ST, Ann WS. CO_2 capture and conversion using Mg-MOF-74 prepared by a sonochemical method. *Energy Environ Sci* 2012;**5**:6465−73.
152. Kim J, Yang ST, Choi SB, Sim J, Kim J, Ahn WS. Control of catenation in CuTATB-*n* metal-organic frameworks by sonochemical synthesis and its effect on CO_2 adsorption. *J Mater Chem* 2011;**21**: 3070−6.
153. Hernández JG, Friscic T. Metal-catalyzed organic reactions using mechanochemistry. *Tetrahedron Lett* 2015;**56**:4253−65.
154. Friscic T, Halasz I, Strukil V, Eckert-Maksic M, Dinnebier RE. Clean and efficient synthesis using mechanochemistry: coordination polymers, metal-organic frameworks and metallodrugs. *Croat Chem Acta* 2012;**85**:367−78.
155. Bennett TD, Cao S, Tan JC, Keen DA, Bithell EG, Beldon PJ, et al. Facile mechanosynthesis of amorphous zeolitic imidazolate frameworks. *J Am Chem Soc* 2011;**133**:14546−9.
156. Bennett TD, Simoncic P, Moggach SA, Gozzo F, Macchi P, Keen DA, et al. Reversible pressure-induced amorphization of a zeolitic imidazolate framework (ZIF-4). *Chem Commun* 2011;**47**: 7983−5.
157. Bennett TD, Keen DA, Tan JC, Barney ER, Goodwin AL, Cheetham AK. Thermal amorphization of zeolitic imidazolate frameworks. *Angew Chem Int Ed Engl* 2011;**50**:3067−71.
158. Mueller U, Puetter H, Hesse M, Wessel H, Schubert M, Huff J, et al., inventors; BASF Aktiengesellschaft, BASF AG, assignees. Method for electrochemical production of a crystalline porous metal organic skeleton material. United States patent US No. 2011105776. 2011 May 5.
159. Joaristi AM, Juan-Alcaiz J, Serra-Crespo P, Kapteijn F, Gascon J. Electrochemical synthesis of some archetypical Zn^{2+}, Cu^{2+}, and Al^{3+} metal organic frameworks. *Cryst Growth Des* 2012;**12**: 3489−98.
160. Sun S, Murray CB, Weller D, Folks L, Moser A. Monodisperse FePt nanoparticles and ferromagnetic FePt nanocrystal superlattices. *Science* 2000;**287**:1989−92.
161. Mokari T, Zhang M, Yang P. Shape, size, and assembly control of PbTe nanocrystals. *J Am Chem Soc* 2007;**129**:9864−5.
162. Peng X, Manna L, Yang W, Wickham J, Scher E, Kadavanich A, et al. Shape control of CdSe nanocrystals. *Nature* 2000;**404**:59−61.
163. Manna L, Milliron DJ, Meisel A, Scher EC, Alivisatos AP. Controlled growth of tetrapod-branched inorganic nanocrystals. *Nat Mater* 2003;**2**:382−5.
164. Truong NP, Whittaker MR, Mak CW, Davis TP. The importance of nanoparticle shape in cancer drug delivery. *Expet Opin Drug Deliv* 2015;**12**:129−42.
165. Seoane B, Dikhtiarenko A, Mayoral A, Tellez C, Coronas J, Kapteijn F, et al. Metal organic framework synthesis in the presence of surfactants: towards hierarchical MOFs? *CrystEngComm* 2015;**17**: 1693−700.
166. Qiu LG, Li ZQ, Wu Y, Wang W, Xu T, Jiang X. Facile synthesis of nanocrystals of a microporous metal-organic framework by an

ultrasonic method and selective sensing of organoamines. *Chem Commun* 2008:3642−4.
167. Morris W, Wang S, Cho D, Auyeung E, Li P, Farha OK, et al. Role of modulators in controlling the colloidal stability and polydispersity of the UiO-66 metal-organic framework. *ACS Appl Mater Interfaces* 2017;**9**:33413−8.
168. Gutov OV, Molina S, Escudero-Adán EC, Shafir A. Modulation by amino acids: toward superior control in the synthesis of zirconium metal-organic frameworks. *Chemistry* 2016;**22**:13582−7.
169. Xu X, Lu Y, Yang Y, Nosheen F, Wang X. Tuning the growth of metal-organic framework nanocrystals by using polyoxometalates as coordination modulators. *Sci China Mater* 2015;**58**:370−7.
170. Rosnes MH, Nesse FS, Opitz M, Dietzel PDC. Morphology control in modulated synthesis of metal-organic framework CPO-27. *Microporous Mesoporous Mater* 2019;**275**:207−13.
171. Bentz KC, Ayala S, Kalaj M, Cohen SM. Polyacids as modulators for the synthesis of UiO-66. *Aust J Chem* 2019;**72**:848−51.
172. Müller K, Singh Malhi J, Wohlgemuth J, Fischer RA, Wöll C, Gliemann H, et al. Water as a modulator in the synthesis of surface-mounted metal-organic framework films of type HKUST-1. *Dalton Trans* 2018;**47**:16474−9.
173. Abánades Lázaro I, Wells CJR, Forgan RS. Multivariate modulation of the Zr MOF UiO-66 for defect-controlled combination anticancer drug delivery. *Angew Chem Int Ed Engl* 2020;**59**:5211−7.
174. Horcajada P, Serre C, Grosso D, Boissiere C, Perruchas S, Sanchez C, et al. Colloidal route for preparing optical thin films of nanoporous metal-organic frameworks. *Adv Mater* 2010;**21**:1931−5.
175. Reineke TM, Eddaoudi M, Fehr M, Kelley D, Yaghi OM. From condensed lanthanide coordination solids to microporous frameworks having accessible metal sites. *J Am Chem Soc* 2015;**121**:1651−7.
176. Kerbellec N, Catala L, Daiguebonne C, Gloter A, Stephan O, Bünzli JC, et al. Luminescent coordination nanoparticles. *New J Chem* 2008;**32**:584−7.
177. Cho W, Lee HJ, Oh M. Growth-controlled formation of porous coordination polymer particles. *J Am Chem Soc* 2008;**130**:16943−6.
178. Hatakeyama W, Sanchez TJ, Rowe MD, Serkova NJ, Liberatore MW, Boyes SG. Synthesis of gadolinium nanoscale metal-organic framework with hydrotropes: manipulation of particle size and magnetic resonance imaging capability. *ACS Appl Mater Interfaces* 2011;**3**:1502−10.
179. Bhat M, Gaikar VG. Characterization of interaction between butylbenzene sulfonates and cetyl pyridinium chloride in a mixed aggregate system. *Langmuir* 2000;**16**:1580−92.
180. Garay AL, Pichon A, James SL. Solvent-free synthesis of metal complexes. *Chem Soc Rev* 2007;**36**:846−55.
181. Friscic Tomislav. New opportunities for materials synthesis using mechanochemistry. *J Mater Chem* 2010;**20**:7599−605.
182. Furukawa Y, Ishiwata T, Sugikawa K, Kokado K, Sada K. Nano- and microsized cubic gel particles from cyclodextrin metal-organic frameworks. *Angew Chem Int Ed Engl* 2012;**51**:10566−9.
183. Qiu C, Wang J, Qin Y, Fan H, Xu X, Jin Z. Green synthesis of cyclodextrin-based metal-organic frameworks through the seed-mediated method for the encapsulation of hydrophobic molecules. *J Agric Food Chem* 2018;**66**:4244−50.
184. Li H, Lv N, Li X, Liu B, Feng J, Ren X, et al. Composite CD-MOF nanocrystals-containing microspheres for sustained drug delivery. *Nanoscale* 2017;**9**:7454−63.
185. Kritskiy I, Volkova T, Sapozhnikova T, Mazur A, Tolstoy P, Terekhova I. Methotrexate-loaded metal-organic frameworks on the basis of γ-cyclodextrin: design, characterization, *in vitro* and *in vivo* investigation. *Mater Sci Eng C Mater Biol Appl* 2020;**111**:110774.
186. Zhuang J, Kuo CH, Chou LY, Liu DY, Weerapana E, Tsung CK. Optimized metal-organic-framework nanospheres for drug delivery: evaluation of small-molecule encapsulation. *ACS Nano* 2014;**8**:2812−9.
187. Chen X, Tong R, Shi Z, Yang B, Liu H, Ding S, et al. MOF nanoparticles with encapsulated autophagy inhibitor in controlled drug delivery system for antitumor. *ACS Appl Mater Interfaces* 2018;**10**:2328−37.
188. Noorian SA, Hemmatinejad N, Navarro JAR. BioMOF@cellulose fabric composites for bioactive molecule delivery. *J Inorg Biochem* 2019;**201**:110818.
189. Lyu F, Zhang Y, Zare RN, Ge J, Liu Z. One-pot synthesis of protein-embedded metal-organic frameworks with enhanced biological activities. *Nano Lett* 2014;**14**:5761−5.
190. Wu X, Ge J, Yang C, Hou M, Liu Z. Facile synthesis of multiple enzyme-containing metal-organic frameworks in a biomolecule-friendly environment. *Chem Commun* 2015;**51**:13408−11.
191. Vassaki M, Papathanasiou KE, Hadjicharalambous C, Chandrinou D, Turhanen P, Choquesillo-Lazarte D, et al. Self-sacrificial MOFs for ultra-long controlled release of bisphosphonate anti-osteoporotic drugs. *Chem Commun* 2020;**56**:5166−9.
192. Devautour-Vinot S, Martineau C, Diaby S, Ben-Yahia M, Miller S, Serre C, et al. Caffeine confinement into a series of functionalized porous zirconium MOFs: a joint experimental/modeling exploration. *J Phys Chem C* 2013;**117**:11694−704.
193. Javanbakht S, Nezhad-Mokhtari P, Shaabani A, Arsalani N, Ghorbani M. Incorporating Cu-based metal-organic framework/drug nanohybrids into gelatin microsphere for ibuprofen oral delivery. *Mater Sci Eng C Mater Biol Appl* 2019;**96**:302−9.
194. He Y, Hou X, Guo J, He Z, Guo T, Liu Y, et al. Activation of a gamma-cyclodextrin-based metal-organic framework using supercritical carbon dioxide for high-efficient delivery of honokiol. *Carbohydr Polym* 2020;**235**:115935.
195. Simon-Yarza T, Giménez-Marqués M, Mrimi R, Mielcarek A, Gref R, Horcajada P, et al. A smart metal-organic framework nanomaterial for lung targeting. *Angew Chem Int Ed Engl* 2017;**56**:15565−9.
196. Noorian SA, Hemmatinejad N, Navarro JAR. Bioactive molecule encapsulation on metal-organic framework *via* simple mechanochemical method for controlled topical drug delivery systems. *Microporous Mesoporous Mater* 2020;**302**:110199.
197. Wang Z, Cohen SM. Postsynthetic modification of metal-organic frameworks. *Chem Soc Rev* 2009;**38**:1315−29.
198. Morris W, Briley WE, Auyeung E, Cabezas MD, Mirkin CA. Nucleic acid−metal organic framework (MOF) nanoparticle conjugates. *J Am Chem Soc* 2014;**136**:7261−4.
199. Cao SL, Yue DM, Li XH, Smith TJ, Li N, Zong MH, et al. Novel nano-/micro-biocatalyst: soybean epoxide hydrolase immobilized on UiO-66-NH2 MOF for efficient biosynthesis of enantiopure (*R*)-1,2-octanediol in deep eutectic solvents. *ACS Sustain Chem Eng* 2016;**4**:3586−95.
200. Cunha D, Gaudin C, Colinet I, Horcajada P, Maurin G, Serre C. Rationalization of the entrapping of bioactive molecules into a series of functionalized porous zirconium terephthalate MOFs. *J Mater Chem B* 2013;**1**:1101−8.
201. Xu Z, Li M, Li X, Liu X, Ma F, Wu S, et al. Antibacterial activity of silver doped titanate nanowires on Ti implants. *ACS Appl Mater Interfaces* 2016;**8**:16584−94.
202. Xu H, Zhang G, Xu K, Wang L, Yu L, Xing MMQ, et al. Mussel-inspired dual-functional PEG hydrogel inducing mineralization and inhibiting infection in maxillary bone reconstruction. *Mater Sci Eng C Mater Biol Appl* 2018;**90**:379−86.
203. Lin S, Liu X, Tan L, Cui Z, Yang X, Yeung KWK, et al. Porous iron-carboxylate metal-organic framework: a novel bioplatform with sustained antibacterial efficacy and nontoxicity. *ACS Appl Mater Interfaces* 2017;**9**:19248−57.
204. Gallis DFS, Butler KS, Agola JO, Pearce CJ, McBride AA. Antibacterial countermeasures *via* metal-organic framework-supported sustained therapeutic release. *ACS Appl Mater Interfaces* 2019;**11**:7782−91.
205. Zhang X, Liu L, Huang L, Zhang W, Wang R, Yue T, et al. The highly efficient elimination of intracellular bacteria *via* a metal organic framework (MOF)-based three-in-one delivery system. *Nanoscale* 2019;**11**:9468−77.

206. Guo A, Durymanov M, Permyakova A, Sene S, Serre C, Reineke J. Metal organic framework (MOF) particles as potential bacteria-mimicking delivery systems for infectious diseases: characterization and cellular internalization in alveolar macrophages. *Pharm Res (N Y)* 2019;**36**:53.
207. Yu M, You D, Zhuang J, Lin S, Dong L, Weng S, et al. Controlled release of naringin in metal-organic framework-loaded mineralized collagen coating to simultaneously enhance osseointegration and antibacterial activity. *ACS Appl Mater Interfaces* 2017;**9**:19698−705.
208. Wang S, Wang Y, Peng Y, Yang X. Exploring the antibacteria performance of multicolor Ag, Au, and Cu nanoclusters. *ACS Appl Mater Interfaces* 2019;**11**:8461−9.
209. Tran CD, Prosenc F, Franko M, Benzi G. One-pot synthesis of biocompatible silver nanoparticle composites from cellulose and keratin: characterization and antimicrobial activity. *ACS Appl Mater Interfaces* 2016;**8**:34791−801.
210. Shakya S, He Y, Ren X, Guo T, Maharjan A, Luo T, et al. Ultrafine silver nanoparticles embedded in cyclodextrin metal-organic frameworks with GRGDS functionalization to promote antibacterial and wound healing application. *Small* 2019;**15**:e1901065.
211. Yang Y, Wu X, He C, Huang J, Yin S, Zhou M, et al. Metal-organic framework/Ag-based hybrid nanoagents for rapid and synergistic bacterial eradication. *ACS Appl Mater Interfaces* 2020;**12**:13698−708.
212. Mohamed NA, Davies RP, Lickiss PD, Ahmetaj-Shala B, Reed DM, Gashaw HH, et al. Chemical and biological assessment of metal organic frameworks (MOFs) in pulmonary cells and in an acute *in vivo* model: relevance to pulmonary arterial hypertension therapy. *Pulm Circ* 2017;**7**:643−53.
213. Wyszogrodzka-Gaweł G, Dorożyński P, Giovagnoli S, Strzempek W, Pesta E, Węglarz WP, et al. An inhalable theranostic system for local tuberculosis treatment containing an isoniazid loaded metal organic framework Fe-MIL-101-NH_2-from raw MOF to drug delivery system. *Pharmaceutics* 2019;**11**:687.
214. Wyszogrodzka G, Dorożyński P, Gil B, Roth WJ, Strzempek M, Marszałek B, et al. Iron-based metal-organic frameworks as a theranostic carrier for local tuberculosis therapy. *Pharm Res (N Y)* 2018;**35**:144.
215. Duan Y, Ye F, Huang Y, Qin Y, He C, Zhao S. One-pot synthesis of a metal-organic framework-based drug carrier for intelligent glucose-responsive insulin delivery. *Chem Commun* 2018;**54**:5377−80.
216. Yang XX, Feng P, Cao J, Liu W, Tang Y. Composition-engineered metal-organic framework-based microneedles for glucose-mediated transdermal insulin delivery. *ACS Appl Mater Interfaces* 2020;**12**:13613−21.
217. Kim SN, Park CG, Huh BK, Lee SH, Min CH, Lee YY, et al. Metal-organic frameworks, NH_2-MIL-88(Fe), as carriers for ophthalmic delivery of brimonidine. *Acta Biomater* 2018;**79**:344−53.
218. Gandara-Loe J, Souza BE, Missyul A, Giraldo G, Tan JC, Silvestre-Albero J. MOF-based polymeric nanocomposite films as potential materials for drug delivery devices in ocular therapeutics. *ACS Appl Mater Interfaces* 2020;**12**:30189−97.
219. Zhang H, Jiang W, Liu R, Zhang J, Zhang D, Li Z, et al. Rational design of metal organic framework nanocarrier-based codelivery system of doxorubicin hydrochloride/verapamil hydrochloride for overcoming multidrug resistance with efficient targeted cancer therapy. *ACS Appl Mater Interfaces* 2017;**9**:19687−97.
220. Zhang L, Wang Z, Zhang Y, Cao F, Dong K, Ren J, et al. Erythrocyte membrane cloaked metal-organic framework nanoparticle as biomimetic nanoreactor for starvation-activated colon cancer therapy. *ACS Nano* 2018;**12**:10201−11.
221. Jiang W, Zhang H, Wu J, Zhai G, Li Z, Luan Y, et al. Cus@MOF-based well-designed quercetin delivery system for chemo-photothermal therapy. *ACS Appl Mater Interfaces* 2018;**10**:34513−23.
222. Huang J, Li N, Zhang C, Meng Z. Metal-organic framework as a microreactor for *in situ* fabrication of multifunctional nanocomposites for photothermal-chemotherapy of tumors *in vivo*. *ACS Appl Mater Interfaces* 2018;**10**:38729−38.
223. Gao S, Zheng P, Li Z, Feng X, Yan W, Chen S, et al. Biomimetic O_2-evolving metal-organic framework nanoplatform for highly efficient photodynamic therapy against hypoxic tumor. *Biomaterials* 2018;**178**:83−94.
224. Meng X, Deng J, Liu F, Guo T, Liu M, Dai P, et al. Triggered all-active metal organic framework: ferroptosis machinery contributes to the apoptotic photodynamic antitumor therapy. *Nano Lett* 2019;**19**:7866−76.
225. Min H, Wang J, Qi Y, Zhang Y, Han X, Xu Y, et al. Biomimetic metal-organic framework nanoparticles for cooperative combination of antiangiogenesis and photodynamic therapy for enhanced efficacy. *Adv Mater* 2019;**31**:e1808200.
226. Haddad S, Abánades Lázaro I, Fantham M, Mishra A, Silvestre-Albero J, Osterrieth JWM, et al. Design of a functionalized metal-organic framework system for enhanced targeted delivery to mitochondria. *J Am Chem Soc* 2020;**142**:6661−74.
227. Yao J, Liu Y, Wang J, Jiang Q, She D, Guo H, et al. On-demand CO release for amplification of chemotherapy by MOF functionalized magnetic carbon nanoparticles with NIR irradiation. *Biomaterials* 2019;**195**:51−62.
228. Ku MS, Dulin W. A biopharmaceutical classification-based right-first-time formulation approach to reduce human pharmacokinetic variability and project cycle time from first-in-human to clinical proof-of-concept. *Pharm Dev Technol* 2012;**17**:285−302.
229. Xu J, Wu L, Guo T, Zhang G, Wang C, Li H, et al. A "ship-in-a-bottle" strategy to create folic acid nanoclusters inside the nanocages of γ-cyclodextrin metal-organic frameworks. *Int J Pharm* 2019;**556**:89−96.
230. Hartlieb KJ, Ferris DP, Holcroft JM, Kandela I, Stern CL, Nassar MS, et al. Encapsulation of ibuprofen in CD-MOF and related bioavailability studies. *Mol Pharm* 2017;**14**:1831−9.
231. Moussa Z, Hmadeh M, Abiad MG, Dib OH, Patra D. Encapsulation of curcumin in cyclodextrin-metal organic frameworks: dissociation of loaded CD-MOFs enhances stability of curcumin. *Food Chem* 2016;**212**:485−94.
232. Zhang G, Meng F, Guo Z, Guo T, Peng H, Xiao J, et al. Enhanced stability of vitamin a palmitate microencapsulated by γ-cyclodextrin metal-organic frameworks. *J Microencapsul* 2018;**35**:249−58.
233. He H, Han H, Shi H, Tian Y, Sun F, Song Y, et al. Construction of thermophilic lipase-embedded metal-organic frameworks *via* biomimetic mineralization: a biocatalyst for ester hydrolysis and kinetic resolution. *ACS Appl Mater Interfaces* 2016;**8**:24517−24.
234. Liang K, Coghlan CJ, Bell SG, Doonan C, Falcaro P. Enzyme encapsulation in zeolitic imidazolate frameworks: a comparison between controlled co-precipitation and biomimetic mineralisation. *Chem Commun* 2016;**52**:473−6.
235. Abuçafy MP, Caetano BL, Chiari-Andréo BG, Fonseca-Santos B, do Santos AM, Chorilli M, et al. Supramolecular cyclodextrin-based metal-organic frameworks as efficient carrier for anti-inflammatory drugs. *Eur J Pharm Biopharm* 2018;**127**:112−9.
236. Wu YN, Zhou M, Li S, Li Z, Li J, Wu B, et al. Magnetic metal-organic frameworks: γ-Fe_2O_3@MOFs *via* confined *in situ* pyrolysis method for drug delivery. *Small* 2014;**10**:2927−36.
237. Yin X, Yang B, Chen B, He M, Hu B. Multifunctional gold nanocluster decorated metal-organic framework for real-time monitoring of targeted drug delivery and quantitative evaluation of cellular therapeutic response. *Anal Chem* 2019;**91**:10596−603.
238. Dong K, Zhang Y, Zhang L, Wang Z, Ren J, Qu X. Facile preparation of metal-organic frameworks-based hydrophobic anticancer drug delivery nanoplatform for targeted and enhanced cancer treatment. *Talanta* 2019;**194**:703−8.
239. Wang GD, Chen H, Tang W, Lee D, Xie J. Gd and Eu co-doped nanoscale metal-organic framework as a t1−t2 dual-modal contrast agent for magnetic resonance imaging. *Tomography* 2016;**2**:179−87.
240. Meng X, Gui B, Yuan D, Zeller M, Wang C. Mechanized azobenzene-functionalized zirconium metal-organic framework for on-command cargo release. *Sci Adv* 2016;**2**:e1600480.

241. Jia Q, Li Z, Guo C, Huang X, Song Y, Zhou N, et al. A γ-cyclodextrin-based metal-organic framework embedded with graphene quantum dots and modified with PEGMA *via* SI-ATRP for anticancer drug delivery and therapy. *Nanoscale* 2019;**11**:20956−67.
242. Wu MX, Gao J, Wang F, Yang J, Song N, Jin X, et al. Multistimuli responsive core-shell nanoplatform constructed from Fe_3O_4@MOF equipped with pillar[6]arene nanovalves. *Small* 2018;**14**:e1704440.
243. Silva JYR, Proenza YG, da Luz LL, de Sousa Araújo S, Filho MAG, Junior SA, et al. A thermo-responsive adsorbent-heater-thermometer nanomaterial for controlled drug release: (ZIF-8,EuxTby)@AuNP core−shell. *Mater Sci Eng C Mater Biol Appl* 2019;**102**:578−88.
244. Ramezani MR, Ansari-Asl Z, Hoveizi E, Kiasat AR. Fabrication and characterization of Fe(III) metal-organic frameworks incorporating polycaprolactone nanofibers: potential scaffolds for tissue engineering. *Fibers Polym* 2020;**21**:1013−22.
245. Wang D, Zhou J, Chen R, Shi R, Zhao G, Xia G, et al. Controllable synthesis of dual-MOFs nanostructures for pH-responsive artemisinin delivery, magnetic resonance and optical dual-model imaging-guided chemo/photothermal combinational cancer therapy. *Biomaterials* 2016;**100**:27−40.
246. Lajevardi A, Sadr MH, Yaraki MT, Badiei A, Armaghan M. A pH-responsive and magnetic Fe_3O_4@silica@MIL-100 (Fe)/β-CD nanocomposite as a drug nanocarrier: loading and release study of cephalexin. *New J Chem* 2018;**42**:9690−701.
247. Gwon K, Han I, Lee S, Kim Y, Lee DN. Novel metal-organic framework-based photocrosslinked hydrogel system for efficient antibacterial applications. *ACS Appl Mater Interfaces* 2020;**12**:20234−42.
248. Luo D, Wang C, Tong Y, Liu C, Xiao Y, Zhu Z, et al. An NIF-doped ZIF-8 hybrid membrane for continuous antimicrobial treatment. *RSC Adv* 2020;**10**:7360−7.
249. Wuttke S, Zimpel A, Bein T, Braig S, Stoiber K, Vollmar A, et al. Validating metal-organic framework nanoparticles for their nanosafety in diverse biomedical applications. *Adv Healthc Mater* 2017;**6**:1600818.
250. Schütz CA, Juillerat-Jeanneret L, Mueller H, Lynch I, Riediker M. Therapeutic nanoparticles in clinics and under clinical evaluation. *Nanomedicine* 2013;**8**:449−67.
251. Lucena FR, de Araújo LC, Rodrigues Mdo D, da Silva TG, Pereira VR, Militão GC, et al. Induction of cancer cell death by apoptosis and slow release of 5-fluoracil from metal-organic frameworks Cu-BTC. *Biomed Pharmacother* 2013;**67**:707−13.
252. Lu K, He C, Lin W. Nanoscale metal-organic framework for highly effective photodynamic therapy of resistant head and neck cancer. *J Am Chem Soc* 2014;**136**:16712−5.
253. Ruyra À, Yazdi A, Espín J, Carné-Sánchez A, Roher N, Lorenzo J, et al. Synthesis, culture medium stability, and *in vitro* and *in vivo* zebrafish embryo toxicity of metal-organic framework nanoparticles. *Chemistry* 2015;**21**:2508−18.
254. Nel AE, Mädler L, Velegol D, Xia T, Hoek EM, Somasundaran P, et al. Understanding biophysicochemical interactions at the nano-bio interface. *Nat Mater* 2009;**8**:543−57.
255. Huxford RC, Dekrafft KE, Boyle WS, Liu D, Lin W. Lipid-coated nanoscale coordination polymers for targeted delivery of antifolates to cancer cells. *Chem Sci* 2012;**3**:198−201.
256. Lu K, Aung T, Guo N, Weichselbaum R, Lin W. Nanoscale metal-organic frameworks for therapeutic, imaging, and sensing applications. *Adv Mater* 2018;**30**:e1707634.
257. Bellido E, Guillevic M, Hidalgo T, Santander-Ortega MJ, Serre C, Horcajada P. Understanding the colloidal stability of the mesoporous MIL-100(Fe) nanoparticles in physiological media. *Langmuir* 2014;**30**:5911−20.
258. Li X, Lachmanski L, Safi S, Sene S, Serre C, Grenèche JM, et al. New insights into the degradation mechanism of metal-organic frameworks drug carriers. *Sci Rep* 2017;**7**:13142.
259. Liu WG, Truhlar DG. Computational linker design for highly crystalline metal-organic framework nu-1000. *Chem Mater* 2017;**29**:8073−81.
260. Kundu T, Mitra S, Patra P, Goswami A, Díaz Díaz D, Banerjee R. Mechanical downsizing of a gadolinium(III)-based metal-organic framework for anticancer drug delivery. *Chemistry* 2014;**20**:10514−8.
261. Grall R, Hidalgo T, Delic J, Garcia-Marquez A, Chevillard S, Horcajada P. *In vitro* biocompatibility of mesoporous metal (III; Fe, Al, Cr) trimesate MOF nanocarriers. *J Mater Chem B* 2015;**3**:8279−92.
262. Orellana-Tavra C, Mercado SA, Fairen-Jimenez D. Endocytosis mechanism of nano metal-organic frameworks for drug delivery. *Adv Healthc Mater* 2016;**5**:2261−70.
263. Rojas S, Baati T, Njim L, Manchego L, Neffati F, Abdeljelil N, et al. Metal-organic frameworks as efficient oral detoxifying agents. *J Am Chem Soc* 2018;**140**:9581−6.
264. Yang D, Yang G, Gai S, He F, An G, Dai Y, et al. Au25 cluster functionalized metal-organic nanostructures for magnetically targeted photodynamic/photothermal therapy triggered by single wavelength 808 nm near-infrared light. *Nanoscale* 2015;**7**:19568−78.
265. Bian R, Wang T, Zhang L, Li L, Wang C. A combination of tri-modal cancer imaging and *in vivo* drug delivery by metal-organic framework based composite nanoparticles. *Biomater Sci* 2015;**3**:1270−8.
266. Parayath NN, Nehoff H, Taurin S, Greish K. Prospects of nanocarriers for oral delivery of bioactives using targeting strategies. *Curr Pharm Biotechnol* 2016;**17**:683−99.
267. Mrsny RJ. Oral drug delivery research in Europe. *J Control Release* 2012;**161**:247−53.
268. Javanbakht S, Pooresmaeil M, Hashemi H, Namazi H. Carboxymethylcellulose capsulated Cu-based metal-organic framework-drug nanohybrid as a pH-sensitive nanocomposite for ibuprofen oral delivery. *Int J Biol Macromol* 2018;**119**:588−96.
269. Chowdhuri AR, Laha D, Pal S, Karmakar P, Sahu SK. One-pot synthesis of folic acid encapsulated upconversion nanoscale metal organic frameworks for targeting, imaging and pH responsive drug release. *Dalton Trans* 2016;**45**:18120−32.
270. Lin W, Hu Q, Jiang K, Yang Y, Yang Y, Cui Y, et al. A porphyrin-based metal-organic framework as a pH-responsive drug carrier. *J Solid State Chem* 2016;**237**:307−12.
271. Hidalgo T, Giménez-Marqués M, Bellido E, Avila J, Asensio MC, Salles F, et al. Chitosan-coated mesoporous MIL-100(Fe) nanoparticles as improved bio-compatible oral nanocarriers. *Sci Rep* 2017;**7**:43099.
272. Chen Y, Li P, Modica JA, Drout RJ, Farha OK. Acid-resistant mesoporous metal-organic framework toward oral insulin delivery: protein encapsulation, protection, and release. *J Am Chem Soc* 2018;**140**:5678−81.
273. Zhou Y, Liu L, Cao Y, Yu S, He C, Chen X. A nanocomposite vehicle based on metal-organic framework nanoparticle incorporated biodegradable microspheres for enhanced oral insulin delivery. *ACS Appl Mater Interfaces* 2020;**12**:22581−92.
274. Pan YB, Wang S, He X, Tang W, Wang J, Shao A, et al. A combination of glioma *in vivo* imaging and *in vivo* drug delivery by metal-organic framework based composite nanoparticles. *J Mater Chem B* 2019;**7**:7683−9.
275. Pang Y, Fu Y, Li C, Wu Z, Cao W, Hu X, et al. Metal-organic framework nanoparticles for ameliorating breast cancer-associated osteolysis. *Nano Lett* 2020;**20**:829−40.
276. Kush P, Bajaj T, Kaur M, Madan J, Jain UK, Kumar P, et al. Biodistribution and pharmacokinetic study of gemcitabine hydrochloride loaded biocompatible iron-based metal organic framework. *J Inorg Organomet Polym Mater* 2019;**30**:2827−41.
277. Du X, Fan R, Qiang L, Xing K, Ye H, Ran X, et al. Controlled Zn^{2+}-triggered drug release by preferred coordination of open active sites within functionalization indium metal organic frameworks. *ACS Appl Mater Interfaces* 2017;**9**:28939−48.
278. Mei L, Zhang Z, Zhao L, Huang L, Yang XL, Tang J, et al. Pharmaceutical nanotechnology for oral delivery of anticancer drugs. *Adv Drug Deliv Rev* 2013;**65**:880−90.

279. Castillo-Blas C, de la Peña-O'Shea VA, Puente-Orench I, de Paz JR, Sáez-Puche R, Gutiérrez-Puebla E, et al. Addressed realization of multication complex arrangements in metal-organic frameworks. *Sci Adv* 2017;**3**:e1700773.
280. Smith R, Vitórica-Yrezábal IJ, Hill A, Brammer L. Arene guest selectivity and pore flexibility in a metal-organic framework with semi-fluorinated channel walls. *Philos Trans A Math Phys Eng Sci* 2017;**375**:20160031.
281. Burgaz E, Erciyes A, Andac M, Andac O. Synthesis and characterization of nano-sized metal organic framework-5 (MOF-5) by using consecutive combination of ultrasound and microwave irradiation methods. *Inorg Chim Acta* 2019;**485**:118−24.
282. Feng PL, Perry JJt, Nikodemski S, Jacobs BW, Meek ST, Allendorf MD. Assessing the purity of metal-organic frameworks using photoluminescence: MOF-5, ZnO quantum dots, and framework decomposition. *J Am Chem Soc* 2010;**132**:15487−9.
283. Su F, Jia Q, Li Z, Wang M, He L, Peng D, et al. Aptamer-templated silver nanoclusters embedded in zirconium metal-organic framework for targeted antitumor drug delivery. *Microporous Mesoporous Mater* 2018;**275**:152−62.
284. Wang ZC, Zhang Y, Li ZY. A low cytotoxic metal-organic framework carrier: pH-responsive 5-fluorouracil delivery and anti-cervical cancer activity evaluation. *J Clust Sci* 2018;**29**:1285−90.
285. Lei Z, Yan C, Rui S, Tingguo K, Guangsheng P, Boran W, et al. Synthesis of hollow nanocages MOF-5 as drug delivery vehicle to solve the load-bearing problem of insoluble antitumor drug oleanolic acid. *Inorg Chem Commun* 2018;**96**:20−3.